VNiVERSiDAD D SALAMANCA

CAMPUS OF INTERNATIONAL EXCELLENCE

Department of Medicine, Hematology

Cancer Research Center (IBMCC-CSIC-USAL)

PRECLINICAL EVALUATION OF BH3-MIMETICS TARGETING MCL-1 (S63845) AND BCL-2 (VENETOCLAX) IN MULTIPLE MYELOMA

Doctoral dissertation presented by

Esperanza Macarena Algarín Pachón

Supervisors

Mercedes Garayoa Berrueta, PhD

Enrique M Ocio San Miguel, MD, PhD

Co-supervisor

Javier de las Rivas Sanz, PhD

Tutor

Marcos González Díaz, MD, PhD

June, 2020

Dña. Mercedes Garayoa Berrueta, Doctora en Ciencias Biológicas e Investigadora del Centro de Investigación del Cáncer de Salamanca,

D. Enrique M. Ocio San Miguel, Doctor en Medicina, Jefe de Servicio de Hematología del Hospital Universitario Marqués de Valdecilla de Santander y Responsable de Grupo del Instituto de Investigación Marqués de Valdecilla de Santander,
como directores y,

D. Javier de las Rivas Sanz, Doctor en Bioquímica y Biología Molecular e Investigador Científico del Consejo Superior de Investigaciones Científicas (CSIC) en el Centro de Investigación del Cáncer de Salamanca (Laboratorio 19),
como co-director y,

D. Marcos González Díaz, Doctor en Medicina, Investigador Principal del Centro de Investigación del Cáncer de Salamanca (Laboratorio 12), Jefe de Servicio de Hematología del Hospital Universitario de Salamanca y Catedrático de la Universidad de Salamanca del área de conocimiento de "Enfermería",
como tutor,

CERTIFICAN

Que el trabajo realizado bajo nuestra dirección y tutoría por Dña. Esperanza Macarena Algarín Pachón titulado "Preclinical evaluation of BH3-mimetics targeting MCL-1 (S63845) and BCL-2 (venetoclax) in multiple myeloma", reúne las condiciones de originalidad y calidad científica requeridas para optar al grado de Doctor, con mención "Doctor International", por la Universidad de Salamanca.

Y para que así conste a los efectos oportunos, firmamos el presente certificado en Salamanca, a 23 de junio de 2020,

Fdo.

Dra. Mercedes Garayoa

Dr. Enrique M. Ocio

Dr. Javier de las Rivas

Dr. Marcos González

Esta Tesis Doctoral ha sido realizada con las siguientes ayudas:

- Proyectos de Acción Estratégica en Salud del Instituto de Salud Carlos III – Fondo de Investigación Sanitaria y FEDER (PI 15/0067 y PI 15/2156)
- Proyectos de la Gerencia Regional de Salud (GRS 1604/A/17)
- Beca predoctoral financiada por la Consejería de Educación de la Junta de Castilla y León y el Fondo Social Europeo [convocatoria publicada en el Boletín Oficial de Castilla y León (BOCyL) nº 221 del 16 de noviembre de 2016 y resuelta en el BOCyL nº 126 del 4 julio de 2017. BDNS (Identificador): 322354)]

ABBREVIATIONS

ADCC	Antibody dependent cellular cytotoxicity
ADCP	Antibody dependent cell phagocytosis
AKT	Kinase B protein
AML	Acute myeloid leukemia
AP-1	Activator protein 1
APAF1	Apoptotic peptidase activating factor 1
AvrgFC	Average log2-fold change
BAD	BCL-2 associated agonist of cell death
BAK	BCL-2 homologous antagonist/killer
BAX	BCL-2 associated X
BCL-2	B-Cell lymphoma 2
BCL-2A1	BCL-2 related protein A1
BCL-B	BCL-2 like protein 10
BCL-W	BCL-2-like protein 2
BCL-X_L	BCL-2 like 1- extra large
BCL2L1	BCL-2 like 1
BCMA	B-cell maturation antigen
BH3	BCL-2 homology domain 3
BID	BH3 interacting domain death agonist
BIK	BCL-2 interacting killer
BIM	BCL-2 interacting mediator of cell death
BLI	Bioluminescence imaging
BM	Bone marrow
BMF	BCL-2 modifying factor
BOK	BCL-2 related ovarian killer protein
BRAF	V-raf murine sarcoma viral oncogene homolog B
Cas9	CRISPR-associated protein 9
CBFA2T3	CBFA2/RUNX1 partner transcriptional co-repressor 3
CCND1	Cyclin D1
CCND2	Cyclin D2
CCND3	Cyclin D3
CDC	Complement-dependent cytotoxicity
CDKN2C	Cyclin dependent kinase inhibitor 2C
CI	Combination index
CLL	Chronic lymphocytic leukemia
CLPB	Caseinolytic mitochondrial matrix peptidase chaperone subunit B
CpG	Cytosine-phosphodiester bond-guanine
CRBN	Cereblon
CRISPR	Clustered regularly interspaced short palindromic repeats
CRISPRa	CRISPR activation
CRISPRi	CRISPR interference

CRL	Cullin-RING ligases
crRNA	CRISPR RNA
CSN	Constitutive photomorphogenesis 9 signalosome
CUL4A	Cullin 4A
CUL5	Cullin 5
CYLD	CYLD lysine 63 deubiquitinase
dCas9	Dead Cas9
DDB1	Damage specific DNA binding protein 1
$DiOC_6$	3,3'-dihexyloxacarbocyanine iodide
DIS3	DIS3 exosome endoribonuclease and 3'-5' exoribonuclease
DNA	Deoxyribonucleic acid
DSB	Double strand break
ERK	Extracellular signal-regulated kinases
FAM46C	Family with sequence similarity 46 member C
Fc	Fragment crystallizable region
FDA	United States Food and Drug Administration
FGFR3	Fibroblast growth factor receptor 3
H3K27me3	Trimethylation of lysine 27 on histone H3
H3K36me2	Dimethylation of lysine 36 on histone H3
HDAC	Histone deacetylase
HDR	Homology directed repair
HIST1H1E	Histone cluster 1 H1 family member E
HRK	Harakiri BCL-2 interacting protein
HY	Hyperdiploidy
IC_{50}	Half-maximal inhibitory concentration
iFISH	Interphase fluorescence in situ hybridization
IFN-α	Interferon alpha
IFN-γ	Interferon gamma
Ig	Immunoglobulin
IgH	Immunoglobulin heavy chain
IgL	Immunoglobulin light chain
IKZF1	Ikaros
IKZF3	Aiolos
IL2	Interleukin 2
IL6	Interleukin 6
IMiDs	Immunomodulatory agents
IMWG	International Myeloma Working Group
IP	Immunoprecipitation
JAK	Janus kinase
KRAB	Krüppel associated box
KRAS	V-ki-ras2 Kirsten rat sarcoma viral oncogene homolog
LTB	Lymphotoxin beta
mAb	Monoclonal antibody

MAF	Avian musculoaponeurotic fibrosarcoma
MAFB	Avian musculoaponeurotic fibrosarcoma homolog B
MAPK	Mitogen-activated protein kinase
MCL-1	Myeloid cell leukemia sequence 1
MDR1	Multidrug resistance 1
MDR1i	Multidrug resistance 1 inhibitor
MGUS	Monoclonal gammopathy of undetermined significance
miRNA	microRNA
MM	Multiple myeloma
MMSET	Nuclear receptor binding SET domain protein 2
MRI	Magnetic resonance imaging
mRNA	Messenger ribonucleic acid
MSC	Mesenchymal stromal cell
MTT	3-4,5-dimethylthiazol-2-yl-2,5-dipheniltetrazolium bromide
MYC	V-myc avian myelocytomatosis viral oncogene homolog
NC	Negative control
NDMM	Newly diagnosed multiple myeloma
NFκB	Nuclear factor kappa B
NHEJ	Non-homologous DNA end joining
NK	Natural killer
NRAS	Neuroblastoma RAS viral oncogene homolog
ORR	Overall response rate
PAM	Protospacer adjacent motif
PBS	Phosphate buffered saline
PC	Plasma cell
PEG	Polyethylene glycol
PI	Proteasome inhibitor
PI3K	Phosphatidyl inositol 3-kinase
PMAIP1 / NOXA	Phorbol-12-myristate-13-acetate-induced protein 1
POU2AF1	POU class 2 homeobox associating factor 1
pre-miRNA	Precursor microRNA
pri-miRNA	Primary precursor microRNA
PSMC6	Proteasome 26S subunit, ATPase 6
PUMA	BCL-2 binding component 3
qRT-PCR	Quantitative real-time polymerase chain reaction
RB1	Retinoblastoma 1
RISC	RNA-induced silencing complex
RNA	Ribonucleic Acid
RNF7	Ring finger protein 7
RRMM	Relapse/refractory multiple myeloma
RUNX3	RUNX family transcription factor 3
sgRNA	Single guide RNA
SLAMF7	Signaling lymphocyte activating molecule F7

SMM	Smoldering multiple myeloma
STAT	Signal transducers and activators of transcription
TP53	Tumor protein P53
TPGS	D-α-tocopheryl polyethylene glycol 1000 succinate
tracrRNA	Trans-activating crRNA
TRAF3	TNF receptor associated factor 3
UBE2D3	Ubiquitin conjugating enzyme E2 D3
UBE2F	Ubiquitin conjugating enzyme E2 F
UBE2G1	Ubiquitin conjugating enzyme E2 G1
UTR	Untranslated region
XIAP	X-linked inhibitor of apoptosis
ΔΨm	Mitochondrial membrane potential

TABLE OF CONTENTS

1.INTRODUCTION

1.1. MULTIPLE MYELOMA

Multiple myeloma (MM) is a hematologic neoplasm characterized by the proliferation of clonal plasma cells (PCs) in the bone marrow (BM). The substitution of normal BM cells by MM cells results in cytopenias responsible, among other factors, for the immunodeficiency observed in these patients, and also in the production of monoclonal immunoglobulins (Igs) that can lead to renal failure. Other symptoms as hypercalcemia and osteolysis are direct consequences of the interaction of malignant PCs with the BM microenvironment.

MM is the second most common hematological malignancy after non-hodgkin lymphoma[11], with 138,509 new cases and 98,437 deaths in 2016 over the world. Its incidence is higher in better-developed countries, such as the United States, Western Europe and Australia[2]. This disease is more frequent in the elderly, with a median age at diagnosis of about 70 years, and only 37% of MM patients are younger than 65 years[3].

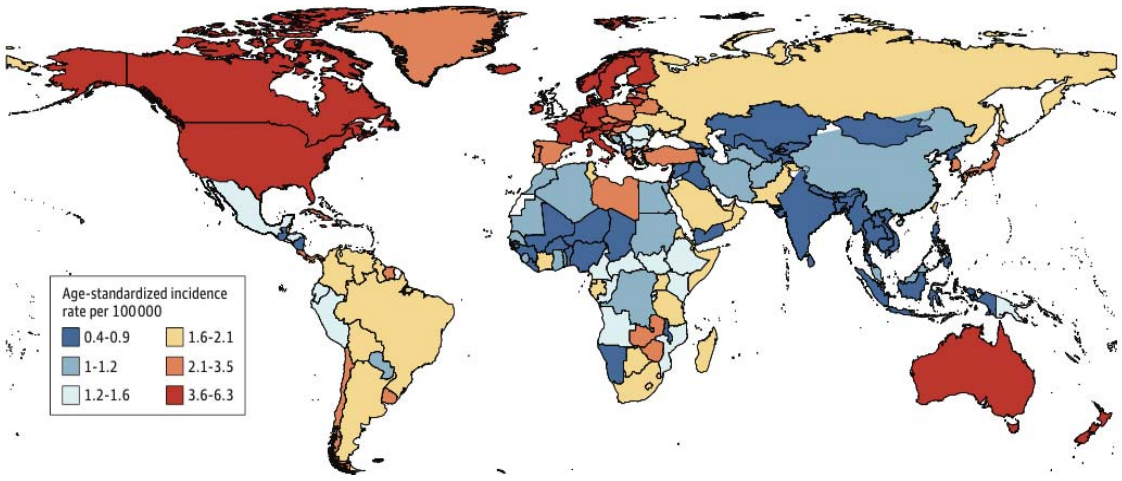

Figure 1. Global incidence rate of MM (2016)[2].

The diagnosis of this disease according to the International Myeloma Working Group (IMWG) criteria is based on monoclonal Ig levels (> 3 g/dL), the infiltration of clonal PCs in the BM (≥10% cellularity in morphological examination or a biopsy-proven plasmacytoma) and the presence of CRAB features (acronym derived from the clinical manifestations of this disease: Hypercalcemia, Renal insufficiency, Anemia and bone lytic lesions) or, in absence of these, the existence of myeloma-defining events, including

validated biomarkers such as involved-to-uninvolved serum free light chains ratio ≥100, the presence of >1 focal lesions in the magnetic resonance imaging (MRI) or ≥60% of plasma cell infiltration in the bone marrow[4].

MM seems to progress generally from premalignant asymptomatic states. The monoclonal gammopathy of undetermined significance (MGUS), with an overall risk of transformation to MM of 1% per year[5], is defined by a serum monoclonal Ig concentration <3 g/dL, <10% clonal PCs in the BM, and the absence of CRAB or any other myeloma-defining events. Some patients also experience an intermediate stage between MGUS and MM known as smoldering multiple myeloma (SMM), defined by a monoclonal Ig level of >3 g/dL and/or a clonal marrow plasmacytosis of 10-60% and the absence of myeloma-defining events. The annual risk of progression from SMM to symptomatic MM is 10% per year during the first 5 years after diagnosis[6] and decreases thereafter. Currently, MGUS and SMM patients do not receive any treatment, only an observational clinical follow-up. However, several clinical trials are currently revealing that the treatment of SMM patients with high-risk of progression to MM, delays the development of MM and may prolong survival of these patients[7,8].

1.2. MULTIPLE MYELOMA PATHOPHYSIOLOGY

Primary and secondary genetic abnormalities, epigenetic alterations and the influence of the BM microenvironment play a fundamental role in the ontogenesis, heterogeneity and progression of MM.

1.2.1. Genetic alterations

The initiation and progression of MM are highly dependent on genetic aberrations acquired by tumor cells at the time of onset and during the evolution of the disease.

1.2.1.1. Primary genetic events

PCs are antibody-secreting cells that represent the terminal differentiation stage of the B cell lineage. Antibodies, essential to prevent infections, are composed by two heavy (IgH) and two light (IgL) chains linked by disulfide bonds. Three different genomic mechanisms affecting the IgH and IgL loci and occurring during PC differentiation enable the production

of a diverse repertoire of antibodies with high affinity for specific antigens: V(D)J recombination, class switch recombination and somatic hypermutation. Several enzymes take part in these processes generating double-strand DNA breaks in the Ig loci, later ligated by proteins of the non-homologous end-joining (NHEJ) pathway. Occasionally, DNA breaks can aberrantly fuse to other genomic regions containing specific oncogenes, causing translocations that confer a growth advantage to PCs and can lead to the development of MM[9]. Clonal translocations involving the IgH locus on chromosome 14 are common in this disease and usually limited to a set of recurrent partner oncogenes:

- translocations t(11;14), t(12;14), and t(6;14), leading to the overexpression of *CCND1* (15-20%), *CCND2* (~1%) or *CCND3* (1-4%) cyclin D genes are the most frequent in newly diagnosed MM (NDMM) patients.
- t(4;14) resulting in the upregulation of nuclear receptor binding SET domain protein 2 (*MMSET*) and fibroblast growth factor receptor 3 (*FGFR3*) is the second most common translocation, occurring in ~15% of NDMM.
- translocations t(14;16) and t(14;20) involving avian musculoaponeurotic fibrosarcoma (*MAF*) and avian musculoaponeurotic fibrosarcoma homolog B (*MAFB*) transcription factors are only present in approximately 5% of NDMM cases[10,11].

Translocations t(4;14), t(14;16) and t(14;20) are considered as high-risk cytogenetic factors in MM patients, regardless of treatment[12,13]. The t(11;14) translocation was historically considered to confer a better prognosis, however this has been recently challenged[14].

The second type of founding genetic event, almost mutually exclusive with translocations of the IgH locus, is aneuploidy. Within this group of alterations, hyperdiploidy (HY) is the most frequent entity, being present in around 40% of NDMM patients. Co-occurring trisomies of some of the odd chromosomes: 3, 5, 7, 9, 11, 15 and 19, are found in this subgroup of patients possibly as a result of chromosome segregation errors occurring during PC differentiation. As compared with IgH translocations, HY tend to have a better prognosis[10,11].

Nevertheless, these primary cytogenetic abnormalities are insufficient to produce fully malignant MM cells, since they are already present at the same frequency in asymptomatic MGUS patients[15] and only a small proportion of them develops MM.

1.2.1.2. *Secondary genetic events*

In MM cells, clonal genetic events are usually accompanied by other cytogenetic abnormalities that lead to malignant transformation.

The most common secondary genetic events in MM are monosomy of chromosome 13 or 13q deletion, which are present in 35-40% and 6-10% of MM patients, respectively[16]. Among the genes situated in that region we can highlight the retinoblastoma 1 (*RB1*) tumor suppressor gene that prevents cell cycle progression. A recent study suggests the monosomy 13 to be an adverse prognostic factor whereas partial deletion seems to exhibit the opposite effect[17].

Other highly frequent alterations are those found in chromosome 1. Amplification of 1q and deletion of 1p occur in 40% and 20-25% of MM patients respectively. Notably, the *MCL1* gene, which encodes for an anti-apoptotic protein essential for MM cell survival, is located in 1q21, whereas the region usually lost in 1p32 includes the cyclin dependent kinase inhibitor 2C (*CDKN2C*), that regulates the G1/S cell cycle checkpoint. Both of these alterations are associated with poor prognosis[18,19].

Deletion of 17p is present in ~10% of NDMM, and its frequency increases in relapse/refractory MM patients (RRMM), being considered as an indicator of disease progression. This alteration is associated with the loss of the tumor suppressor P53 (*TP53*) gene, a marker of poor outcome as well as of genomic instability[20].

Another alteration that might be related to disease progression is the t(8;14) involving the v-myc avian myelocytomatosis viral oncogene homolog (*MYC)*. Unlike other IgH translocations, the t(8;14) translocation is found at sub-clonal levels in ~5% of NDMM [21,22]. Only sometimes it is present in MGUS, and is more common in RRMM than in NDMM[10,11].

Finally, different mutations contributing to MM progression have also been recently identified by several large-scale studies. Despite the heterogeneity of the mutational landscape in MM, most frequently mutated genes belong to a limited number of pathways. Particularly, around 40% of MM patients harbor mutations in v-ki-ras2 Kirsten rat sarcoma viral oncogene homolog (*KRAS)* and/or neuroblastoma RAS viral oncogene homolog (*NRAS*), which cause the activation of RAS/mitogen-activated protein kinase (MAPK) pathway. Moreover, mutations in genes belonging to the nuclear factor kappa B (NFκB) pathway, although at lower frequency, have also been reported, such as TNF receptor associated factor 3 (*TRAF3*) (4%), lymphotoxin beta (*LTB*) (3%) or CYLD lysine 63 deubiquitinase (*CYLD*) (3%)[23,24].

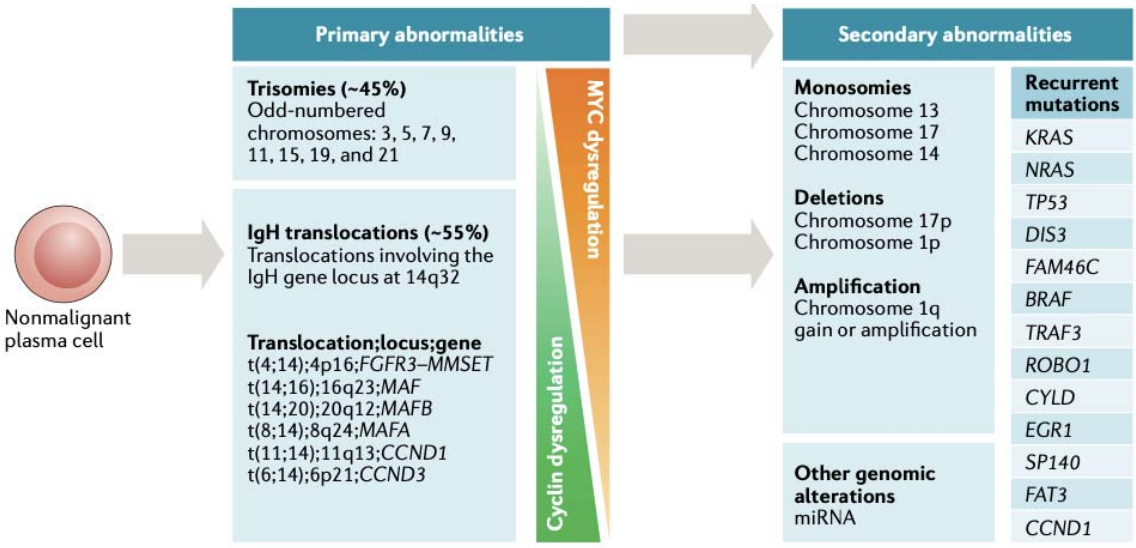

Figure 2. Primary and secondary genetic events in MM[11].

1.2.2. Epigenetic alterations

Additionally to the well-known genetic aberrations, emerging data in the last decades suggest that epigenetic features such as aberrant DNA methylation, histone post-translational modifications and abnormal microRNA (miRNA) expression may also play an important role in MM pathogenesis.

1.2.2.1. *DNA methylation*

Deoxyribonucleic acid (DNA) methylation is a biological process essential for cell differentiation and other important functions. It consists on the covalent addition of a methyl group to the aromatic ring of cytosine residues of cytosine-phosphodiester bond-guanine (CpG) dinucleotides. Within the mammalian genome, most methylated CpG dinucleotides are located at intragenic and intronic regions. On the contrary, most unmethylated CpG pairs are found in CpG-rich regions, known as CpG islands, which are found in the proximal region of the promoters of genes. Methylation of CpG islands has been associated with transcriptional silencing.

Similarly to other cancers, MM is characterized by regional DNA hypermethylation embedded in extensive hypomethylated regions. The global DNA hypomethylation is believed to occur in early myelomagenesis and advances during the transition from MGUS to MM, resulting into genomic instability. Indeed, this global DNA hypomethylation has been correlated with disease progression and poor prognosis. On the other hand, hypermethylation of tumor suppressor genes has been observed in the late stage of the malignancy. Among genes frequently hypermethylated in MM are cyclin-dependent kinase inhibitors, apoptosis regulators, negative regulators of the Wnt/ β-Catenin and the Janus kinase (JAK)/ signal transducer and activator of transcription (STAT) signaling pathways and tumor suppressors, whose transcriptional silencing promotes the progression of the disease.

Interestingly, it has also been recently reported hypermethylated sites out of CpG islands in MM cells. However, the relevance of DNA methylation in these regions is largely unknown[25,26].

1.2.2.2. *Histone epigenetic modifications*

Other well-studied epigenetic changes are post-translational modifications of histones. The amino terminal domains of histones, known as tails, are subjected to different epigenetic modifications that affect the chromatin structure being able to elicit gene transcription activation or repression.

One of the best characterized chromosomal abnormality involving histone modifying enzymes in MM, is the t(4;14) translocation. As previously mentioned, this genetic aberration leads to the overexpression of *MMSET*, a gene that encodes for a histone methyltransferase that catalyzes the dimethylation of lysine 36 on histone H3 (H3K36me2), a gene activation mark. Moreover, increased H3K36me2 levels in *MMSET* overexpressing cells has also been associated with a global reduction of the trimethylation of lysine 27 on histone H3 (H3K27me3), a modification related to gene repression. Therefore, the augmented expression of *MMSET* alters the whole chromatin structure resulting in an aberrant expression of genes involved in different key survival processes[25,26].

1.2.2.3. *microRNAs*

MicroRNAs (miRNAs) are short 20-22 nucleotide ribonucleic acid (RNA) molecules that function as negative regulators of gene expression in eukaryotic organisms. miRNAs are primarily transcribed as a polyadenylated primary precursor (pri-miRNA), that is subsequently processed by the RNA III endonuclease Drosha, giving rise to a precursor miRNA (pre-miRNA) of approximately 70-nucleotides in length. Pre-miRNAs are transported to the cytoplasm by exportin 5, where they are cleaved by the RNase III type endonuclease Dicer and transformed into a 20-nucleotide miRNA duplex. The mature miRNA strand of the duplex, together with the protein Argonaute-2, is further assembled into a ribonucleoprotein complex known as RNA-induced silencing complex (RISC), while the other strand is typically degraded. Then, the mature miRNA in complex with RISC is able to recognize complementary sequences in the 3′ untranslated region (3′ UTR) of target messenger RNAs (mRNAs) preventing their translation into proteins (if there is total complementarity) or promoting mRNA degradation (in case of imperfect complementarity) [27].

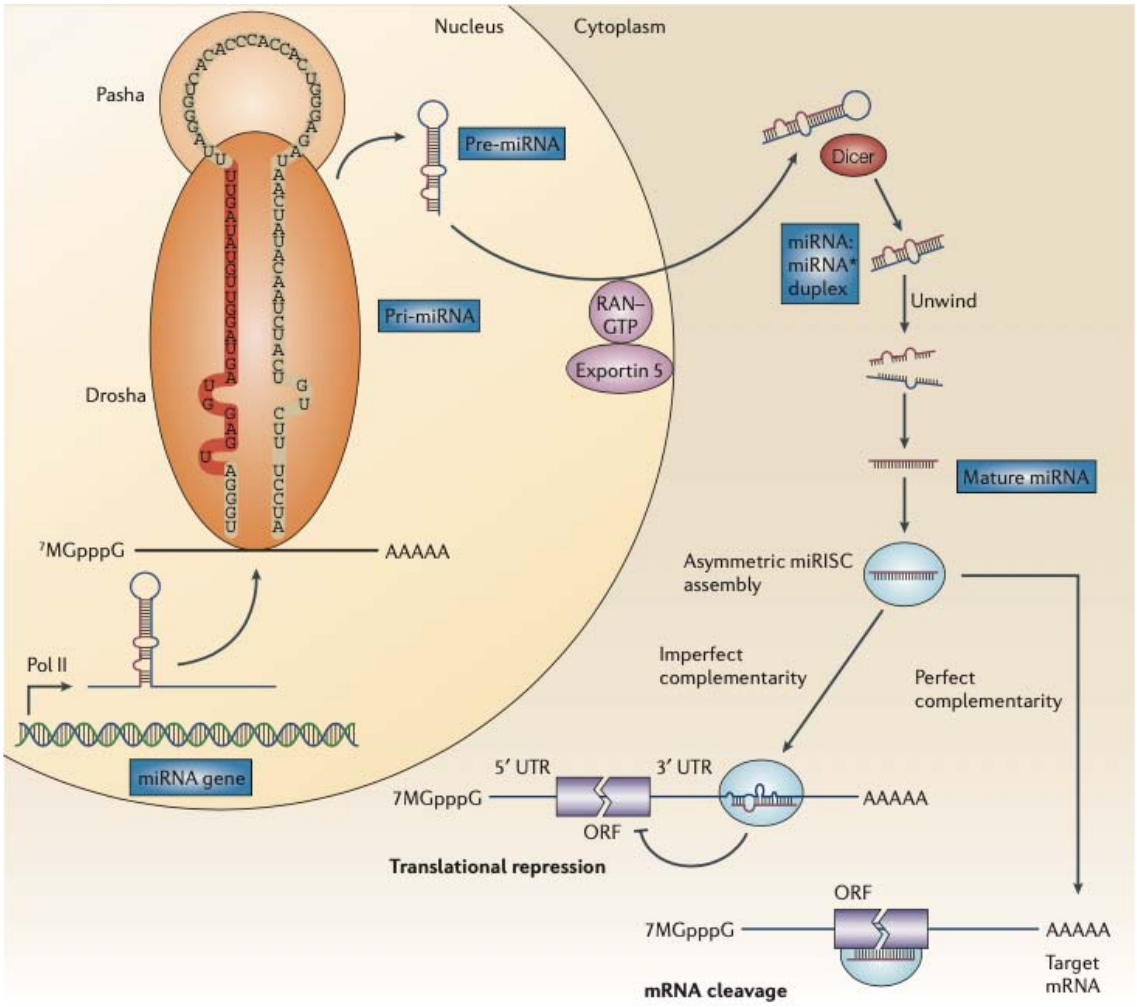

Figure 3. Biogenesis and mechanism of action of miRNAs[28].

The hypothesis that miRNAs may play an important role in cancer arose from the discovery that these noncoding RNAs are frequently present in the regions of the genome where cancer related genes, such as oncogenes and tumor suppressor genes, are encoded. In addition, miRNA expression profile studies performed using normal, MGUS, and MM PCs revealed different miRNA signatures for each of these stages. For instance, Pichiorri *et al.* identified miR-21, miR-106b/-25 cluster and miR-181a/b to be overexpressed in PCs from MM and MGUS patients with respect to normal PCs from healthy donors. Moreover, the upregulation of miR-32 and miR-17/92 cluster was exclusively detected on MM PCs[29]. In addition, miR-221 and miR-222 were also found overexpressed in MM cells with certain genetic features, such as HY and the traslocation t(4;14), as compared with donor PCs[30]. On the other hand, several miRNAs underexpressed on MM cells as compared with normal PCs have also been found, such as the miR-15a/-16 cluster[31], and correlated with different MM genetic subgroups[32].

Several mechanisms responsible for miRNA deregulation have been identified in MM such as DNA copy number variations, methylation of CpG islands, altered expression of transcription factors, defects in miRNA biogenesis and modifications affecting the availability of miRNA binding sites in the target 3´UTR mRNA seed sequence[33].

1.2.3. Influence of the bone marrow microenvironment

MM is not exclusively determined by genetic and epigenetic features, but the crosstalk between MM cells and the BM microenvironment, where they reside, is crucial for the development and progression of this disease. The MM BM microenvironment is composed by a cellular compartment that includes hematopoietic (immune cells and osteoclasts) and non-hematopoietic cells [adipocytes, endothelial cells, fibroblasts, osteoblasts and mesenchymal stromal cells (MSCs)]; and a non-cellular compartment constituted by the extracellular matrix and soluble factors such as cytokines, chemokines or growth factors, which are generally produced by the cellular compartment[34].

MSCs are self-renewing precursor cells essential for the formation and function of the BM microenvironment. Due to their multipotent capacity, they can differentiate into a variety of cells residing in the BM such as adipocytes, osteoblasts and fibroblasts, that altogether support the normal hematopoiesis. However, the close interplay between MSCs and MM cells is known to have bidirectional consequences that lead to the creation of a BM niche more prone to support the development of MM disease[35]. On the one hand, cell-cell contact cooperates with paracrine cytokine-induced signaling to activate pathways on MSCs that result in the secretion of soluble factors such as interleukin 6 (IL6), which in turn promote drug resistance, survival and proliferation of MM cells. Moreover, the communication with MM cells reduces the ability of MSCs to differentiate into osteoblasts, thereby contributing to the appearance of osteolytic lesions frequently found in MM patients[35]. On the other hand, these interactions also lead to changes in MM PCs, such as the activation of several cellular signaling pathways [phosphatidyl inositol 3-kinase (PI3K)/ kinase B protein (AKT), JAK/STAT, RAS/MAPK and NFκB] that support proliferation, migration, drug resistance, as well as the expression of anti-apoptotic proteins on MM cells[36].

After interaction with BM-MSCs, the expression of many genes belonging to a great diversity of molecular networks (e. g. oncogenic kinases, cytokines, chemokines and

chemokine receptors, oncogenic transcription factors, cell cycle regulators, hypoxia response genes or anti-apoptotic BCL-2 family members… among others) has been found to be differentially expressed in MM cells[37]. This might be, at least in part, consequence of the regulatory effect exerted by BM-MSCs on MM cells through miRNAs, which affect the expression of their target mRNAs (Figure 4)[38]. It is known that the interaction with the BM milieu induces the downregulation of tumor suppressor miRNAs and the upregulation of oncomiRNAs on MM cells, resulting in augmented tumor cell proliferation, migration and/or survival. In this regard, miR-29b, which is downregulated in MM cells, has been demonstrated to increase tumor-cell adhesion to BM-MSCs, reducing the expression of factors such as IL-8, MMP2, and VEGF-A, which promote angiogenesis and disease progression[39]. Similarly, enforced expression of miR-199a, found to be downregulated on MM cells after hypoxia, leading to increased HIF-1α levels, has also been reported to augment the adhesion of MM cells to BM-MSCs in those conditions[40]. Additionally, the ectopic expression of miR-34a on MM cells has been shown to overcome the proliferative advantage conferred by BM-MSCs *in vitro* and *in vivo* using a SCID-synth-hu model[41]. Moreover, the expression of miR-30 was reported to be reduced on MM cells after their interaction with BM-MSCs, resulting in an enhanced BCL9 expression. BCL9 is a transcriptional coactivator of the Wnt signaling pathway, which promotes MM cell proliferation, survival, migration and drug resistance[42]. On the contrary, adherence to BM-MSCs upregulated miR-125a levels in MM cells, which directly target *TP53* transcript and consequently induces cell growth, migration, and survival in MM cells harboring a wild-type p53 gene[43].

Other miRNAs also altered in MM cells in presence of the stromal BM microenvironment are involved in other biological processes such as drug resistance. For instance, Hao *et al.* reported that IL6 secreted by BM-MSCs led to miR-15a/-16 suppression in MM cells, protecting them from apoptosis induced by bortezomib[44]. Similarly, adherence to BM-MSCs has been found to increase miR-21 expression in MM cells, conferring resistance to apoptosis triggered by dexamethasone, doxorubicin and bortezomib[45]. Levels of miR-125b, which targets *IRF4* mRNA, were downregulated in MM cells after stromal interaction and promoted myeloma growth and survival[46]. Gulla *et al.* observed an overexpression of miR-221/222 in MM cells when co-cultured with BM-MSCs, and miR-221/222 inhibition overcame melphalan resistance of tumor cells[47]. Moreover, the transfer of EVs containing specific RNA species such as miRNAs, from BM-MSCs to MM

cells has also been reported to promote growth, survival, homing and proteasome inhibitor resistance in myelomatous cells[48].

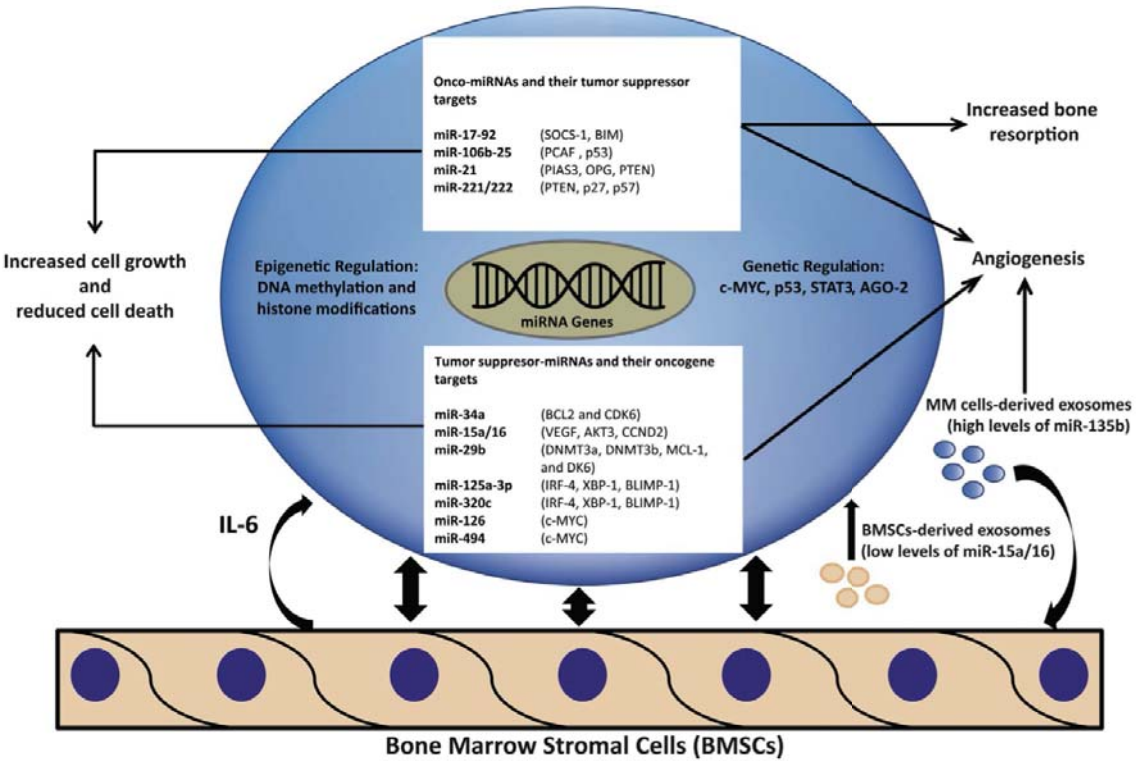

Figure 4. Deregulation of miRNAs in MM cells after interaction with the BM milieu[25].

1.3. APPROVED DRUGS FOR THE TREATMENT OF MULTIPLE MYELOMA

Until the early 1990s, the therapeutic armamentarium for MM was limited to corticosteroids and alkylating agents, being the median survival of 2-3 years. The appearance of immunomodulatory agents (IMiDs) and several other targeted agents such as proteasome inhibitors (PIs), histone deacetylase (HDAC) inhibitors and, more recently, monoclonal antibodies (mAbs) have markedly prolonged the survival of both, young and elderly MM patients over the last two decades[49,50]. In fact, the median overall survival has at least doubled in the last decade, reaching 7-10 years[50].

1.3.1. Glucocorticoids

Glucocorticoids such as prednisone and dexamethasone are steroid hormones that have been used for the treatment of MM for over 50 years, first as single agents and later in combination with other drugs to induce superior clinical response rates.

These agents bind to cytosolic glucocorticoid receptors and then translocate to the nucleus to modulate the expression of important transcription factors such as NFκB and activator protein 1 (AP-1), ultimately inducing apoptosis[51].

1.3.2. Alkylating agents

Alkylating agents substitute hydrogen atoms on DNA for alkyl groups, resulting in the cross-linking of strands of DNA and consequently in the inhibition of DNA, RNA, and protein synthesis, thereby triggering apoptosis.

Melphalan is a DNA-alkylating nitrogen mustard derivative that, in combination with corticosteroids, constituted the standard therapy for MM for over 40 years until the introduction of PIs and IMiDs. Cyclophosphamide is another alkylator, that is also frequently used in combination with dexamethasone or prednisone and generally a third party compound, being mainly PIs, but also IMiDs or even mAbs.

More recently another alkylating agent, bendamustine, was licensed in Europe in combination with prednisone at frontline for those MM patients unsuitable for transplantation and not able to receive thalidomide and bortezomib[52]. Currently, bendamustine is scarcely used, but several trials have evaluated its combination with PIs or IMiDs in RRMM patients.

1.3.3. Proteasome inhibitors

There are currently three PIs approved for the treatment of MM, all of them majorly targeting the proteasome β-5 catalytic subunit: bortezomib, carfilzomib and ixazomib. Bortezomib, also binding to the β-1 and β-2 proteasomal subunits, was the first PI approved by the United States Food and Drug Administration (FDA) in 2003 for RRMM, and was later incorporated in many different combinations for relapsed and newly diagnosed patients. Carfilzomib was approved in 2012 for RRMM in combination with

dexamethasone, based on a phase II trial showing a higher response rate and longer progression free survival and overall survival than bortezomib + dexamethasone in MM patients non-refractory to PIs[53]. It was also latterly approved in combination with lenalidomide and dexamethasone for RRMM after 1-3 prior lines of therapy[54]. Moreover, carfilzomib has also demonstrated to be effective in MM patients relapsing after treatment with bortezomib[55]. The last PI to be approved was ixazomib, that belongs to the same family as bortezomib and has similar properties except for the advantage that it is the only orally bioavailable approved PI. Ixazomib has been shown to be effective in bortezomib-resistant RRMM patients and is also approved for patients in first relapses in combination with lenalidomide and dexamethasone[56].

The activity of PIs in this disease is based on the high Ig production rate of MM cells. Generally, an elevated protein synthesis results in the production of misfolded and non-functional proteins that have to be rapidly degraded by the proteasome to prevent their accumulation through the unfolded protein response. Thus, MM cells are thought to be especially sensitive to proteasome inhibition, which leads to proteotoxic stress induction and triggering of apoptosis[57].

Furthermore, PIs cause pleiotropic effects on tumor cells, including blockade of NF-κB activity, cell cycle arrest, apoptosis induction, inhibition of DNA repair enzymes and inhibition of adhesion to BM-MSCs (extensively reviewed in [58,59]). Additionally, these agents have been reported to have bone anabolic and anti-resorptive effects, thereby being also beneficial for the MM associated bone disease[60].

1.3.4. Immunomodulatory agents

Thalidomide was the first-in-class IMiD approved by the FDA in 2006 for NDMM patients in combination with dexamethasone[61]. However, this agent was subsequently substituted by more potent and effective second generation IMiDs, including lenalidomide and pomalidomide.

Currently, lenalidomide has become a backbone for combination with PIs, mAbs or other agents in the relapsed and the newly diagnosed situation, both in transplant eligible and ineligible patients. On the other hand, pomalidomide is effective and approved in RRMM patients previously treated with lenalidomide, both in combination with dexamethasone[62], with bortezomib and dexamethasone[63] and more recently with the anti-CD38 mAb isatuximab[64].

It was not until 2010, when cereblon (CRBN) was identified as the primary target of IMiDs. CRBN is one of the four components of the of the cullin-4 RING E3 ligase complex that mediates the ubiquitination and subsequent proteasomal degradation of target proteins. IMiDs' binding to CRBN results in the alteration of the substrate specificity of this complex, leading to the degradation of two key PC transcription factors, Ikaros (*IKZF1*) and Aiolos (*IKZF3*). Moreover, Ikaros and Aiolos loss also leads to IRF4 and c-Myc downregulation, essential transcription factors for MM PCs[65]. In addition, regarding their immunomodulatory properties, IMiDs induce the production of interleukin 2 (IL2) and interferon gamma (IFNγ) by immune effector cells, resulting in the potentiation of NK and T cells proliferation and cytotoxicity[66].

1.3.5. Histone deacetylase inhibitors

Panobinostat is an HDAC inhibitor approved, in combination with bortezomib and dexamethasone, for the treatment of RRMM patients previously treated with bortezomib and an IMiD. However, there are some concerns about its safety and tolerability, mainly based on asthenia, thrombocytopenia and gastro-intestinal toxicity[67].

The cytotoxic effect of panobinostat is mainly based on two mechanisms of action: reversion of the deacetylation state of histones, that leads to the transcriptional activation of tumor-suppressor genes, and the acetylation of non-histone proteins, such as tubulin. This last mechanism leads, among other consequences, to the blockage of the aggresome pathway that ends up in an overproduction of misfolded proteins thay synergistically cooperates with proteasome inhibition[68].

1.3.6. Monoclonal antibodies

Three mAbs, daratumumab, isatuximab and elotuzumab are currently approved for the treatment of MM. The two first ones target the transmembrane glycoprotein CD38, while elotuzumab binds to the signaling-lymphocyte-activating molecule F7 (SLAMF7). Both of them are surface proteins highly expressed by MM cells.

On the one hand, mAbs can exert their action through classic immune effector mechanisms [antibody dependent cellular cytotoxicity (ADCC), antibody dependent cellular phagocytosis (ADCP) and complement-dependent cytotoxicity (CDC)]. ADCC is mediated by NK cells expressing CD16, a receptor that recognizes the fragment crystallizable region (Fc) of mAbs bound to the target antigen present on MM cell surface,

activating the release of granzymes and perforins, which induce the lysis of the tumor cell. ADCP is mediated by macrophages that internalize and degrade antibody-opsonized tumor cells. Finally, CDC is triggered when the C1q complement factor is activated through its binding to the Fc of an antibody bound to the MM cell. As a result, pores generate in the myeloma cell surface leading to lysis of these cells. On the other hand, CD38 is also expressed in non-tumor immune cells, and therefore, mAbs targeting this antigen also exhibit immunomodulatory activities, such as a decrease in regulatory T and B lymphocytes and myeloid-derived suppressor cells. Moreover, crosslinks formed between antigen-bound antibody on MM cells and receptors on effector cells may also play an important role in direct cytotoxicity of MM cells[69,70].

Daratumumab and similarly isatuximab, are able to induce CDC, ADCC, ADCP and decrease the subpopulation of CD38-expressing regulatory T cells favoring the increase of helper and cytotoxic T-cell populations. Moreover, crosslinking of daratumumab on MM cells leads to loss of membrane integrity[70]. Finally, daratumumab, and particularly isatuximab also inhibits the enzymatic activity of CD38, which acts as an ectoenzyme that catalyzes the synthesis of nucleotides involved in calcium fluxes regulation and activation of signaling pathways critical for different biological processes. Elotuzumab acts primarily through ADCC, but also triggers the ADCP mechanism and enhances the anti-myeloma NK cell activity by crosslinking SLAMF7 on both cell types[71].

In contrast to elotuzumab, daratumumab and isatuximab exhibit single agent activity in heavily pretreated MM patients[72,73]. However, most interesting outcomes are those from the combination of these drugs with PIs and IMiDs. Daratumumab is approved in combination with bortezomib + dexamethasone and lenalidomide + dexamethasone for the treatment of RRMM patients, and has now moved to the newly diagnosed setting in combination with previous standards such as melphalan + prednisone + bortezomib or lenalidomide + dexamethasone. Similarly, isatuximab has been very recently approved in combination with pomalidomide an dexamethasone for the treatment of RRMM patients[64]. Elotuzumab is approved in combination with IMiDs (lenalidomide or pomalidomide) and dexamethasone for the treatment of RRMM.

1.3.7. Exportin inhibitors

Transport of proteins and mRNAs into and out of the nucleus is controlled by the nuclear pore complex (NPC). The function of exportins is to mediate the transport of proteins and mRNAs out of the nucleus through the NPC. Particularly, exportin-1 (XPO1) is one of the best-characterized nuclear exporters, responsible for transporting most of the tumor suppressors, growth regulators and oncoprotein mRNAs including p53, p21, forkhead box protein O (FOXO), cyclins, RB and c-Myc among others and is over-expressed in several cancers, including MM. Selinexor is novel drug that establishes a reversible covalent bond with cysteine 528 in the cargo binding pocket of XPO1, thereby inducing apoptosis of tumor cells by impeding the translocation of key tumor suppressor proteins and growth regulatory factors into the cytoplasm. This agent has shown very promising results in the clinic in combination with standard treatments and in 2019, based on the 21% ORR reached in the STORM trial evaluating selinexor + dexamethasone in RRMM patients refractory to at least two PIs, two IMiDs and an anti-CD38 monoclonal antibody, what has resulted in the approval of this drug by the FDA[74].

1.4. ANTI-APOPTOTIC PROTEINS AS NOVEL TARGETS IN MULTIPLE MYELOMA

Despite the success in the treatment of MM during the past 20 years, MM is still an incurable disease. Initial treatment employing one or more of the previously described approved drugs frequently induces responses, but MM patients eventually relapse or generate resistance to these therapies. Therefore, new agents or combinations of drugs are still necessary for the treatment of MM. In order to design and discover novel molecules, it is important to deepen into the main pathogenetic mechanisms of tumor cells, one of such is apoptosis evasion.

1.4.1. Apoptosis evasion: a hallmark of tumor cells

Apoptotic evasion has been postulated as one of the main mechanisms by which tumor cells survive[75]. Apoptosis is an evolutionarily conserved cell death pathway crucial for tissue homeostasis that may be initiated through extrinsic or intrinsic pathways (Figure 5). The extrinsic pathway is triggered by the binding of cell-surface death receptors belonging to the tumor necrosis factor superfamily to their ligands, which leads to the recruitment and activation of the caspase 8 initiator. The intrinsic pathway, which is tightly regulated

by the B-cell lymphoma 2 (BCL-2) protein family, is initiated by intracellularly sensed stress signals and ultimately leads to the permeabilization of the outer mitochondrial membrane and the release of apoptogenic proteins such as Smac/DIABLO, that neutralizes caspase-inhibitory proteins like the X-linked inhibitor of apoptosis (XIAP); or cytochrome c, which interacts with the apoptotic peptidase activating factor 1 (APAF1) adaptor molecule, forming the apoptosome that promotes the activation of the caspase 9 initiator. Lastly, the extrinsic and the intrinsic apoptotic pathways converge on the activation of the common effector caspases 3 and 7, which are responsible for the final triggering of apoptosis. Importantly, the activation of the extrinsic pathway can lead to the activation of the intrinsic pathway via cleavage of BH3 interacting domain death agonist (BID) by caspase 8, resulting in amplification of the death signal[76].

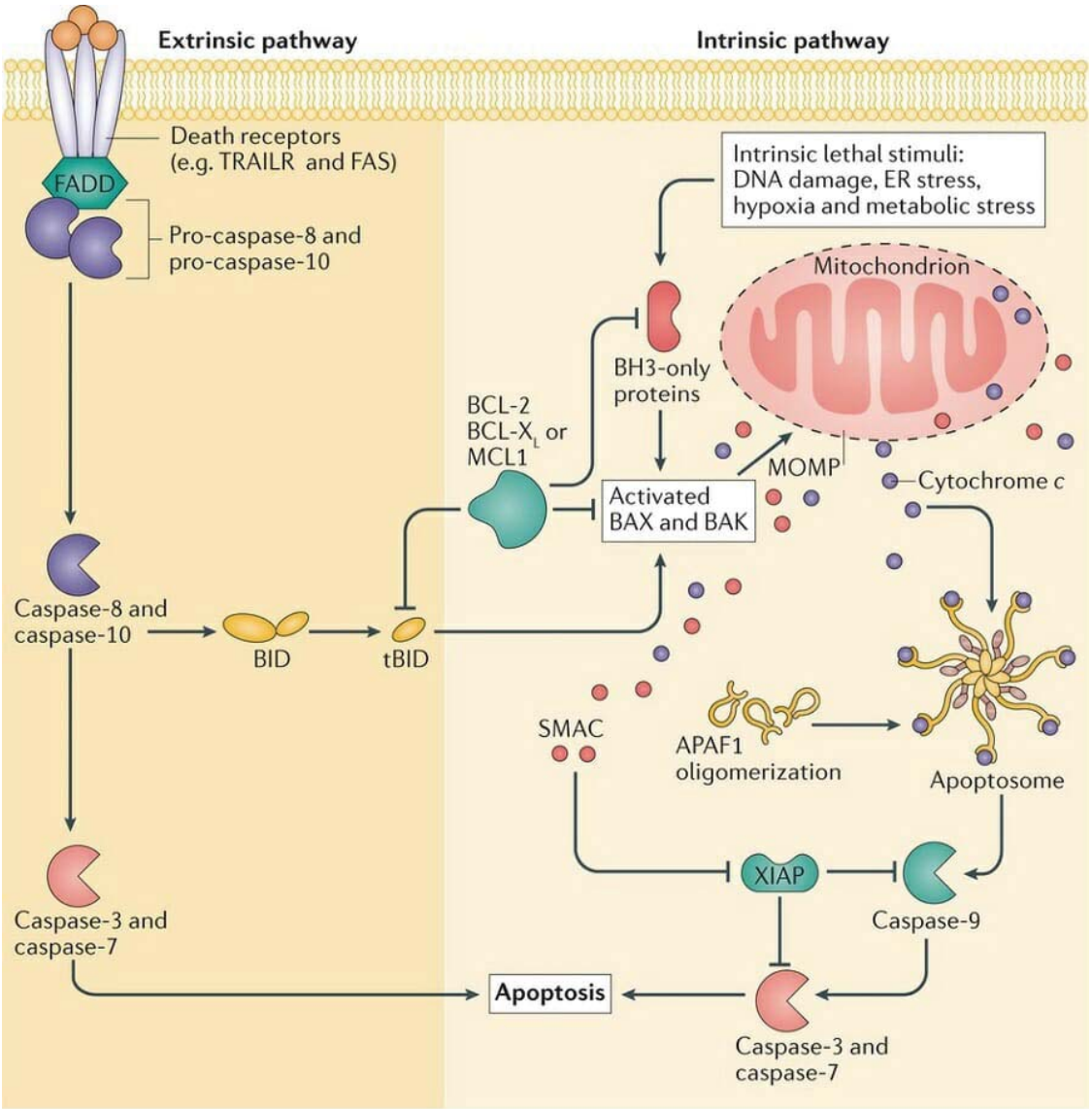

Figure 5. Extrinsic and intrinsic apoptotic pathways[77].

The members of the BCL-2 family of proteins regulating the intrinsic apoptotic pathway are classified into three groups according to their structure and function (Figure 6):

- Anti-apoptotic multidomain proteins: BCL-2, BCL-2-like protein 1 extra-large (BCL-X_L), BCL-2-like protein 2 (BCL-W), BCL-2 related protein A1(BCL2A1/BFL1), BCL-2 like protein 10 (BCL-B) and MCL-1.
- Pro-apoptotic BCL-2 homology domain 3 (BH3)-only proteins: subdivided into sensitizers [BCL-2 associated agonist of cell death (BAD), BCL-2 modifying factor (BMF), harakiri BCL-2 interacting protein (HRK), BCL-2 interacting killer (BIK) and phorbol-12-myristate-13-acetate-induced protein 1 (NOXA)] and activators [BCL-2-interacting mediator of cell death (BIM), BID and BCL-2-binding component 3 (PUMA)].
- Effector pro-apoptotic multidomain proteins: BCL-2 homologous antagonist/killer (BAK), BCL-2 associated X (BAX) and BCL-2-related ovarian killer protein (BOK).

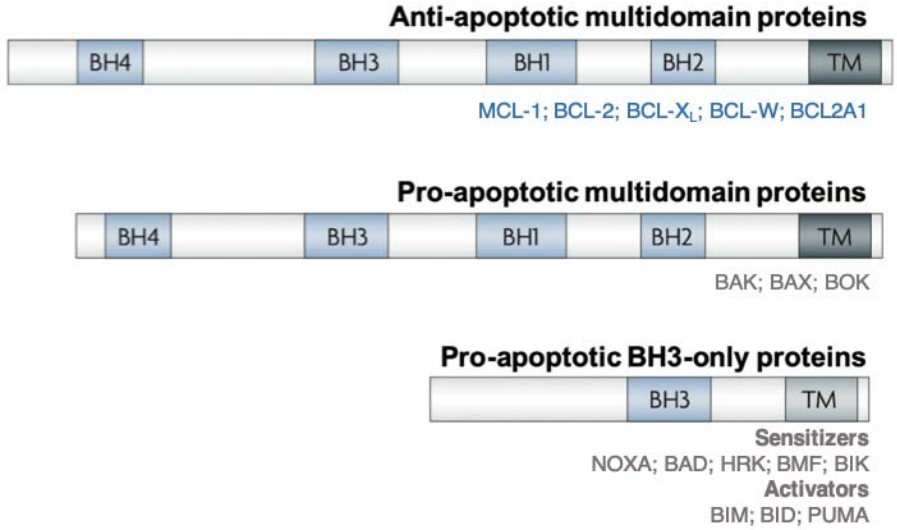

Figure 6. Classification of BCL-2 family members according to their structure and function (modified from[78]).

The activation of the effectors BAX, BAK and BOK by their interaction with BH3-only activators (BIM, BID and PUMA) is ultimately responsible for triggering apoptosis. Under normal conditions, anti-apoptotic proteins sequester these BH3-only activators to prevent them interacting with BAX, BAK, and BOK, thereby avoiding apoptosis. However,

in response to stress stimuli, BH3-only activators are either activated through transcriptional, post-transcriptional or post-translational mechanisms, or displaced from the anti-apoptotic proteins by BH3-only sensitizers, and they become able to interact with BAX, BAK and BOK. These interactions induce conformational changes in the pro-apoptotic effector proteins that allow them to homo-oligomerize and generate pores on the outer mitochondrial membrane, causing its permeabilization. In addition, BH3-only sensitizers are also involved in displacing BAX, BAK and BOK from anti-apoptotic proteins, favoring the interplay between BH3-only activators and pro-apoptotic effector proteins. Whereas BH3-only activators are promiscuous and bind to most anti-apoptotic proteins, BH3-only sensitizers have distinct binding specificities. For instance, BAD binds only to BCL-2, BCL-X_L and BCL-W, whereas NOXA binds just to MCL-1 and BCL2A1(Figure 7)[76,79,80].

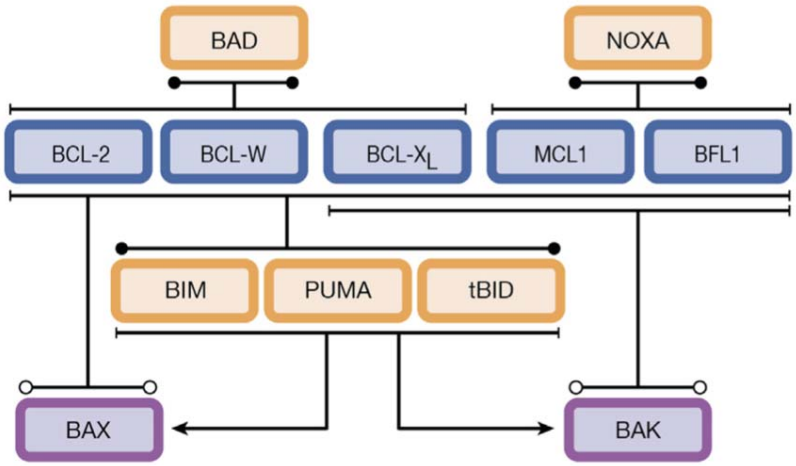

Figure 7. Interactions established among BCL-2 family proteins regulating the intrinsic apoptotic pathway[80].

Despite the oncogenic stress, genomic instability and cellular hypoxia characteristic of cancer, tumor cells can keep the intrinsic apoptotic pathway inactivated by modulating the proteins belonging to the BCL-2 family[81]. In this regard, BCL-2, BCL-X_L or MCL-1 anti-apoptotic proteins have been reported to be overexpressed in various tumors[82]. The increased expression of these proteins has been reported to be prompted by signaling pathways usually hyperactivated in cancer cells such as the PI3K/AKT signaling pathway, which may induce the overexpression of *MCL1*; or by miRNAs downregulated in some tumors like miR-15 and miR-16, leading to increased expression

of *BCL2*, or diminished levels of miR-29b, miR-101 and miR-193a, which result in increased translation of *MCL1* mRNAs. At post-translational level, tumor cells can also promote the stability of anti-apoptotic proteins. BCL-2 and BCL-X_L are quite stable proteins; MCL-1, however, is a protein with a short half-life and fast turnover, and when its transcription is suppressed following an apoptotic stimulus, MCL-1 protein levels rapidly decrease. Emerging evidence suggests that tumor cells are able to induce the phosphorylation on certain amino acid residues on MCL-1 resulting in the stabilization of this protein[83].

Other mechanism of apoptotic evasion employed by tumor cells is the downregulation of pro-apoptotic proteins. For instance, *TP53* is a tumor suppressor gene that in normal conditions induces the expression of pro-apoptotic proteins (including BAX, PUMA and NOXA) in response to different stimuli, has been found to be frequently mutated or inactivated in tumor cells. Moreover, cancer cells may also enhance the degradation of specific pro-apoptotic proteins through different post-translational modifications. Generally, phosphorylation by pro-survival kinases [e.g. AKT and extracellular signal-regulated kinases (ERK)] frequently leads to the suppression of pro-apoptotic proteins. For example, BIM stability depends on ERK phosphorylation at S69, which promotes its degradation through the ubiquitin-proteasome pathway[81]. Moreover, in contrast to BAK, BAX is mostly localized in the cytosol and it translocates to the mitochondria only during apoptosis. Phosphorylation of BAD by AKT prompts its sequestration in the cytosol, thereby preventing its pro-apoptotic activity[84].

1.4.2. BH3-mimetics in multiple myeloma

In the last years, many academic and industry laboratories have been focused on the development of agents able to inhibit anti-apoptotic proteins, with the aim of inducing apoptosis in tumor cells. Apoptosis induction using BH3-mimetics, molecules targeting the BH3-binding groove of anti-apoptotic proteins to which pro-apoptotic proteins usually bind, is nowadays a particularly exciting research field due to the selectivity and efficacy demonstrated by these drugs.

The first remarkable BH3-mimetics to be explored were the dual BCL-2/BCL-X_L inhibitor ABT-737 and its orally bioavailable equivalent ABT-293 (navitoclax). Despite the notable efficacy exhibited by navitoclax in preclinical studies, the inhibition of BCL-X_L (an

important survival factor for platelets) caused the development of severe thrombocytopenia setting a dose-limiting toxicity in the clinic[85]. Due to the high dependence of cancer, mainly solid tumors, on BCL-X_L, significant efforts in developing selective inhibitors targeting exclusively this anti-apoptotic protein and with an appropriate therapeutic window are still ongoing.

The orally bioavailable selective BCL-2 inhibitor venetoclax was subsequently developed, and has been the first BH3-mimetic approved by the FDA, particularly for the treatment of patients with relapsed or refractory chronic lymphocytic leukemia (CLL) with deletion of 17p[86]. Venetoclax binds to BCL-2 impeding its activity as an inhibitor of pro-apoptotic BCL-2 family members, ultimately inducing apoptosis[87]. In MM, a phase I clinical trial of venetoclax in monotherapy proved to be effective in highly pretreated RRMM patients, predominantly in the subgroup of patients harboring the t(11;14) translocation, with an ORR of 40% in this subset of MM patients. Interestingly, almost none of the patients without the t(11;14) translocation responded to the treatment (ORR 6%)[88]. Combinations with standard of care agents capable of sensitizing MM cells to venetoclax have subsequently been investigated. The combination of venetoclax with dexamethasone, an agent inducing the upregulation of BCL-2 and BIM favoring its interaction[89], has been investigated in MM patients harboring the t(11;14), achieving an ORR of 45% in the phase 2 study[90]. Venetoclax has also been combined with PIs, since it was demonstrated that bortezomib sensitizes MM cells to the BCL-2 inhibitor by increasing the expression of NOXA[91]; then NOXA displaces MCL-1 (which has been associated with venetoclax resistance[75,92]) from BIM and induces its degradation[93]. The clinical trial phase 1 assessing the venetoclax + bortezomib + dexamethasone combination initially showed excellent results regarding the efficacy (ORR 67%) in MM patients bearing different cytogenetic alterations (no differences in ORR attributable to the t(11;14) translocation), and specially in those non-refractory to bortezomib (ORR 90%)[94]. However, the confirmatory phase 3 study, surprisingly revealed a significant increased risk of death in the venetoclax experimental arm[95], that was toned down with longer follow up[96]. Other combinations currently being evaluated are venetoclax + carfilzomib + dexamethasone and venetoclax + bortezomib + dexamethasone + daratumumab. Apart from venetoclax, S55746 is another BH3-mimetic targeting BCL-2 in early clinical development, but results have not been published so far.

It is well known that MM cells are generally more dependent on MCL-1 than on BCL-2[97–99], partly due to cytokines such as IL6, which are released by MSCs from the BM tumor microenvironment[100]. In fact, *MCL1* has been shown to be overexpressed in MM cells, especially in those harboring t(4;14) and t(14;16) high-risk translocations[101], and associated with relapse and shorter survival[102]. Three BH3-mimetics targeting MCL-1 are currently in early clinical investigation: AZD-5991, AMG-176 and S64315/MIK655. All these agents, similarly to venetoclax with BCL-2, bind to MCL-1 preventing its interaction with pro-apoptotic proteins, thereby activating the apoptotic intrinsic pathway on tumor cells. Although results from clinical trials have not been reported so far, AZD-5991, AMG-176 and S63845 (tool compound of S64315/MIK655) have demonstrated potent single agent anti-tumoral effect *in vitro* and *in vivo* in diverse hematological malignancies, including MM[103–105].

1.5. CLUSTERED REGULARLY INTERSPACED SHORT PALINDROMIC REPEATS ASSOCIATED PROTEIN 9 (CRISPR/Cas9) SCREENS

1.5.1. CRISPR/Cas9 technology

CRISPR/Cas9 is a technology based on a prokaryotic adaptive immune system (Figure 8). This system consists first on the integration of short DNA fragments of foreign sequences, such as plasmids and viruses, into CRISPR loci of the host genome[106]. Consequently, prokaryotes become capable to transcript RNA sequences complementary to those invading plasmid or viral targets, known as CRISPR RNA (crRNAs), when they are reinfected[107]. Ir order to form a complex with and guide the endonuclease Cas9 to cleave the invasive nucleo acid, crRNAs previously hybridize with a trans-activating crRNA (tracrRNA)[108]. In addition, the frequently used *Streptococcus pyogenes* Cas9 needs to recognize a short 3 base pairs upstream sequence “NGG”, known as the protospacer adjacent motif (PAM), juxtaposed to the target sequence to induce the cleavage (Figure 9)[109].

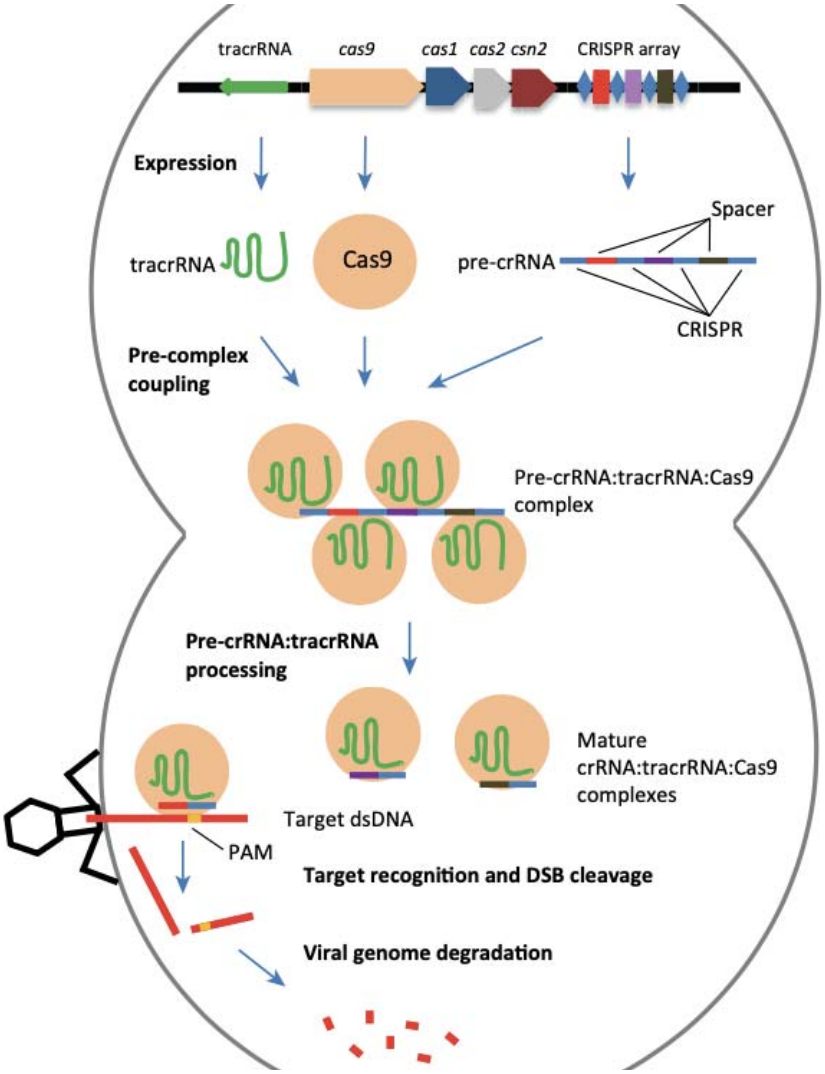

Figure 8. CRISPR/Cas9 system in prokaryotes[110].

This system is now extensively used to modify gene expression in a sequence-specific manner in eukaryotic cells in order to study gene function and to uncover biological mechanisms. The crRNA and tracrRNA can be artificially fused to synthetize a single guide RNA (sgRNA). When a sgRNA complementary to a DNA sequence located adjacent to a PAM is expressed together with the endonuclease Cas9 into an eukaryotic cell, the sgRNA is used to recognize that sequence, and the Cas9 performs a double-strand break (DSB) through its HNH nuclease domain, that cleaves the complementary strand, and its RuvC-like domain, which cleaves the noncomplementary strand (Figure 9).

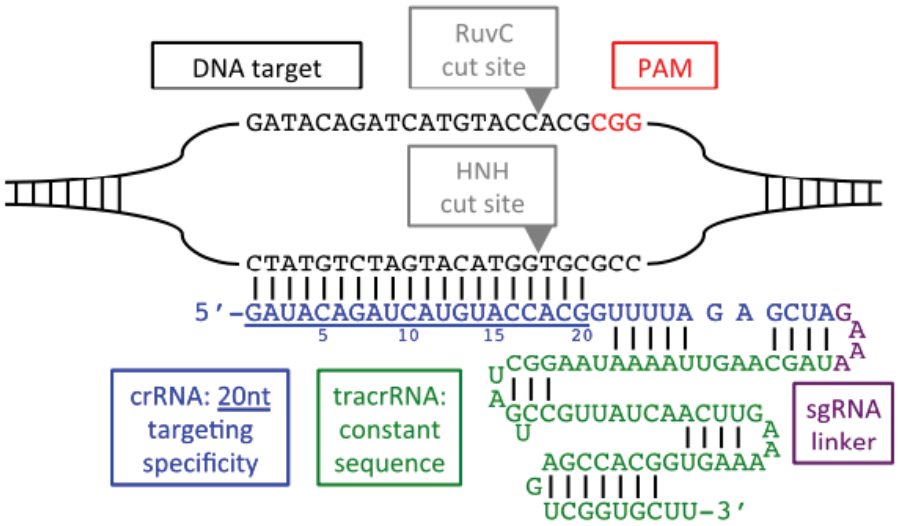

Figure 9. Schematic of interaction of sgRNA and DNA[111].

Following the DSB, the genome is generally repaired by the error-prone non-homologous end-joining (NHEJ) pathway or the high-fidelity homology-directed repair (HDR) pathway. The NHEJ pathway introduces small insertions and/or deletions that frequently result in a frame-shift mutation and the subsequent premature stop codon. As a consequence, if the DSB occurs in a protein-coding region, these indels will result into a non-functional protein. Cells predominantly use the NHEJ since HDR requires a template homologous to the regions flanking the break, which is only close enough during the cell cycle S phase. However, HDR can be used to introduce a specific alteration in the targeted genomic region, such as a point mutation or an insertion, by providing an exogeneous template[112].

Besides gene editing through the formation of DSBs, gene expression can be also regulated by engineering the Cas9 protein. The introduction of certain mutations in the HNH (H840A) and RuvC (D10A) domains results in a catalytically inactive dead Cas9 (dCas9). This mutant dCas9, despite being enzymatically inactive, retains its RNA-guided DNA binding ability. Thus, when fused to a transcription repressor or activator domain, it can be used to, respectively reduce or increase transcription using sgRNA targeting a location relative to the transcription start site. For instance, the transcription repressor domain Krüppel-associated box (KRAB), besides hampering transcription by constituting a steric interference for the RNA polymerase machinery, also induces heterochromatin formation blocking the initiation of transcription and elongation, thereby repressing gene expression. On the other hand, for example, the transcription activator effector VP64 (four

copies of the well-characterized *Herpes simplex* virus transcription activator protein VP16) has been demonstrated to augment gene expression when fused to dCas9. These dCas9-based transcriptional repression and activation systems are commonly known as CRISPR interference (CRISPRi) and CRISPR activation (CRISPRa), respectively (Figure 10)[113].

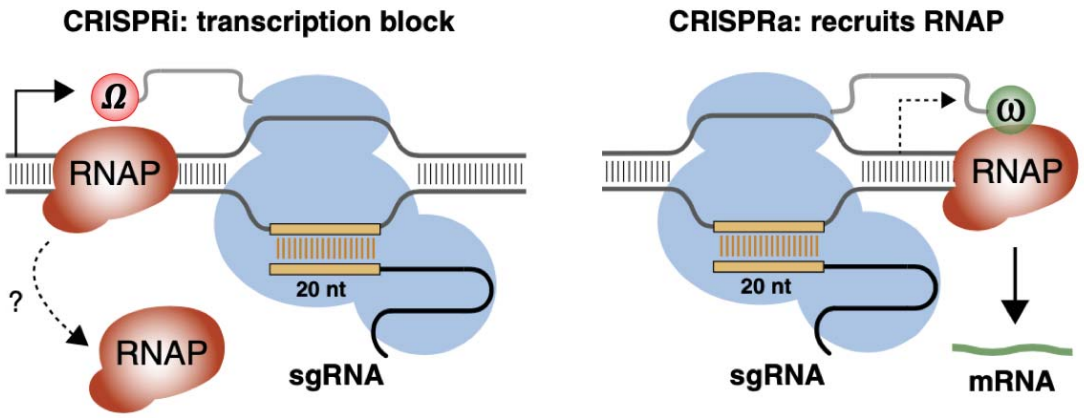

Figure 10. Molecular mechanisms underlying CRISPRi and CRISPRa. Stable binding of the dCas9: repressor domain(Ω)-sgRNA complex to DNA blocks the progression of RNA polymerase (RNAP), repressing transcription. However, the activator domain (ω) fused to dCas9 recruits RNAP via direct interactions, activating transcription (modified from[114]).

1.5.2. CRISPR/Cas9 screens as a tool for identifying genes conferring sensitivity/resistance to therapeutic agents

In the last years, the CRISPR/(d)Cas9 technology has been adapted for genome-wide screens, consisting on the simultaneous testing of thousands of individual perturbations, by the production of large pooled libraries containing multiple sgRNAs targeting all genes from the human genome, which allows the genetic characterization of a phenotype of interest (Figure 11).

Pooled sgRNAs libraries are introduced into lentiviral vectors through traditional cloning methods. Cells stably expressing (d)Cas9 can be generated either before or simultaneously to the sgRNA library transduction, which has to be performed in conditions that assure that each cell is infected by just one viral particle, thereby harboring a single alteration. Once both elements, the sgRNA library and (d)Cas9, are stably expressed in host cells and permanent genomic modifications are produced, a selective pressure is

introduced. Depending on the goal, to identify perturbations that cause cells to die or provide a survival advantage, cells depleted (negative selection) or enriched (positive selection) after selection will be analyzed (Figure 11). Negative selection is generally used to uncover vulnerabilities, genes essential to specific cell types, whereas positive selection is an approach for elucidating genes conferring resistance to targeted drugs[115].

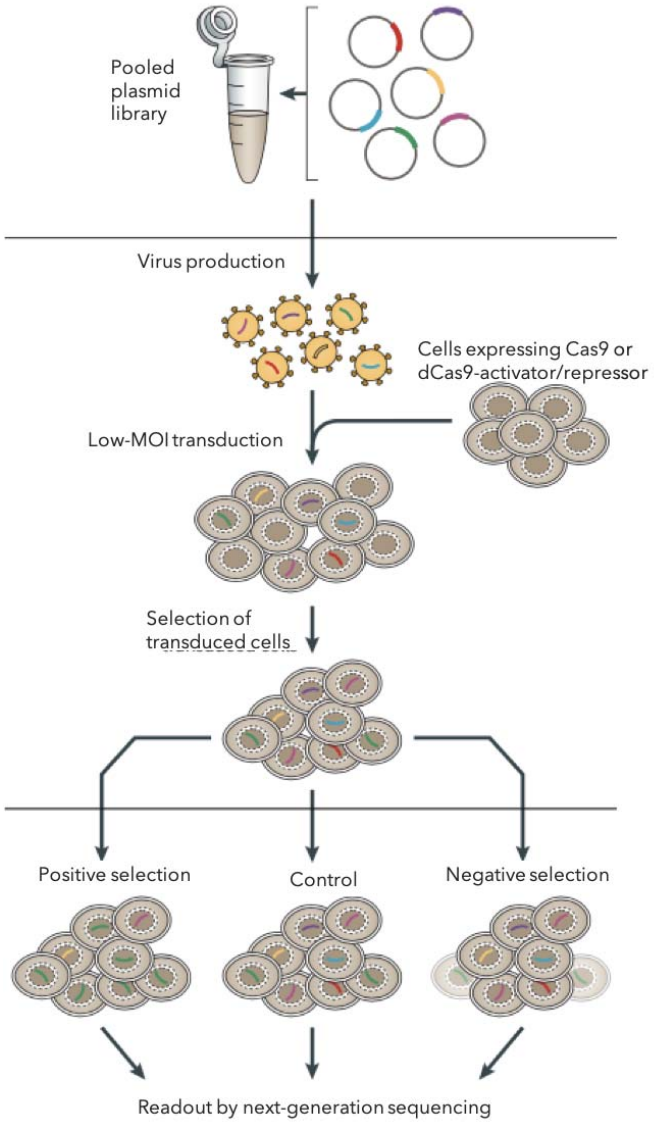

Figure 11. Screen strategies with pooled libraries (image modified from[115]).

In MM, CRISPR knockout screens have been already performed following a positive selection strategy to reveal key genes involved in the resistance to PIs and IMiDs. Regarding PIs, residual surviving RPMI-8226 cells were subjected to DNA sequencing 15

days after CRISPR library transduction, having been treated for the first week with bortezomib. As a result, proteasome 26S subunit ATPase 6 (*PSMC6*) knockout MM cells were identified to be partially resistant to bortezomib-induced apoptosis[116]. On the other hand, the whole-genome screen of CRISPR-Cas9 reported by Sievers *et al.* showed that CRBN is essential for the anti-myeloma effect of lenalidomide in the sensitive MM.1S cell line. Moreover, the knockout of other genes including an additional subunit of the $CRL4^{CRBN}$ ubiquitin ligase (DDB1), all 9 subunits of the constitutive photomorphogenesis 9 signalosome (CSN) and E2 ubiquitin-conjugating enzymes [ubiquitin conjugating enzyme E2 G1 (UBE2G1) and D3 (UBE2D3)] were also found to confer resistance to lenalidomide[117]. Similarly, the genome-scale CRISPR-Cas9 screen implemented in MM.1S cells treated with pomalidomide for 21 days revealed that the inactivation of several CSN subunits confers resistance to this IMiD. This mechanism of resistance was found to be based on the decrease of CRBN levels induced by some of the knockouts of CSN subunits, since this complex inhibits the SCF^{Fbxo7} E3 ligase, which induces CRBN degradation[118].

Regarding novel anti-myeloma agents currently under preclinical and/or clinical development, mAbs against the B cell maturation antigen (BCMA), a cell-surface protein specifically expressed by MM cells, are showing promising results. However, tumor cells are known to lose the targeted antigen as a mechanism of resistance to mAbs. In a recent study, CRISPRi and CRISPRa screens have been used as a tool for identifying genes upregulating BCMA expression on MM cells. For this purpose, after the transduction of the correspondent CRISPRi or CRISPRa library in the AMO1 cell line, cells expressing high expression of BCMA were sorted by flow cytometry using a fluorescent tagged antibody and subjected to next-generation sequencing. Thus, knockdown of all the subunits of the γ-secretase complex and various subunits of the Sec61 translocon complex were found to upregulate BCMA. Moreover, the overexpression of the mucin family and several genes involved in transcriptional regulation such as POU class 2 homeobox associating factor 1 (*POU2AF1*), CBFA2/RUNX1 partner transcriptional co-repressor 3 (*CBFA2T3*), mastermind like transcriptional coactivator 2 (*MAML2*) or RUNX family transcription factor 3 (*RUNX3*), also resulted into increased BCMA expression on the surface of MM cells. This study is important since it reveals potential combinations with drugs modulating the expression of the identified genes that could overcome the resistance developed by MM cells to anti-BCMA mAbs[119].

In addition, during the last year, several CRISPR screens have been done to uncover novel mechanisms of resistance to BH3-mimetics in tumor cells, although not in MM. Two independent CRISPR knockout screens have been published revealing genes involved in resistance to BCL-2 inhibition in acute myeloid leukemia (AML) using venetoclax. The one reported by Nechiporuk and colleagues, which was based on a positive selection, validated *TP53*, *BAX* and *PMAIP1* (NOXA) as genes involved in the mitochondrial apoptotic pathway whose inactivation confers resistance to venetoclax[120]. More broadly, the study performed by Chen *et al.* analyzed positively and negatively selected genes after 8 and 16 days of treatment with venetoclax, identifying genes that confer resistance or synergize with this agent. According with the previously described study, *TP53, BAX* and *PMAIP1* (NOXA) were among the positively selected genes in the screen. On the contrary, *MDM2*, encoding an E3 ubiquitin ligase that targets p53 for degradation, *MCL1* and other *genes* such as the caseinolytic mitochondrial matrix peptidase chaperone subunit B (*CLPB*) involved in mitochondrial structure and function, were depleted in the final long-term treated cell population[121]. Regarding BH3 mimetics targeting MCL-1, two whole-genome CRISPR screens have been implemented with S63845 and AZD-5991 in melanoma and ovarian tumor cell lines and in lung cancer cells, respectively. When screened with S63845, *BCL2L1* (BCL-X_L) knockout cells were strongly depleted after treatment revealing its role in resistance to this agent. Moreover, non-expressing *WSB2* cells, a relatively unknown gene that contains a domain proposed to recruit ubiquitination factors to bound proteins, were also negatively selected[122]. In lung cancer, a CRISPRi screen evaluating AZD-5991 confirmed BCL-X_L knockdown to re-sensitize tumor cells to MCL-1 inhibition. Moreover, knockdown of several members of a cullin-RING ligase complex (CRL) including cullin 5 (*CUL5)*, ubiquitin conjugating enzyme E2 F (*UBE2F)* and ring finger protein 7 (*RNF7)* also re-sensitized tumor cells to AZD-5991 treatment[123].

2. HYPOTHESIS AND OBJETIVES

HYPOTHESIS

Promising results have been obtained with the BCL-2 inhibitor venetoclax in MM patients harboring the translocation t(11;14). Moreover, it is well-known the essential role of MCL-1 for MM cell survival. The gene encoding for this anti-apoptotic protein is located in 1q, a region frequently amplified in MM cells and associated with bad prognosis. Considering these findings, we hypothesize that these anti-apoptotic proteins may constitute attractive novel targets for the treatment of, at least, certain subgroups of MM patients. Moreover, the evaluation of the preclinical efficacy and mechanisms of action of venetoclax and the MCL-1 inhibitor S63845, alone or in combination, could help in predicting their potential success in the clinic and their prospective incorporation into the anti-myeloma armamentarium.

However, it is a fact that MM patients always develop resistance mechanisms to anti-myeloma agents. In this regard, we postulate that the efficacy of venetoclax and S63845 may be modified by the presence of the stromal BM microenvironment. This effect could be due to changes on anti-apoptotic proteins expression, perhaps mediated by miRNAs deregulated on MM cells as a consequence of the interaction with BM-MSCs derived from MM patients. On the other hand, we also presume the existence of genetic features inherently present in the tumor cell involved in the resistance/sensitivity to venetoclax or S63845. In other hematological malignancies genome-wide CRISPR screens have been used to reveal these features. Here, we propose to perform CRISPRa screens with venetoclax and S63845 in MM. Overall, revealing more information regarding potential mechanisms of resistance, either mediated by the BM microenvironment or features intrinsic to MM cells, and how to overcome them using suitable combinations will allow MM patients to benefit more from these BH3-mimetics.

AIMS

- **Aim 1.** Evaluation of the efficacy and mechanism of action of single and dual inhibition of BCL-2 and MCL-1 with S63845 and venetoclax in MM.

  1.1. To determine the *in vitro* and *ex vivo* efficacy of venetoclax and S63845 in monotherapy on different MM cell lines and primary tumor cells isolated from MM patients, and its correlation with basal BCL-2 protein family levels and cytogenetic alterations.

1.2. To study the mechanism of action of venetoclax and S63845 as single agents in MM cell lines: analysis of apoptosis, cell cycle and BCL-2 family protein interactions.

*1.*3. To evaluate the *in vitro, ex vivo* and *in vivo* efficacy of the combination of venetoclax with S63845 on different MM cell lines, primary tumor cells isolated from MM patients and in an animal model of disseminated MM.

1.4. To investigate the mechanism of action of the combination of venetoclax with S63845 in MM cell lines: analysis of apoptosis, cell cycle and BCL-2 family proteins interactions.

- **Aim 2.** Evaluation of the stroma-induced resistance to S63845 and venetoclax mediated by miRNAs targeting MCL-1 and BCL-2 in MM.

  2.1. Evaluation of the *in vitro* efficacy of venetoclax and S63845 in the presence of MSCs derived from MM patients (pMSCs).

  2.2. Analysis of changes produced on MCL-1 and BCL-2 expression when MM cell lines are cultured in the presence of the stromal BM microenvironment (pMSCs).

  2.3. Description of miRNAs targeting MCL-1 and BCL-2 deregulated on MM cells when co-cultured with pMSCs.

  2.4. Study of modifications on the interactions between anti-apoptotic proteins and BIM induced by the presence of the stromal BM milieu in untreated or S63845 or venetoclax treated MM cells.

  *2.*5. Assesment of the ability of the S63845 + venetoclax combination to overcome the protective effect exerted by pMSCs.

- **Aim 3.** Identification of genes modulating the response to S63845 and venetoclax in MM by genome-wide CRISPR/Cas9 activation screens.

  3.1. Identification of candidate genes whose activation may sensitize or confer resistance to venetoclax or S63845 by whole-genome CRISPR activation screens.

3.2. Individual validation of the sensitivity or resistance conferred by selected candidate genes by performing S63845 or venetoclax dose-response analyses.

3. MATERIALS AND METHODS

Drugs

S63845 was provided by the Institut de Recherches Servier and Novartis Pharmaceuticals, Inc. Venetoclax was purchased from LC Laboratories and dexamethasone was obtained from Sigma-Aldrich. For experiments in chapter 3, S63845 and venetoclax were purchased from MedChemExpress (#HY-100741 and #HY-15531) and the MDR1 inhibitor HM30181 (MDR1i) was obtained from EMD Millipore (#533794).

Cell lines, primary samples and cultures

The human myeloma cell lines, MM.1S, MM.1R, U266 and NCI-H929 were purchased from ATCC; RPMI-8226, JJN3, KMS12-BM, HEK293 and OPM-2 were obtained from DSMZ; KMS11 from JCRB and LentiX-293T from Takara Bio. The human myeloma cell line MM144 was a generous gift from Dr. S. Rudikoff (National Cancer Institute, National Institutes of Health, Bethesda, MD, USA). The origin of MM1S-luc and RPMI-8226-luc cell lines (luciferase-expressing) has been explained previously[124]. MM.1S-dCas9-VP64 was obtained by transduction with the Lenti dCAS-VP64_Blast vector (Addgene #61425) [containing the blasticidin resistance gene expressed from a SV40 promoter; and the dCas9 (mutations D10A and N863A in SpCas9) gene fused to the transactivation domain VP64 expressed from a EF1a promoter]. Authentication and *in vitro* growth conditions of MM cell lines have already been described[124].

BM samples from MM patients were obtained following approval from the University Hospital of Salamanca Review board and after written informed consent from patients. Research with human samples was conducted in accordance to ethical standards and principles expressed in the Declaration of Helsinki. pMSCs were isolated and expanded as previously reported[124] and used to establish co-cultures with MM cell lines. Specifically, MM.1S-luc and pMSC co-cultures in 96-well plates were used to test drug cytotoxicities[124,125]. For Western blot and qRT-PCR analyses, 2 x 10^5 primary pMSCs were plated overnight in 60 cm^2 plates and 6 x 10^6 MM cell lines were then added and co-cultured for 48 hours. MM cells were recovered by carefully flushing for protein extraction or RNA expression analyses.

Interphase fluorescence in situ hybridization (iFISH) studies

MM cell lines were fixed in 3/1 methanol/acetic (v/v) and screened by iFISH for the presence of 1q chromosomal alterations with the CDKN2C/CKS1B FISH Probe Kit (CytoTest). A BX60 fluorescence microscope (Olympus) equipped with a X100 oil objective was used for the enumeration of hybridization spots per nuclei. A minimum of 100 interphase nuclei were analyzed. Only those spots with a similar size, intensity and shape were counted in areas with <1% unhybridized cells. 1q amplification was defined by gains of >1 fluorescence signals in >10% of the nuclei.

Cell viability, apoptosis, mitochondrial membrane potential (ΔΨm) and cell cycle assays

Viability of MM cells was evaluated by 3-(4,5-dimethylthiazol-2-yl)-2,5-diphenyltetrazolium bromide (MTT) assay[126]. MM1S-luc cells alone or in co-culture with pMSCs were treated with S63845, venetoclax or their combination for 48 hours. After addition of luciferin, bioluminescence of MM1S-luc cells was considered a surrogate of cell viability. The half-maximal inhibitory concentration (IC_{50}) for each drug was calculated using SigmaPlot graphing software. MM.1S-dCas9-VP64 cell line was plated in quadruplicate into 384-well plates at a density of 1 x 10^3 cells in 50 µL per well in presence of increasing doses of S63845 or venetoclax and vehicle for 48 hours. Cell viability was measured using CellTiter Glo (Promega #G7572). Apoptosis after treatments with S63845, venetoclax or their combination was measured by flow cytometry using an Annexin V/7AAD staining kit (Immunostep). The cell cycle profile and apoptosis induction were evaluated as described elsewhere[127]. Loss of mitochondrial membrane potential was assessed by flow cytometry after 3,3'-dihexyloxacarbocyanine Iodide ($DiOC_6$) staining, as previously explained[128].

***Ex vivo* analysis of apoptosis in freshly isolated patient cells**

BM samples from patients with MM were lysed and cultured as previously described[127] in cell culture medium containing plasma from the same patients for 24 hours. The percentage of annexin-V positive cells was analyzed by flow cytometry of myeloma plasma cells ($CD38^+$, $CD45^-$, $SSC^{low/intermediate}$, $CD56^{-/+}$) and normal lymphocytes ($CD45^+$, SSC^{low}).

Evaluation of potential synergisms

MM.1S, JJN3, RPMI-8226, KMS12-BM and NCI-H929 cell lines were treated with the combination of S63845 + venetoclax or S63845 + venetoclax + dexamethasone at different doses and apoptosis or viability were respectively analyzed by flow cytometry or MTT assay. The synergism of the combinations was analyzed using the Calcusyn program (Biosoft). The analysis is based on the Chou-Talalay method[129], which calculates a combination index (CI) whose values are interpreted as: CI > 1 antagonistic effect; CI = 1 additive effect; CI < 1 synergistic effect.

Immunoblotting

Cells were collected, washed with phosphate buffered saline (PBS) and lysed in ice-cold lysis buffer [140 mM NaCl, 50 mM EDTA (ethylenediaminetetraacetic acid), 10% glycerol, 1% NP-40, 20 mM Tris HCl [tris(hydroxymethyl)aminomethane] pH 7] with protease (sc-29130) and phosphatase (sc-45045) inhibitors from Santa Cruz Biotechnology. Protein extracts were boiled in 4X electrophoresis sample buffer and resolved in 10% SDS-PAGE gels. After electrophoresis, proteins were transferred to Immobilon transfer membranes (Merck Millipore), which were subsequently blocked for 1 hour with 1% BSA TBST solution. Membranes were incubated overnight with a primary antibody. After washing three times with TBST, membranes were incubated with a horseradish peroxidase (HRP)-conjugated appropriate secondary antibody. Bands were visualized by a luminol-based detection system using Clarity Western Peroxide and Luminol/Enhancer Reagents (Bio-Rad). All antibodies were purchased from Cell Signaling Technology except for anti-α-tubulin (Calbiochem), HRP-conjugated secondary antibodies (GE Healthcare), anti-CCND1 (Life Technologies), anti-IRF4 (EMD Millipore) and the anti-BCL-X_L used in experiments from chapter 3 (Santa Cruz Biotechnology). Protein expression levels were determined by densitometry analysis of immunoblot bands (using ImageJ software) and normalized with respect to α-tubulin.

Immunoprecipitation (IP)

MM cells were harvested in lysis buffer with protease and phosphatase inhibitors (Santa Cruz Biotechnology). Protein levels were quantified by Bradford assay, and equal concentrations of cleared lysates were subjected to immunoprecipitation with an anti-BIM

(Cell Signaling Technology), an anti-BCL-2 (Cell Signaling Technology) or an anti-MCL-1 antibody (BD Biosciences). Immunocomplexes were captured through overnight incubation at 4ºC with protein-A or GammaBind sepharose beads (Sigma-Aldrich) for rabbit and mouse antibodies, respectively. Beads were washed, boiled in SDS sample buffer and immunoprecipitates were analyzed by immunoblotting.

Animal models

Animal experiments were conducted according to institutional guidelines for the use of laboratory animals and after granted permission from the University of Salamanca Animal Ethical Committee to carry out animal experimentation. RPMI-8226-luc cells (8 x 10^6) were intravenously injected into the tail of 6-week-old female BALB/c Rag2-/- IL-2Rγc-/- (BRG) mice. Tumor development was monitored by non-invasive bioluminescence imaging (BLI), as previously described[124]. In the first experiment, animals were randomized into four groups (n=4 per group). The control group received S63845 and venetoclax vehicles with the same schema as the respective drugs. The other groups received S63845 (12.5 mg/kg weekly), venetoclax (100 mg/kg, 5 times/week, Monday-Friday), and the respective combination of S63845 + venetoclax. In a second experiment, animals were randomized into two groups (n=3 per group). The control group received S63845, venetoclax and dexamethasone vehicles, whereas the other group received the triple combination of S63845 + venetoclax + dexamethasone. S63845 and venetoclax were administered at the same doses and with the same schema as the first experiment, whereas dexamethasone was administered at 1 mg/kg twice weekly on Monday and Tuesday. To *ex vivo* explore the mechanism of action of the treatments, CB17-SCID mice (The Jackson Laboratory, Bar Harbor, ME) were subcutaneously inoculated into the right flank with 8 x 10^6 RPMI-8226 cells in 100 μL RPMI 1640 medium and 100 μL of Matrigel (BD Biosciences). When plasmacytomas reached a large volume (2 cm diameter), animals were divided into 4 groups (n=2 per group) to receive a single dose of vehicle, S63845 at 12.5 mg/kg, venetoclax at 100 mg/kg, or the respective combination of S63845 + venetoclax. Animals were sacrificed 24 hours after treatment and tumors were excised. Immunoprecipitation with an anti-BIM antibody was performed in proteins extracted from these tumors and subsequently MCL-1 and BCL-2 bound to BIM were analyzed by immunoblotting. S63845 was solubilized in 2% vitamin E D-α-tocopheryl polyethylene glycol 1000 succinate (TPGS) and administered by intravenous injection. Venetoclax was prepared in 60% phosal 50PG, 30% polyethylene glycol (PEG) 400, 10% ethanol, and administered by oral

gavage. Dexamethasone was dissolved in PBS and administered by intraperitoneal injection.

Quantitative real-time PCR (qRT-PCR)

Total RNA was isolated using the Direct-zol and RNA Miniprep kit (Zymo Research), according to manufacturer's instructions. Purity and concentration of isolated RNA was determined by Agilent 2100 Bioanalyzer (Agilent Technologies). miRNA expression was determined by qRT-PCR [TaqMan Advanced miRNA Assays for hsa-miR-193b-3p (478314_mir), hsa-miR-21-5p (477975_mir) and hsa-miR-423-5p (478090_mir; used for normalization) (Applied Biosystems)] following manufacturer's protocol**.** Data were calculated using the $2^{-\Delta Ct}$ method.

Transfections

Cell lines were transfected using the Nucleofector II System (Lonza) with G-16 (MM.1S) and A-23 (HEK293) programs. Cells were transfected with miRIDIAN microRNA Mimics or Negative Non-Targeting Control#1 (Dharmacon); miRCURY LNA Power Inhibitors or Negative Control A (Exiqon); and pmirGLO dual luciferase reporter vector. Cells were harvested 48 hours after transfection for protein extraction or to test the efficacy of S63845 and venetoclax.

Luciferase reporter assay

Double-stranded DNA oligonucleotides containing the wild-type (WT) or mutant (MUT) miR-193b-3p and miR-21-5p binding sites in the 3′-UTR of *MCL1* and *BCL2* mRNAs were ligated between the PmeI and XbaI restriction sites of the pmirGLO dual-luciferase reporter vector (Promega). For luciferase assays, HEK293 cells were co-transfected with 500 ng of plasmid constructs and 50 nM of corresponding miRNA or negative control (NC) mimics. Cells were collected 24 hours after transfection and firefly and *renilla* luciferase activities were measured using the Dual-Luciferase Reporter Assay (Promega) following manufacturer's protocol.

Whole-genome CRISPR activation screens

Library amplification. The human Calabrese sgRNA library (Addgene #1000000111) provided as two pooled half-libraries (A and B; each one containing generally 3 sgRNAs per gene and ~56,500 total sgRNAs), was transformed into STBL4 electrocompetent cells (Thermo Fisher Scientific #11635018) conducting four electroporations using 400 ng of Calabrese A or B sub-libraries. Electroporated cells were grown at 37 ºC for 16 hours and plasmid DNA was isolated using the Plasmid Plus Maxi Kit (Qiagen # 12963). Finally, the plasmid DNA was sequenced to assure that all the sgRNAs were equally represented.

Lentivirus production. To produce lentivirus, 17.5×10^6 LentiX-293T were cultured in four T-175 flasks in antibiotic-free DMEM 10% FBS for each sub-library. For each flask, 20 µg Calabrese A or B sub-library plasmids, 20 µg psPAX2 (Addgene #12260) and 10 µg pMD2.G (Addgene #12259) diluted in 3 mL Opti-MEM were combined with 100 µL Lipofectamine 2000 (Thermo Fisher #11668019) diluted in 3 mL Opti-MEM. The mixture was incubated at room temperature for 30 minutes and then added to MM-dCas9-VP64 cells. 16 h after transfection, media was replaced by fresh antibiotic-free DMEM 10% FBS. Virus supernatant was harvested 24 h post-transfection and filtered with a 0.45 µm filter. Lentivirus quality was determined using the Lenti-X GoStix Plus kit (Takara #631280).

Determination of lentiviral titer. MM.1S-dCas9-VP64 cells were transduced in 24-well plates with a range of virus supernatant volumes (0, 100, 200, 300, 400 y 500 µL) in medium with 8 µg/mL polybrene. Plates were centrifuged at 1500 xg for 2 hours and then transferred to a 37ºC incubator. Sixteen hours after infection, media was replaced by fresh RPMI 10% FBS 0.5% penicillin/streptomycin to remove polybrene. 48h post-transduction, infected cells from each condition were treated with puromycin 2 µg/mL. After seven days, cells were counted for viability. A viral dose resulting in 30% transduction efficiency, corresponding to a multiplicity of infection (MOI) of approximately 0.3, was used for subsequent library screen to ensure that most cells were transduced with an unique sgRNA.

Screens. A total of 2×10^8 MM.1S-Cas9-VP64 cells were infected with the Calabrese sub-libraries A or B to achieve a representation of at least 500 cells per sgRNA, taking into account a 30% transduction efficiency. 48h after transduction, infected cells were treated with puromycin 2 µg/mL for seven days. Selected cells containing sgRNAs

from sub-libraries A or B were split into three biological replicates. Cells were then expanded and 4 weeks post-transduction cells were treated with S63845 + MDR1i, MRD1i, venetoclax or DMSO for 28 days. Doses and duration for each treatment are defined in Figure 3.2.

Genomic DNA isolation and sequencing. Genomic DNA was isolated from 3×10^7 cells using the Blood & Cell Culture DNA Maxi kit (Qiagen #13362). DNA concentration was quantified using a NanoDrop 1000 spectrophotometer (NanoDrop Tech,. Wilmington, DE). PCR was performed in two steps. For the first PCR, thirteen 100 µL reactions with 10 µg DNA from cells using the Phusion® High-Fidelity PCR Master Mix (Biolabs # M0531L) were performed. Primer sequences used to amplify sgRNAs in PCR 1 were

F1: AATGGACTATCATATGCTTACCGTAACTTGAAAGTATTTCG
R1: CTTTAGTTTGTATGTCTGTTGCTATTATGTCTACTATTCTTTCC

PCR 1 cycling conditions were an initial 2.5 minutes at 98 °C; followed by 45 seconds at 98 °C, 50 seconds at 62.5 °C, 60 seconds at 72 °C, for 18 cycles; and a final 5 minutes extension at 72 °C.

A second PCR was performed to attach Illumina adaptors to barcode samples. For the second PCR seven 100 µL reactions using 5 µL of the product from the PCR 1 were performed. Primers for the second PCR included either a 1-9bp variable length sequence to increase library complexity or an 8bp barcode for multiplexing of different biological samples

F2: AATGATACGGCGACCACCGAGATCTACACTCTTTCCCTACACGACGCTC
TTCCGATCT (variable.length.sequence)TCTTGTGGAAAGGACGAAACACCG
R2: CAAGCAGAAGACGGCATACGAGAT(barcode)GTGACTGGAGTTCAGACG
TGTGCTCTTCCGATCTTCTACTATTCTTTCCCCTGCACT

PCR 2 cycling conditions were an initial 2 minutes at 98 °C; followed by 40 seconds at 98 °C, 35 seconds at 62.5 °C, 40 seconds at 72 °C, for 6 cycles; 40 seconds at 98 °C, 60 seconds at 72 °C, for 18 cycles and a final 5 minutes extension at 72 °C.

Resulting amplicons from the PCR 2 were mixed, gel extracted with the QIAquick Gel Extraction Kit (Qiagen #28706), quantified using a NanoDrop 1000 spectrophotometer and sequenced using a NextSeq (Illumina).

Analysis of next generation sequencing data for detection of sgRNAs from CRISPRa screens. For each sample, staggered primer adapters and 5' adapters were removed from the raw reads using cutadapt (v.1.9.1, Marcel Martin, http//journal.embnet.org/index.php/embnetjournal/article/view/200). The trimmed reads (20mers) were aligned to the sgRNA library using bowtie2 (using the parameter settings --norc --local -D 20 -R 3 -N 0 -L 10 -i S,1,0.5 -p 6 for a highly sensitive alignment search). Reads were filtered allowing for alignments with a maximum of 1 base mismatch and the abundance of each sgRNA was calculated. The three biological replicates of the Calabrese A and B sub-libraries corresponding to the same experimental conditions were merged by summing up read counts for each sgRNA. A one-sided test for enrichment and depletion of sgRNAs and sgRNA rank aggregation for each gene was performed using the Mageck-RRA algorithm with default parameter settings[130]. The number of reads for each sgRNA for a given sample were normalized as follows read per sgRNA/total read count per sample x 10^6. Reads per million was then log2-transformed by first adding 1 to all values, which is necessary in order to take the log of sgRNAs with zero reads. The non-targeting sgRNAs was used as control distribution for the rank aggregation procedure based on the RRA algorithm.

Activation of the expression of individual genes

For constitutive overexpression of specific genes, sgRNAs targeting their respective promoter sequences (Table 1) were individually cloned into the Calabrese backbone pXPR_502 vector (Addgene #96923) using the Lenti-X CRISPR/CAS9 System (Takara #632629). Briefly, a sense oligo (oligo 1) containing the sequence of the sgRNA of interest plus the 5´ overhang sequence, cacc, was annealed with the antisense oligo (oligo 2), complementary to the oligo 1, plus the 5´ overhang sequence, aaac, by heating at 95ºC and slowly reducing the temperature using a thermal cycler. The annealed oligo was subsequently ligated to the vector, previously linearized using the BsmBI restriction enzyme. The vector was then transformed into Stellar Competent cells (Takara #636766) following the manufacturer´s instructions. Plasmid DNA from bacteria coming from individual colonies was isolated using the QIAprep Spin Miniprep Kit (Qiagen #27106).

Lentiviral particles were packaged in LentiX-293T cells using Lipofectamine 2000 (Life Technologies) and MM.1S-dCas9-VP64 cells were infected for 16 hours with lentiviral particles and polybrene (8 µg/mL). Infected cells were selected with puromycin (2 µg/mL). Olfactory receptor (OR) genes, whose overexpression do not change MM cell phenotype, were used as controls.

Table 1. Individual sgRNAs used for individual validation.

sgRNA	sequence
BCL2_1	AGAGAATGAAGTAAGAGGAC
BCL2_2	GTTACGCACAGGAAACCGGT
BCL2_3	TTACGCACAGGAAACCGGTC
BCL2A1_1	GACATGATGATACATGGAGGC
BCL2A1_2	GTACGCACGAAAGTGACTAGG
BCL2A1_3	GTGATGATACATGGAGGCTGG
BCL2L1_1	AATCCATACCAGCCACCTCC
BCL2L1_2	AGCCAGGAGTACTCTCCCGG
BCL2L1_3	TACTCCTGGCTCCCAGTAGG
CCND1_1	GAGCCCGGCAGAGAATGGGAG
CCND1_2	GCCCGGCAGAGAATGGGAGC
CCND1_3	GTCCCGCTCCCATTCTCTGCC
IRF1_1	GTTGTAGAGCTAGCGGCGAA
IRF1_2	GCCTGATTTCCCCGAAATGA
IRF1_3	GTTGTAGAGCTAGCGGCGAAG
IRF4_1	GGGGGCCGGGGGTTGGACTG
IRF4_2	GTCCAACCCCCGGCCCCCAC
IRF4_3	ACTTTGCAAGCCGAGAGCCG

sgRNA	sequence
IKZF1_1	CTTTCGCGCTCCCGGCCGAC
IKZF1_2	GCCTGGTCTGAGCCGGCTGG
IKZF1_3	CGCGAAAGCCTGGTCTGAGC
IKZF3_1	GCCGCTGTAACCCCGCGCAC
IKZF3_2	GCGGAACCCGCGGCACTCCG
IKZF3_3	GCCGGTGCGCGGGGTTACAG
MCL1_1	AAAAAGTATTCCCATAAAAG
MCL1_2	AAGGGGCGGCAGCTTCCGGA
MCL1_3	CCCATAAAAGGGGAAAGGGG
OR10G3	GAAAGAGATTGTAAAAACTA
OR12D2	GAATGTCTGTCACTCCCAAG
OR6S1	GACCTGCAATTGGATAAACT
PMAIP1_1	CCATAACGCCGTCTGCGGGG
PMAIP1_2	CTCCCATAACGCCGTCTGCG
PMAIP1_3	GGCGTTATGGGAGCGGACGC

4. RESULTS

CHAPTER 1: PRECLINICAL EVALUATION OF SINGLE AND DUAL INHIBITION OF MCL-1 AND BCL-2 WITH S63845 AND VENETOCLAX IN MULTIPLE MYELOMA

S63845 and venetoclax display anti-myeloma activity *in vitro* , especially in cell lines with low levels of expression of non-targeted anti-apoptotic proteins, and *ex vivo* in freshly isolated PCs from MM patients

A panel of nine representative MM cell lines with different cytogenetic alterations was treated with increasing concentrations of S63845 or venetoclax for 24 and 48 hours (Figure 1.1). Both agents reduced MTT uptake in a dose-dependent and time-independent manner. IC_{50} values for S63845 at 48 hours ranged from 2.6 nM to 465.7 nM, while for venetoclax the IC_{50} was approximately 100 times higher, ranging from less than 1 μM to 20.1 μM.

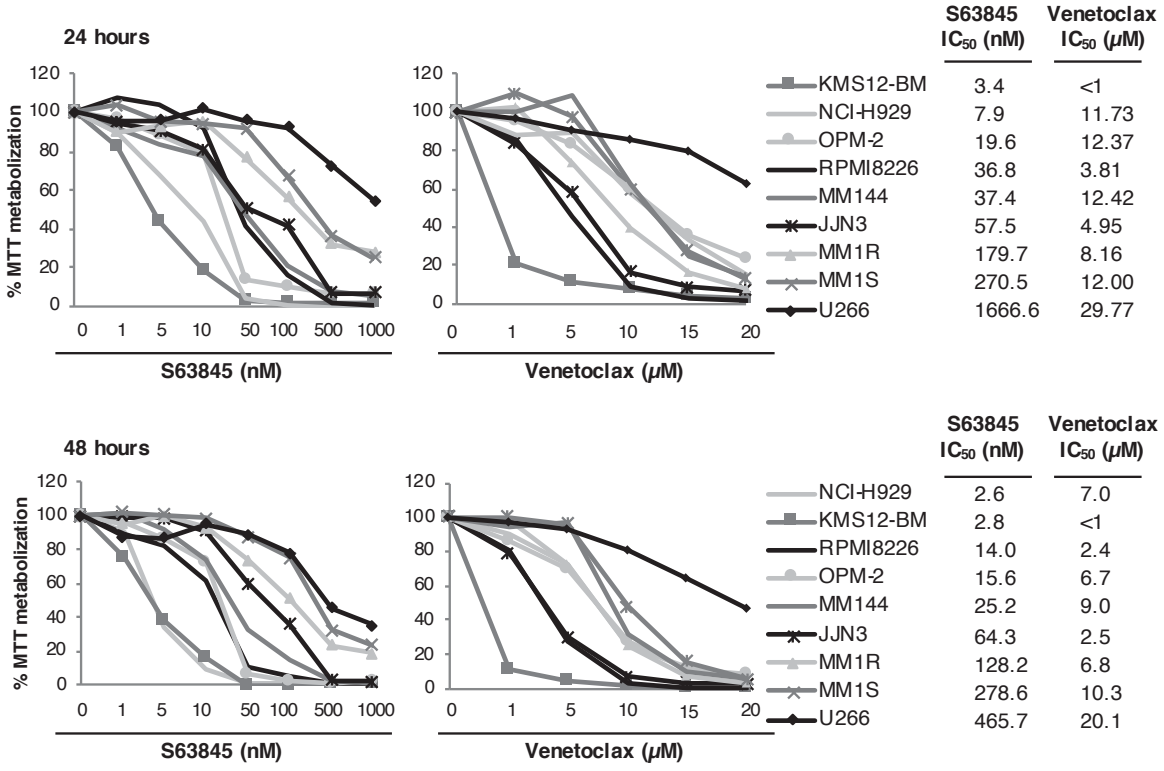

Figure 1.1. S63845 and venetoclax kill MM cell lines in monotherapy. The indicated MM cell lines were incubated with increasing concentrations of S63845 or venetoclax for 24 and 48 hours. Average absorbance is shown relative to the percentage of the control. Data presented are means (n=3) ± SD.

No association was found between any cytogenetic alteration, including p53 mutations, IgH translocations or 1q gains, and sensitivity to S63845 or venetoclax at 48 hours (Tables 1.1 and 1.2). The only remarkable feature was that KMS12-BM, a cell line that harbors the t(11;14) translocation, was distinctly more sensitive to venetoclax, however, the most resistant cell line to this agent, U266, also has this abnormality.

Table 1.1. Sensitivity of MM cell lines to S63845 and their cytogenetic alterations.

MM cell line	S63845 IC_{50} (nM)	TP53 cDNA	IgH translocations	1q gains
NCI-H929	2.6	wild-type	t(4;14)	+
KMS12-BM	2.8	mutated	t(11;14)	+
RPMI8226	14.0	mutated	t (14;16)	+
OPM2	15.6	mutated	t(4;14)	+
MM144	25.2	wild-type	none	+
JJN3	64.3	Not expression	t (14;16)	+
MM.1R	128.2	wild-type	t (14;16)	+
MM.1S	278.6	wild-type	t (14;16)	+
U266	465.7	mutated	t(11;14)	+

Table 1.2. Sensitivity of MM cell lines to venetoclax and their cytogenetic alterations.

MM cell line	Venetoclax IC_{50} (μM)	TP53 cDNA	IgH translocations	1q gains
KMS12-BM	< 1	mutated	t(11;14)	+
RPMI8226	2.4	mutated	t (14;16)	+
JJN3	2.5	Not expression	t (14;16)	+
OPM2	6.7	mutated	t(4;14)	+
MM.1R	6.8	wild-type	t (14;16)	+
NCI-H929	7.0	wild-type	t(4;14)	+
MM144	9.0	wild-type	none	+
MM.1S	10.3	wild-type	t (14;16)	+
U266	20.1	mutated	t(11;14)	+

Subsequently, in order to find predictive markers of response to S63845 or venetoclax, the basal expression of several BCL-2 family proteins was measured in the same nine MM cell lines (Figure 1.2) and the correlation with the sensitivity to both drugs was estimated. S63845 IC_{50} values at 48 hours were not significantly correlated with the expression of any of the BCL-2 family members (data not shown). Intriguingly, although there was no a significant correlation between S63845 sensitivity and the levels of its target

MCL-1, MM cell lines with higher levels of the alternate anti-apoptotic proteins (BCL-X_L or BCL-2) were less sensitive to S63845, with the exception of the KMS12-BM cell line. A similar pattern was observed for venetoclax, as those cell lines with higher levels of BCL-X_L or MCL-1 were, in general, more resistant to this BCL-2 inhibitor. Moreover, cell lines with high levels of BCL-2 were particularly sensitive to venetoclax.

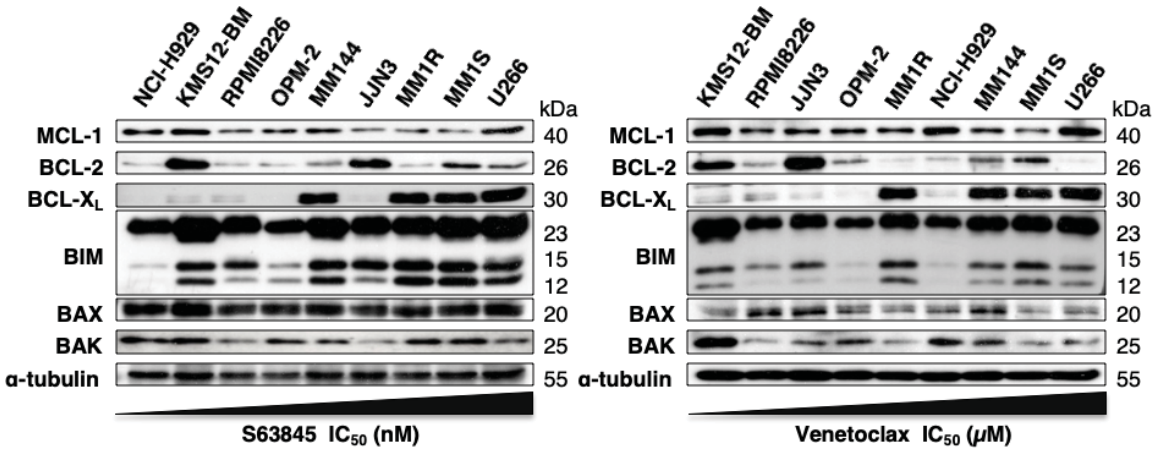

Figure 1.2. Basal expression of some members of the BCL-2 family of proteins. Basal protein levels of six members of the BCL-2 family (MCL-1, BCL-2, BCL-X_L, BIM, BAX and BAK) were analyzed by Western blot in 9 MM cell lines.

The anti-tumoral effect of S63845 and venetoclax was further investigated *ex vivo* in cells isolated from eight MM patients (Figure 1.3). Patients 1 and 2 harbored the t(11;14) translocation, patients 3 to 7 had 1q gain and patient 8 did not bear any of those cytogenetic alterations. S63845 in monotherapy was active in almost all patients, although those patients with 1q amplification (where the locus of the *MCL1* gene is) were significantly more sensitive to this agent (Student's t-test, $p < 0.05$) (Figure 1.4). On the other hand, only patient 2 bearing the t(11;14) translocation was clearly sensitive to venetoclax as single agent. The toxicity on normal lymphocytes was significantly lower to that on tumor cells, suggesting a therapeutic window for both drugs.

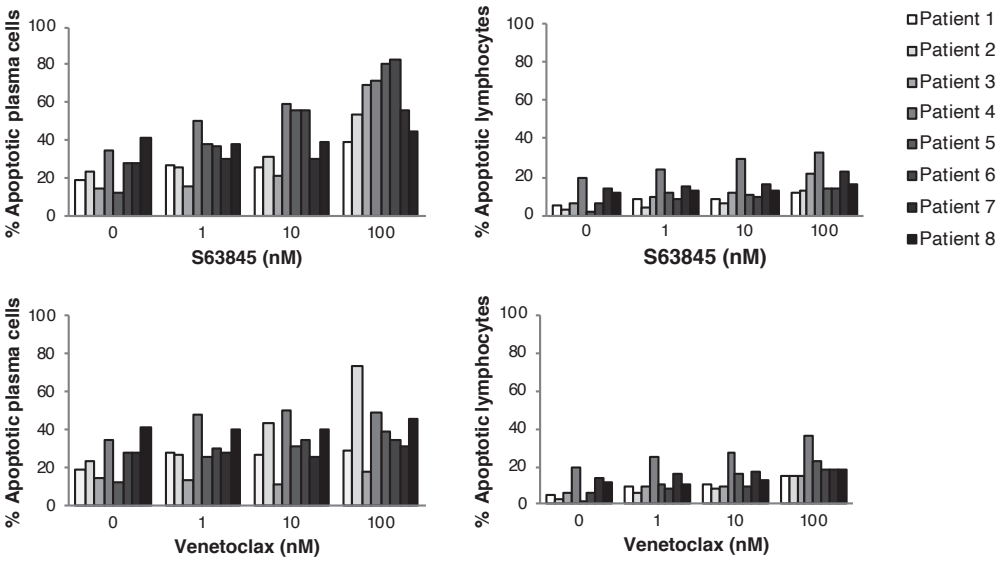

Figure 1.3. S63845 and venetoclax in monotherapy show *ex vivo* anti-myeloma activity with a nice therapeutic window. BM mononuclear cells obtained from eight patients with MM were treated *ex vivo* with increasing doses of S63845 and venetoclax for 24 hours. Apoptosis induction was analyzed in MM cells and normal lymphocytes by flow cytometry.

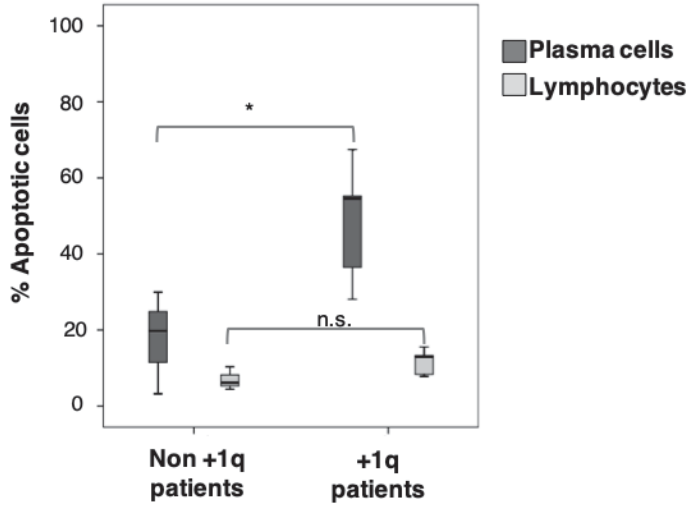

Figure 1.4. S63845 show higher *ex vivo* anti-myeloma activity in monotherapy in MM cells with 1q amplification. Percentage of apoptosis 24 hours after treatment with S63845 100nM was significantly higher (Student's t-test, $p < 0.05$) in plasma cells, but not in lymphocytes, from patients with +1q alterations (n=5) than in the rest of patients (n=3).

S63845 and venetoclax induce apoptosis through a mitochondrial-dependent mechanism

Since S63845 and venetoclax target proteins involved in the intrinsic apoptotic machinery, the activation of this pathway was explored in cell lines with different sensitivity profiles to S63845 and venetoclax (MM.1S, KMS12-BM, JJN3 and NCI-H929). Treating these four cell lines with increasing concentrations of S63845 or venetoclax for 48 hours increased the percentage of annexin V/ propidium iodide-positive cells in a directly dose-response-dependent manner (Figure 1.5). These data confirmed the results obtained from the MTT assay. Moreover, although no time-dependent cytotoxic effect had previously been observed after 24 hours of treatment by MTT, shorter exposures to S63845 or venetoclax in the MM1.S cell line using this flow cytometry technique, revealed a time-dependent increase in the frequency of apoptotic cells (Figure 1.6).

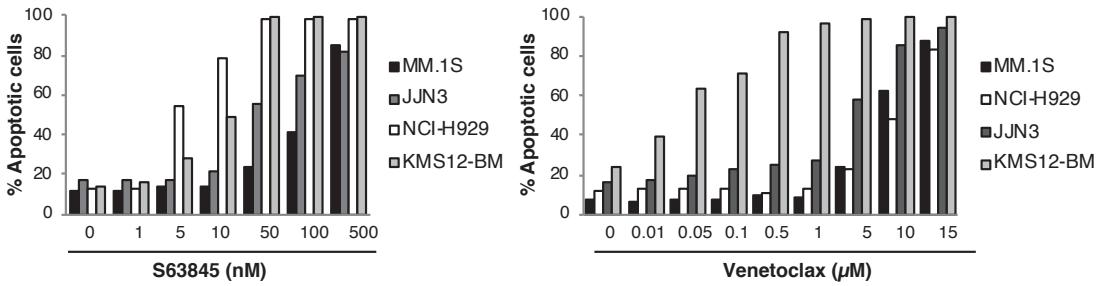

Figure 1.5. Dose-response curves of apoptosis induced by S63845 and venetoclax in MM cells. MM.1S, JJN3, NCI-H929 and KMS12-BM cell lines were treated with increasing concentrations of S63845 or venetoclax for 48 hours, and apoptosis induction was analyzed by flow cytometry after annexin-V and propidium iodide staining. Results are presented as the percentage of apoptotic cells for each condition.

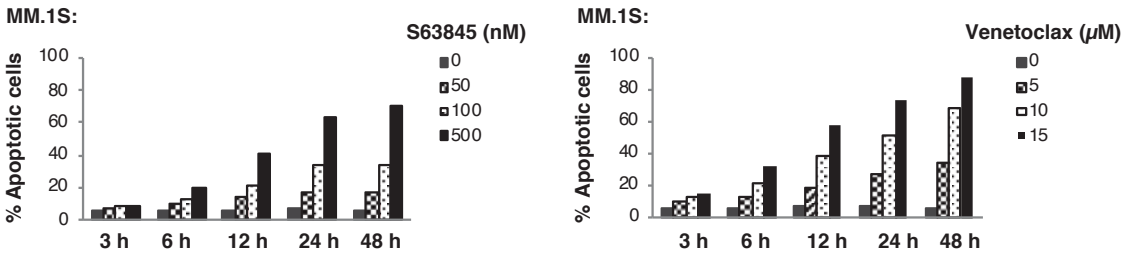

Figure 1.6. Time-response curves of apoptosis induced by S63845 and venetoclax in MM cells. MM.1S cells were treated with the indicated doses of S63845 or venetoclax for 3, 6, 12, 24 and 48 hours, and the induction of apoptosis was analyzed by flow cytometry.

The involvement of the mitochondrial apoptosis pathway was also validated by assessing the loss of mitochondrial membrane potential by flow cytometry after $DiOC_6$ staining in KMS12-BM and MM1S cells, a very sensitive and resistant cell line respectively (Figure 1.7). Treatment with S63845 and venetoclax induced loss of $DiOC_6$ staining in both the most sensitive and the most resistant cell lines. Overall, these data are indicative of the induction of mitochondrial membrane depolarization by these agents and subsequent induction of apoptosis *via* the intrinsic pathway.

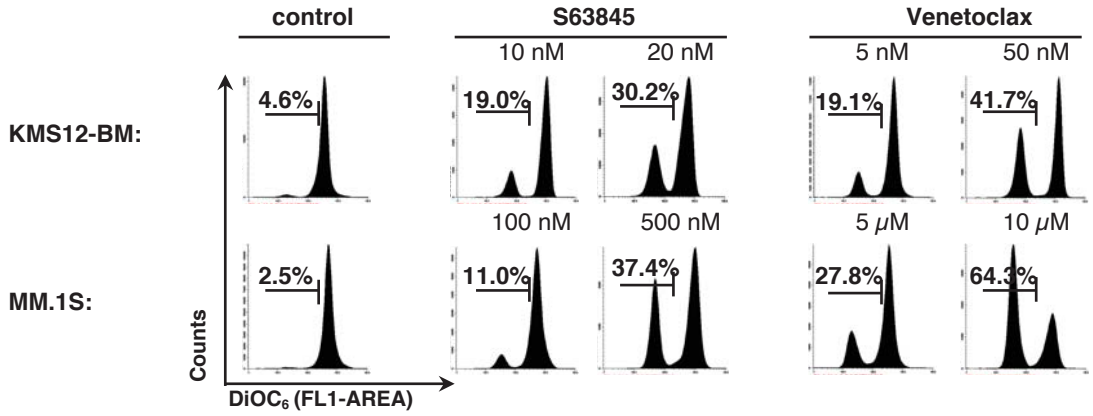

Figure 1.7. S63845 and venetoclax induce apoptosis in MM cells through the mitochondrial intrinsic pathway. Representative examples of loss of mitochondrial membrane potential evaluated by $DiOC_6$ staining after incubation with S63845 and venetoclax for 48 hours in KMS12-BM and MM.1S cell lines. Data shown correspond to representative experiments that were performed at least twice.

A possible effect of S63845 and venetoclax on the cell cycle was also investigated in the same two cell lines (Figure 1.8). The most significant change was an increase in the $subG_0$ phase in KMS12-BM cells, which was indicative of apoptosis. When only analyzing alive cells, S63845 did not substantially modify the cell cycle. By contrast, venetoclax at high doses increased the percentage of cells in the G_0-G_1 phase and decreased that of proliferating cells (S and G_2-M phases) in both cell lines.

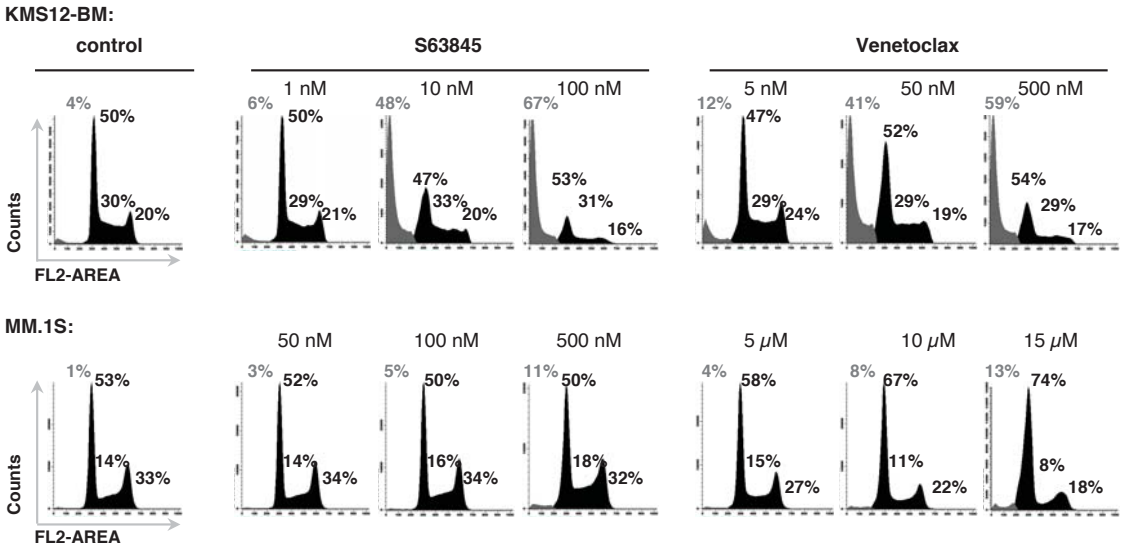

Figure 1.8. Effect of S63845 and venetoclax on the cell cycle in MM cells. KMS12-BM and MM.1S cells were incubated with increasing concentrations of S63845 or venetoclax for 48 hours and the cell-cycle profile was examined by flow cytometry, as shown by representative histograms. The experiment was conducted at least twice. Percentages in the figure are those of cells in subG_0 (apoptotic cells), and in G_0-G_1, S and G_2-M in the non-subG_0 population.

S63845 and venetoclax respectively disrupt MCL-1/BIM and BCL-2/BIM complexes, and shift MM cell dependence to the alternative anti-apoptotic protein

To gain further insight into the mechanisms of apoptosis triggered by S63845 and venetoclax, the expression of their targets along with other important members of the BCL-2 family was first analyzed in MM.1S and KMS12-BM cells after 48 hours of exposure to the drugs. Only modest changes, and no clear reduction of MCL-1 or BCL-2 levels, were observed (Figure 1.9).

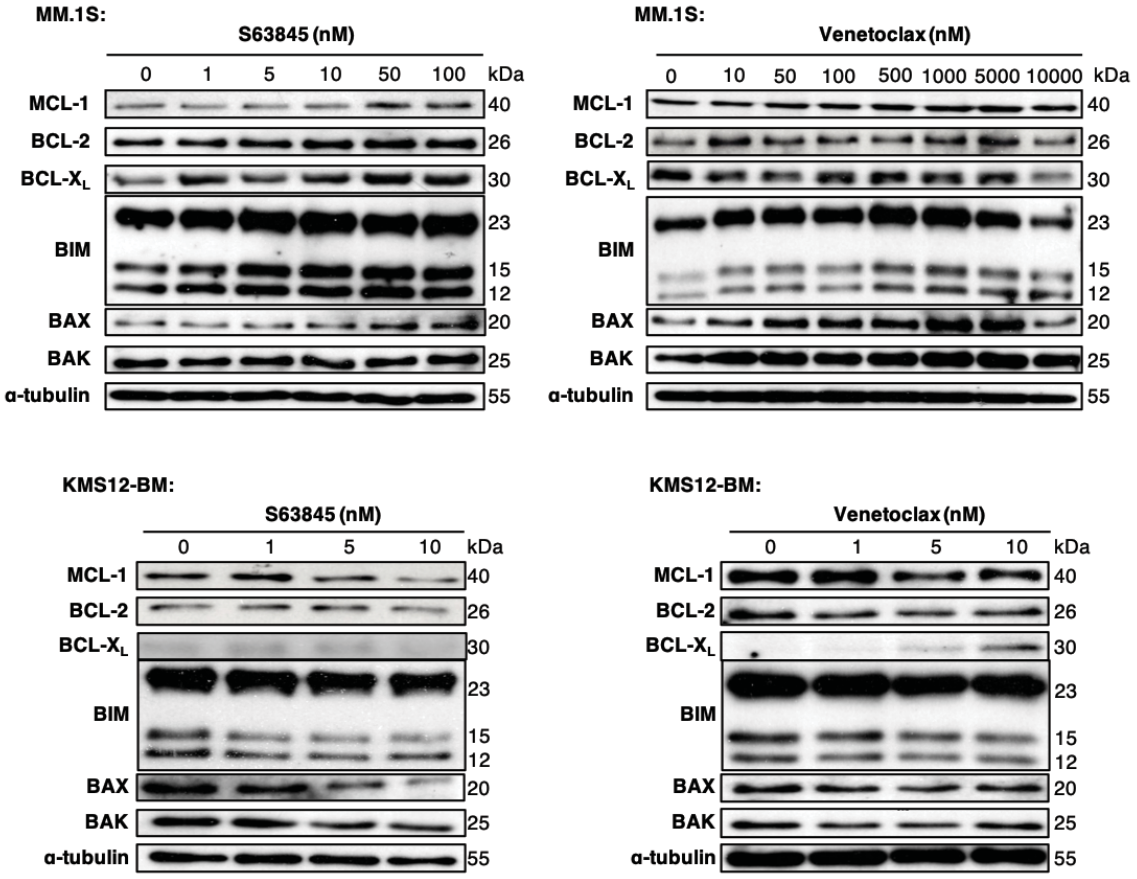

Figure 1.9. S63845 and venetoclax induce modest changes in the expression of BCL-2 family proteins in MM cell lines. Immunoblotting analysis of six BCL-2 family members (MCL-1, BCL-2, BCL-X_L, BIM, BAX and BAK) in MM.1S and KMS12-BM cells after treatment with increasing concentrations of S63845 and venetoclax for 48 hours.

Given that the binding of S63845 and venetoclax to their respective targets, MCL-1 and BCL-2, did not induce their degradation, an alternative mechanism of action was considered, namely the inhibition of their function of sequestering pro-apoptotic proteins. Therefore, the binding of anti-apoptotic proteins to the pro-apoptotic protein BIM was next explored by immunoprecipitation assays. MM.1S, JJN3, NCI-H929 and KMS12-BM cell lines were treated with S63845 or venetoclax for 48 hours, the pro-survival protein BIM was immunoprecipitated, and binding of MCL-1 and BCL-2 to BIM was assessed by immunoblotting (Figure 1.10). S63845 treatment clearly disrupted MCL-1/BIM complexes in the four cell lines tested. Paradoxically, the impairment of the interaction of MCL-1 with BIM was more pronounced in the two cell lines that were less sensitive to this drug, MM.1S and JJN3. However, it was interesting to note a compensatory increase of BCL-2/BIM complexes over control levels after treatment with S63845 that was also particularly evident in the less sensitive cell lines. These results imply that S63845 treatment may

change MM-cell dependence from MCL-1 to BCL-2, particularly in the cell lines that are less sensitive to this drug, thus suggesting a potential mechanism of resistance. On the other hand, and consistent with the results of previous reports, venetoclax impaired BCL-2/BIM complexes in all cell lines tested with the exception of NCI-H929, in which BCL-2 basal expression bound to BIM by immunoblotting could not be detected. Furthermore, venetoclax treatment augmented the binding of MCL-1 to BIM over control levels in MM.1S, JJN3 and KMS12-BM cell lines, suggesting a parallel situation to that observed with S63845.

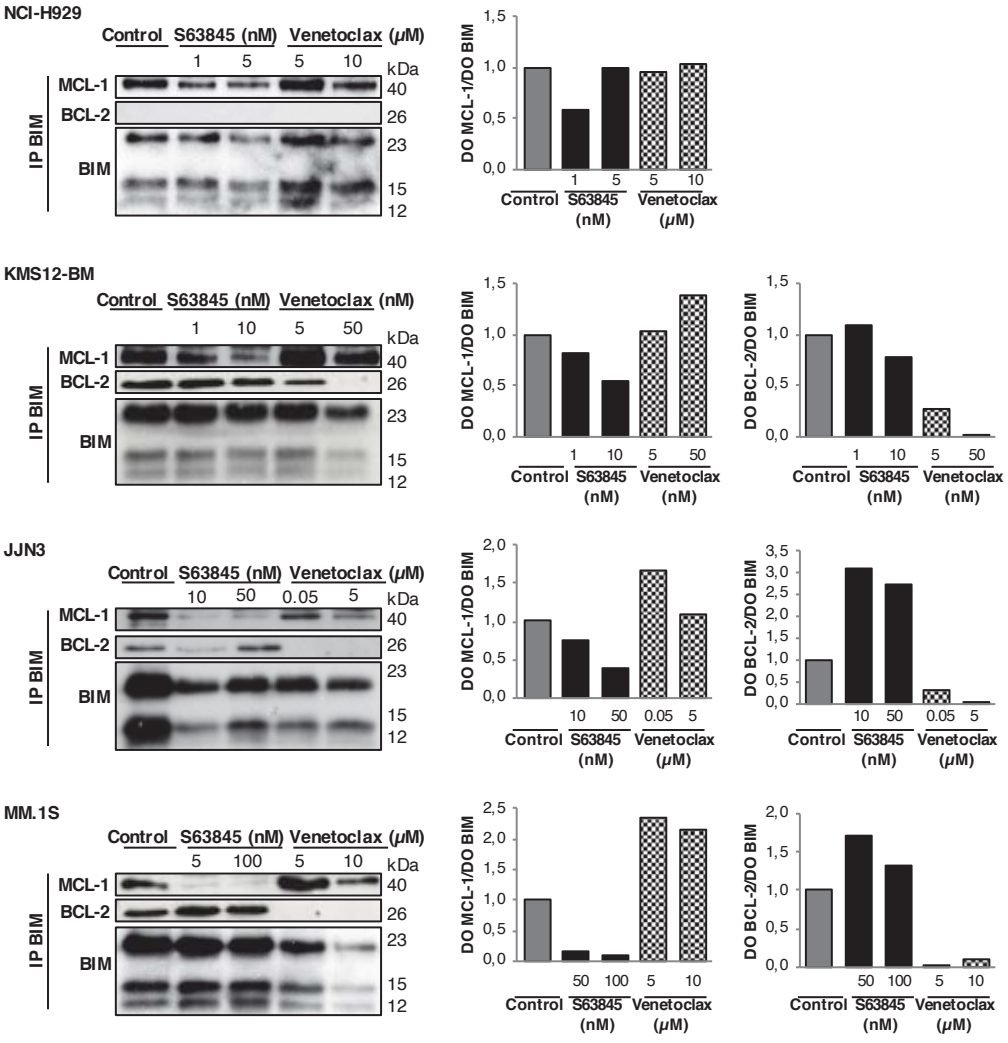

Figure 1.10. S63845 and venetoclax disrupt the binding of their targets to the pro-apoptotic protein BIM and induce changes in MM cell dependence between MCL-1 and BCL-2. NCI-H929, KMS12-BM, JJN3 and MM.1S cells were treated with the indicated concentrations of S63845 or venetoclax for 48 hours and protein lysates were immunoprecipitated for BIM. MCL-1 and BCL-2 bound to BIM were analyzed by immunoblotting. MCL-1 and BCL-2 levels were quantified by densitometry analysis of bands, normalized to those of BIM and depicted as bar diagrams.

S63845 potently synergizes with venetoclax *in vitro*

The observed shift of dependence from MCL-1 to BCL-2 in MM cells treated with S63845, and from BCL-2 to MCL-1 in cells treated with venetoclax as potential mechanisms of evasion to these treatments, particularly in the less sensitive cell lines, supports the potential value of a simultaneous inhibition of both proteins to overcome this resistance. If this is true, the S63845 + venetoclax combination could be a promising strategy to improved the efficacy of either agent in monotherapy. In order to evaluate this hypothesis, the cytotoxic effect of the combination of both agents was evaluated in five myeloma cell lines with different sensitivities to S63845 and venetoclax as single agents (MM.1S being the most resistant and KMS12-BM the most sensitive) by flow cytometry (Figure 1.11). Overall, our *in vitro* findings show that the S63845 + venetoclax combination clearly increased apoptotic cell death and reduced cell viability, with CIs reaching a strong synergism (0.1 < CI < 0.3) in almost all cell lines. This effect was dose- and time-dependent, and very short drug exposures of 3 to 6 hours were sufficient to trigger the apoptotic effect (Figure 1.12).

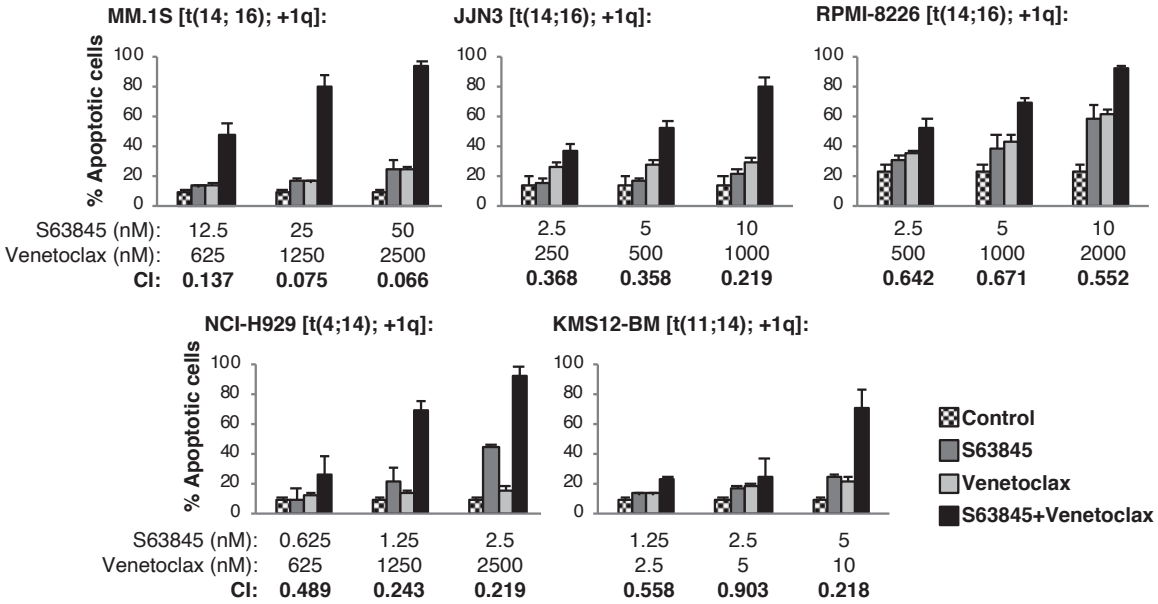

Figure 1.11. S63845 strongly synergizes with venetoclax *in vitro*. MM cell lines were exposed to increasing doses of S63845 + venetoclax for 48 hours, using a constant drug ratio combination design for each cell line. Apoptosis induction was analyzed by flow cytometry and CIs were calculated with the Calcusyn software. Data presented are means (n=3) ± SD.

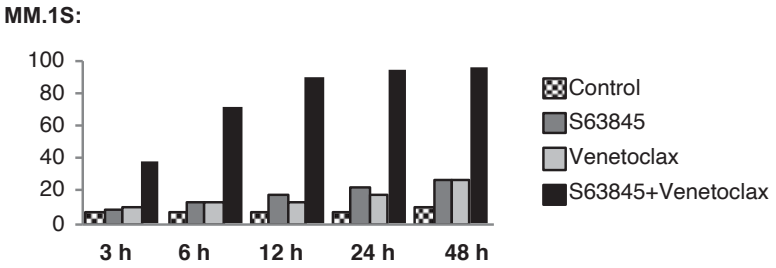

Figure 1.12. The S63845 + venetoclax combination induces a rapid apoptosis induction *in vitro*. MM.1S cells were treated with S63845 50 nM and venetoclax 2.5 μM for 3, 6, 12, 24 and 48 hours, and the induction of apoptosis was analyzed by flow cytometry.

Furthermore, S63845 + venetoclax markedly decreased the mitochondrial membrane potential of MM.1S cells whereas the single treatments at these low concentrations only showed minimal effects (Figure 1.13).

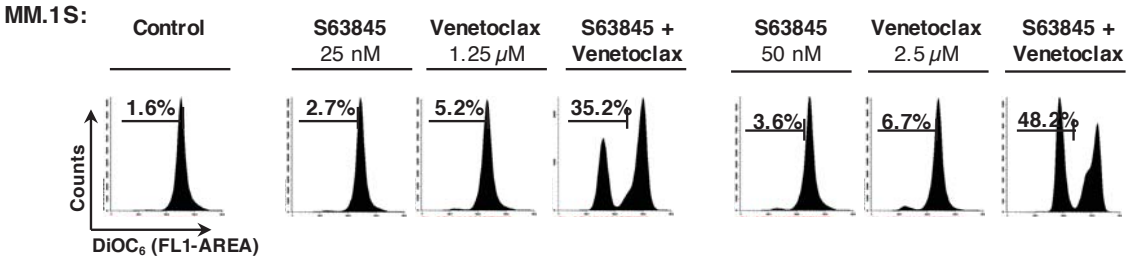

Figure 1.13. S63845 in combination with venetoclax induces apoptosis via the intrinsic apoptotic pathway *in vitro*. Mitochondrial membrane potential changes were evaluated by $DiOC_6$ staining after incubation with S63845 + venetoclax for 48 hours in MM.1S cells. Representative data from an experiment that was conducted twice.

With respect to the cell cycle, the combination induced a cell-cycle blockade, with an increase in the percentage of cells in the non-proliferative phase G_0-G_1 and a decrease in the percentage of those in the S and G_2-M proliferative phases (Figure 1.14). This effect that in the MM.1S cell line was previously observed only with high doses of venetoclax in monotherapy, was clearly potentiated by the combination.

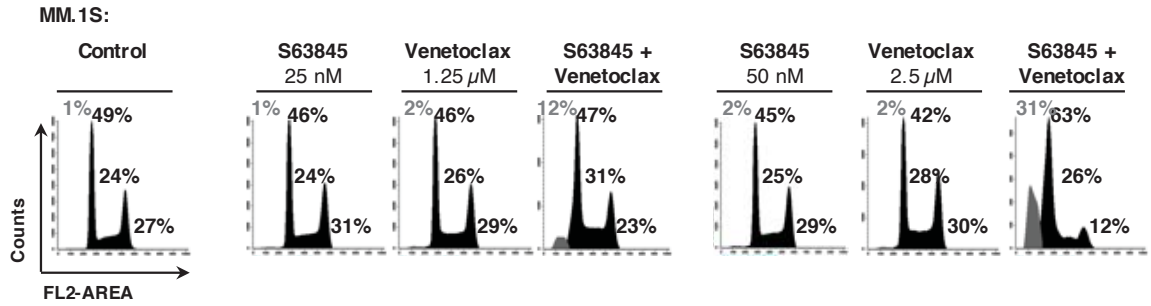

Figure 1.14. Effect of the S63845 + venetoclax combination on the cell cycle on MM cells *in vitro*. Representative histograms of cell-cycle distribution examined by flow cytometry after propidium iodide staining in MM.1S cells incubated with increasing concentrations of S63845 + venetoclax for 48 hours. The experiment was performed at least twice, and percentages in the figure are those of cells in subG$_0$ (apoptotic cells), and in G$_0$-G$_1$, S and G$_2$-M in the non-subG$_0$ population.

Given the clinical interest of the addition of dexamethasone in the currently used backbones of treatment for MM, the triple combination of S63845 + venetoclax + dexamethasone was also evaluated. As observed in Figure 1.15, dexamethasone clearly increased the efficacy of both S63845 and venetoclax, and the triple combination showed an even stronger synergy than the double treatment of S63845 + venetoclax in the MM.1S (best CI = 0.054) and RPMI-8226 (best CI = 0.099) cell lines.

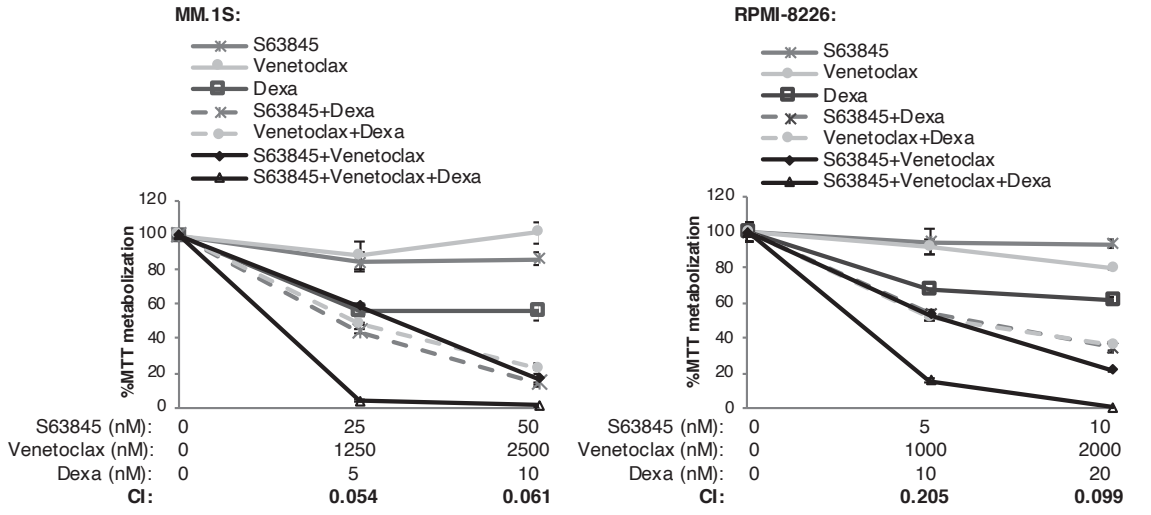

Figure 1.15. The efficacy of the triple combination of S63845 + venetoclax + dexamethasone is superior to the double combination of S63845 + venetoclax. MM.1S and RPMI-8226 cell lines were exposed to increasing concentrations of S63845, venetoclax and dexamethasone and their combinations for 48 hours, maintaining a constant ratio drug combination design. Cell viability was analyzed by MTT assay. CIs for the triple treatments were derived using the Calcusyn software. Data presented are means (n=3) ± SD.

The S63845 + venetoclax combination simultaneously impairs the binding of MCL-1 and BCL-2 to BIM

The hypothesis of a simultaneous disruption of MCL-1/BIM and BCL-2/BIM complexes with S63845 + venetoclax combination was subsequently evaluated in the more sensitive (KMS12-BM) and the less sensitive (MM.1S) cell lines (Figure 1.16). In this case, BCL-X_L/BIM complexes were also evaluated as they could be a potential mechanism of resistance to the simultaneous inhibition of MCL-1 and BCL-2. As previously observed with higher concentrations of the drug, S63845 treatment clearly disrupted MCL-1/BIM complexes, but also induced a compensatory increase of BCL-2/BIM complexes over control levels in both cell lines. BCL-X_L/BIM complexes also augmented after S63845 treatment in the MM.1S cell line, but these complexes were absent in KMS12-BM cells. These results imply that S63845 treatment may also change MM cell dependence from MCL-1 to BCL-2 and also to BCL-X_L in cells particularly dependent on this later protein, thus suggesting again a potential mechanism of resistance. On the other hand, and consistent with previous reports[75,91], venetoclax impaired the formation of BCL-2/BIM complexes and also augmented the binding of MCL-1 to BIM over control levels in KMS12-BM cells and the binding of both MCL-1 and BCL-X_L to BIM in MM.1S cells, suggesting a parallel situation to that observed with S63845. Importantly, after treatment with the S63845 + venetoclax combination, BCL-2/BIM complexes remained low in both cell lines tested. However, in the MM.1S cell line, MCL-1 was still able to interact with BIM, although to a lesser extent than with venetoclax in monotherapy, thereby diminishing the previously described venetoclax escape mechanism. Regarding BCL-X_L/BIM complexes, their increase with S63845 and venetoclax treatments in monotherapy was not further potentiated by the double combination. Whole cell lysates did not show major changes on MCL-1, BCL-2, BCL-X_L and BIM levels in MM.1S and KMS12-BM cells treated with S63845 and venetoclax alone and in combination. Finally, we also immunoprecipitated MCL-1 and BCL-2 anti-apoptotic proteins, and analyzed BIM binding by immunoblotting (Figure 1.17), being the obtained results in accordance with those previously shown from BIM immunoprecipitation.

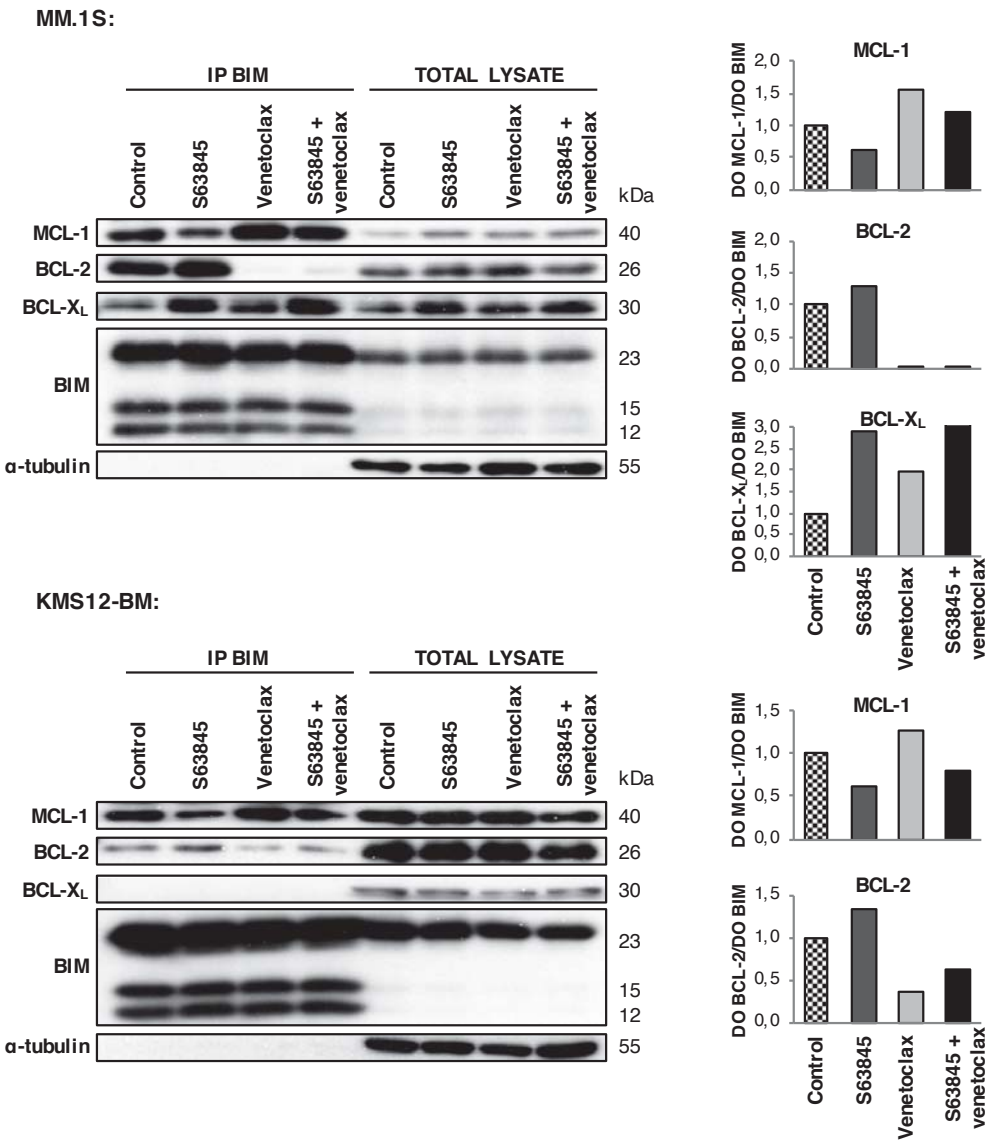

Figure 1.16. The S63845 + venetoclax combination impairs the interactions of MCL-1 and BCL-2 with the pro-apoptotic protein BIM. MM.1S and KMS12-BM cell lines were respectively treated with S63845 (12.5 and 2 nM) and venetoclax (625 and 4 nM), in monotherapy or in combination for 24 hours. Protein lysates were subjected to immunoprecipitation with an anti-BIM antibody, and MCL-1, BCL-2 and BCL-X_L bound to BIM were then analyzed by immunoblotting. Whole cell lysates of each cell line are also shown. MCL-1, BCL-2 and BCL-X_L levels were quantified by densitometry analysis of bands, normalized to those of BIM and depicted as bar diagrams.

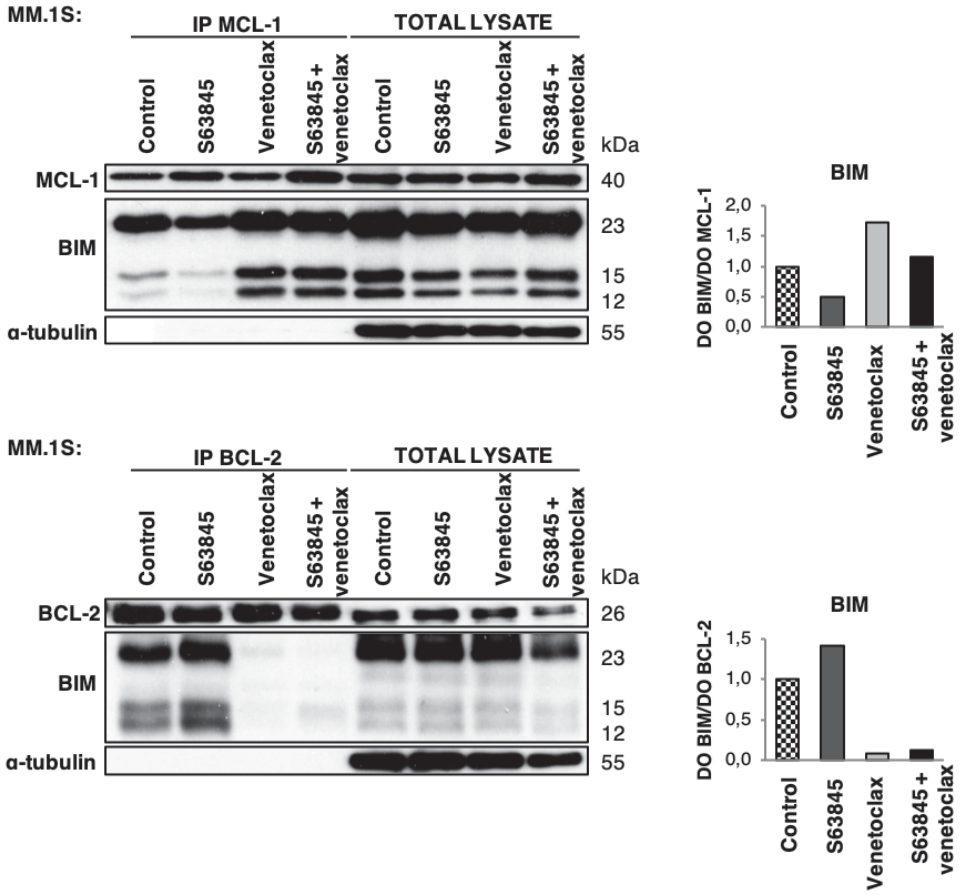

Figure 1.17. S63845 + venetoclax combination disrupts MCL-1/BIM and BCL-2/BIM complexes, and shifts MM cell dependence to the alternative anti-apoptotic protein. MM.1S cells were treated with S63845 12.5 nM and venetoclax 625 nM alone or in combination for 24 hours. Protein lysates were subjected to immunoprecipitation with an anti-MCL-1 or an anti-BCL-2 antibodies, and BIM bound to the anti-apoptotic proteins was then analyzed by immunoblotting. BIM levels were quantified by densitometry analysis of bands, normalized to those of MCL-1 or BCL-2 and depicted as bar diagrams. Whole cell lysates of each cell line are also shown.

S63845 + venetoclax is effective *ex vivo* and *in vivo* with a satisfactory toxicity profile

The anti-tumoral effect of S63845 and venetoclax was further investigated *ex vivo* in cells isolated from the same eight MM patients in which these drugs had been previously tested in monotherapy (Figure 1.18). In five out of the eight evaluated patients (patients 1, 2, 3, 7 and 8), the combination enhanced the apoptotic induction of both agents in monotherapy, but, interestingly, this was particularly evident in patient 2 [venetoclax responder harboring the t(11;14) translocation] and patient 8 [insensitive to both drugs in monotherapy without t(11;14) translocation or +1q gain alterations]. The toxicity on normal

lymphocytes was clearly lower to that on tumor cells, suggesting a therapeutic window for this combination.

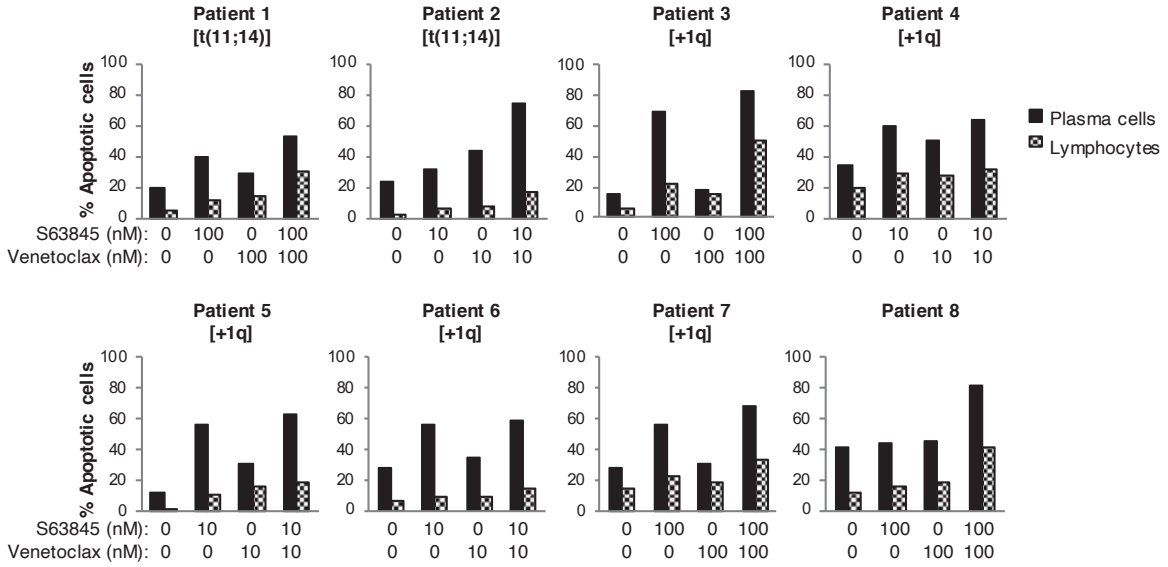

Figure 1.18. S63845 strongly synergizes with venetoclax *ex vivo*. BM cells from eight MM patients were incubated with S63845 and venetoclax as single agents and in combination at indicated doses for 24 hours. Apoptosis induction was analyzed by flow cytometry after annexin-V binding in plasma cells and lymphocytes.

Furthermore, the efficacy of S63845 + venetoclax was explored *in vivo* in an aggressive disseminated model of MM (Figure 1.19). The double treatment delayed tumor growth, and in contrast to the agents in monotherapy, produced a statistically significant benefit with respect to the control from day 19 onwards. It should be noted that at day 32 a mouse treated with S63845 + venetoclax, despite only having a relatively localized bioluminescence signal, developed paralysis and had to be euthanized. Nevertheless, the efficacy in controlling tumor growth translated into improved survival of the mice treated with S63845 + venetoclax, with a median survival of 60 (range 32 to 88 days), compared with 51 days for S63845 (range 38 to 55 days) and 46 days for venetoclax (range 41 to 55 days). These differences did not reach statistical significance possibly due to the low number of mice used and to the mouse with the localized disease that had to be early euthanized. Remarkably, none of the treatment regimens caused a significant reduction in body weight.

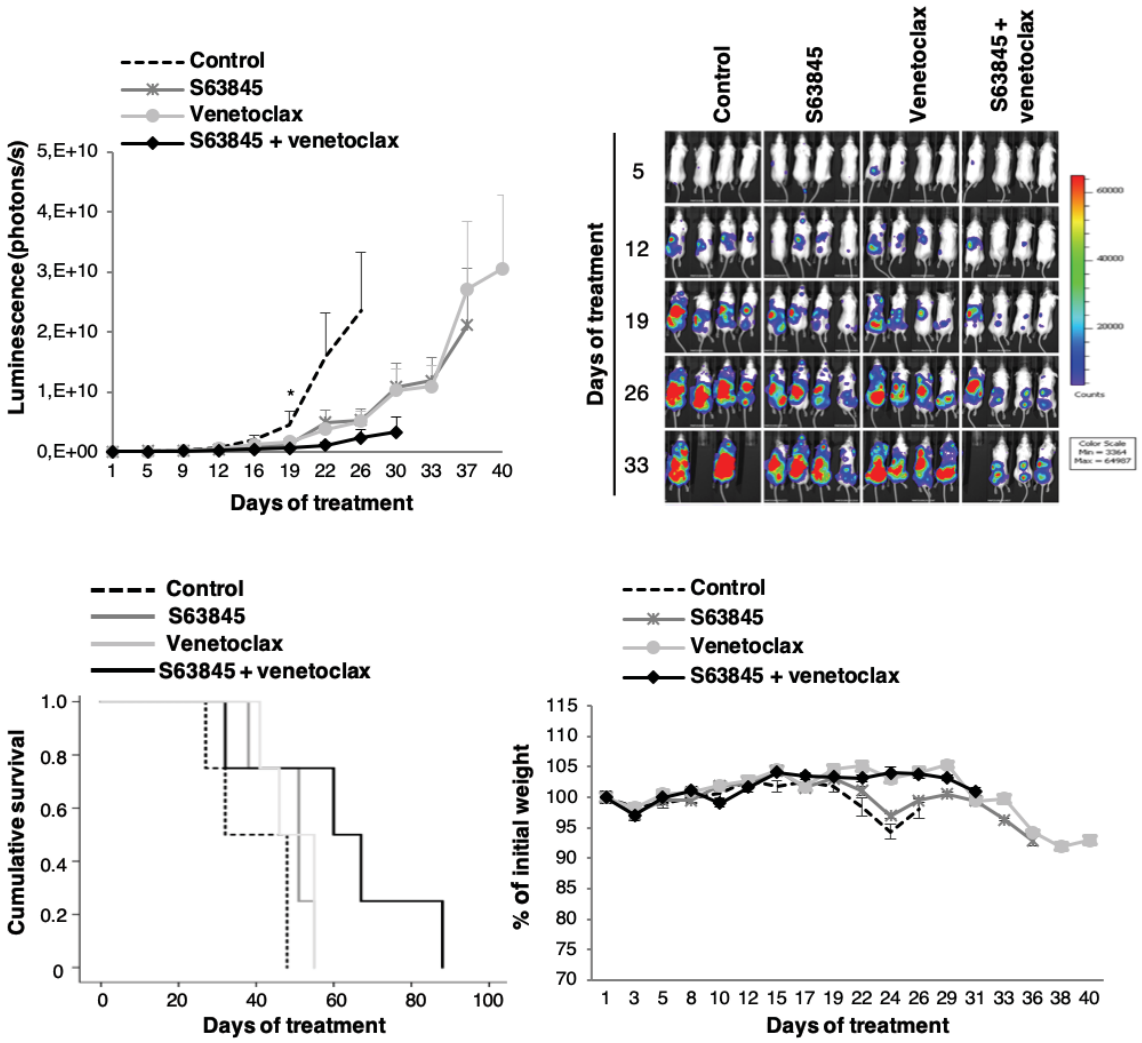

Figure 1.19. The S63845 + venetoclax combination has potent *in vivo* anti-myeloma activity. *In vivo* efficacy of S63845 and venetoclax alone and in combination in an RPMI-8226-luc xenograft model of disseminated MM in BRG mice. Data are summarized as the mean (n=4) ± SEM. Statistically significant differences were calculated by the Kruskal-Wallis test followed by Dunn's post-hoc comparisons (*, $p < 0.05$) (upper left). Images representing the bioluminescence signal of each mouse by treatment group from day 5 to day 33 of treatment (upper right). Kaplan-Meier curves representing the survival of each treatment group (lower left). Percentages of mouse body weight variation (lower right).

As performed *in vitro*, we also evaluated the *in vivo* activity and toxicity of the triple combination of S63845 + venetoclax + dexamethasone in BRG mice. Animals were randomized to receive vehicle (control group) or the triple combination (n=3 per group). S63845 and venetoclax were administered at the same doses and following the same schema as in the previous experiment; dexamethasone was administered intraperitoneally at 1 mg/kg 2 days/week. As shown in Figure 1.20, the triple combination induced approximately 30 days delay in tumor growth compared with the control group. Most

importantly, the tolerability of this triple combination was good, without significant body weight loss or other signs of toxicity.

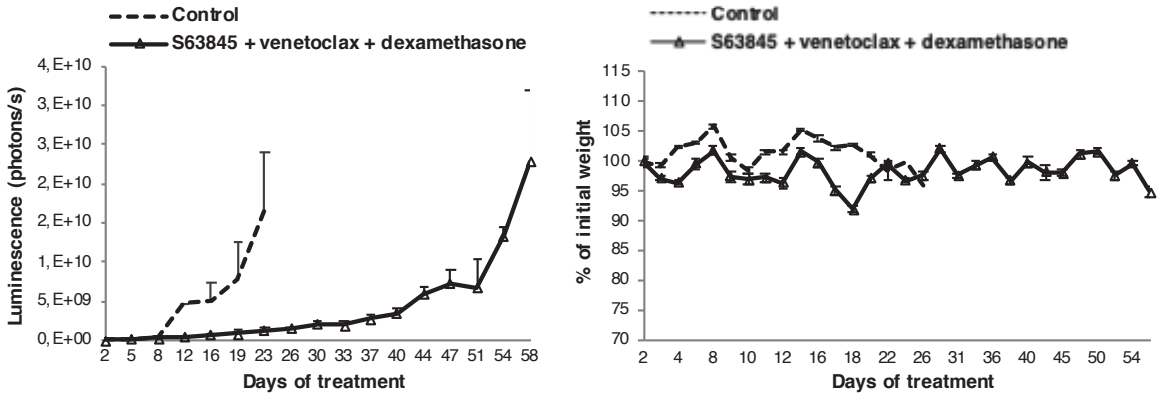

Figure 1.20. The S63845 + venetoclax + dexamethasone combination has potent *in vivo* anti-myeloma activity. *In vivo* efficacy and percentages of mouse body weight variation of S63845 + venetoclax + dexamethasone in an RPMI-8226-luc xenograft model of disseminated MM in BRG mice. Experimental groups included control (vehicle) and S63845 (12.5 mg/kg i.v., weekly) + venetoclax (100 mg/kg p.o., 5 days per week) + dexamethasone (1 mg/kg i.p., 2 days/week) (n = 3 per group). Data are summarized as the mean ± SEM.

Finally, the key mechanistic information obtained *in vitro*, was *in vivo* confirmed in tumor cells from large RPMI-8226 plasmocytomas excised 24 hours after one dose of treatment (Figure 1.21). Despite having received only one dose the day before, and in accordance with the *in vitro* data, treatment with S63845 and venetoclax in monotherapy respectively impaired the binding of MCL-1 and BCL-2, to the pro-apoptotic protein BIM. Moreover, there was a compensatory upregulation of MCL-1/BIM complexes in tumors excised from mice treated with venetoclax, but no increase of BCL-2/BIM complexes was observed in tumors excised from mice treated with S63845. Consistent with previous results, the combination of S63845 + venetoclax was able to counteract the compensatory upregulation of MCL-1 bound to BIM observed in tumors from animals treated with venetoclax in monotherapy and to completely disrupt BCL-2/BIM complexes.

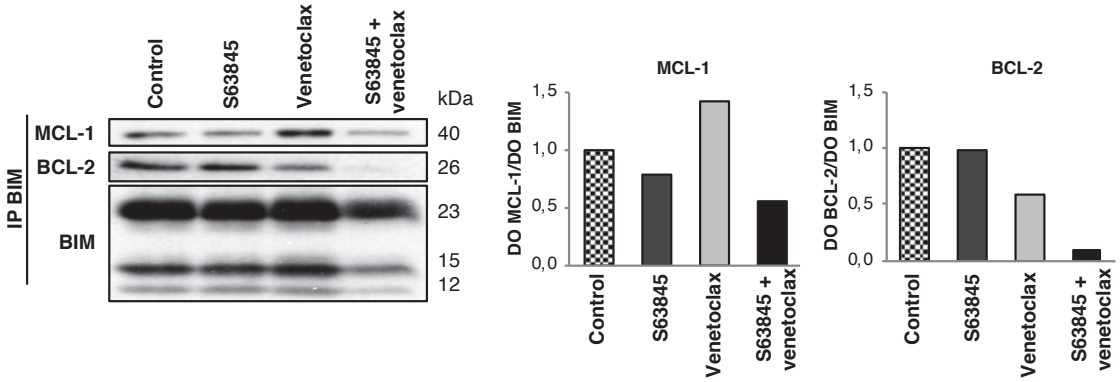

Figure 1.21. The S63845 + venetoclax combination impairs the interactions of MCL-1 and BCL-2 with the pro-apoptotic protein BIM in tumor cells obtained from large plasmocytomas. RPMI-8226 cells were subcutaneously injected in CB17-SCID mice. When plasmacytomas reached 2 cm in one of their diameters, animals received one dose of vehicle, S63845 (12.5 mg/kg), venetoclax (100 mg/kg) or the respective combination (n=2 per group). Tumors were excised 24 hours after treatment and protein lysates from tumors were subjected to immunoprecipitation with an anti-BIM antibody. MCL-1, BCL-2 and BCL-X_L anti-apoptotic proteins bound to BIM were then analyzed by immunoblotting. MCL-1 and BCL-2 and levels were quantified by densitometry analysis of bands, normalized to those of BIM and depicted as bar diagrams.

CHAPTER 2: EVALUATION OF THE STROMA-INDUCED RESISTANCE TO S63845 AND VENETOCLAX MEDIATED BY THE DEREGULATION OF miRNAs TARGETING MCL-1 AND BCL-2 IN MULTIPLE MYELOMA.

Co-culture of MM cells with pMSCs alters the cytotoxic effect of S63845 and venetoclax in monotherapy

Considering the important role of the stromal BM microenvironment mediating drug resistance, first we wanted to investigate whether the co-culture of myeloma cells with pMSCs modified the anti-myeloma effect of S63845 and venetoclax. For this purpose, co-cultures of MM.1S-luc cells and pMSCs were exposed to increasing concentrations of S63845 (1 - 10,000 nM) or venetoclax (0.5 - 10.0 μM) for 48 hours. Despite the proliferative and protective advantage conferred by pMSCs, S63845 and venetoclax (Figure 2.1) were able to reduce MM cell viability in a dose-dependent manner. However, the presence of tumor-associated pMSCs reduced the IC_{50} value of S63845 in MM.1S-luc cells from 94.1 to 81.0 nM, whereas it raised that of venetoclax from 6.2 to 9.8 μM. Importantly, neither S63845 nor venetoclax affected pMSC viability, even at high concentrations (Figure 2.2).

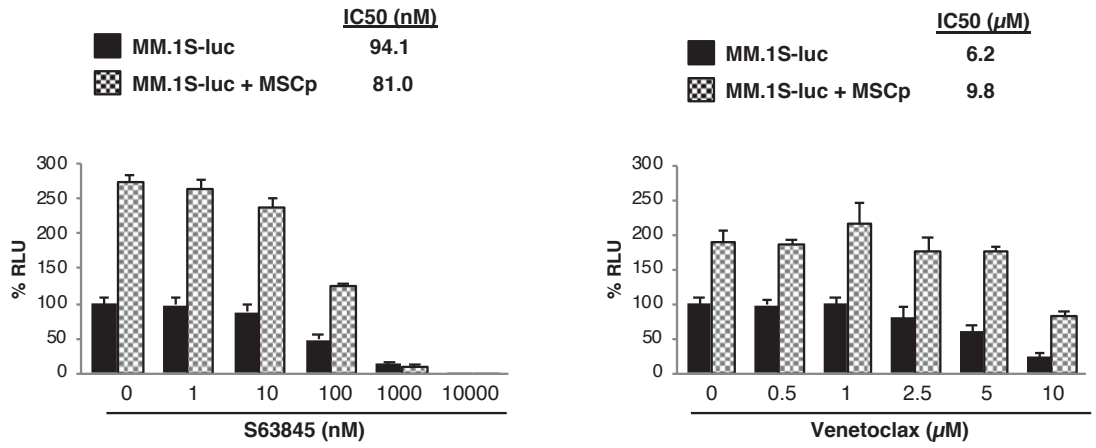

Figure 2.1. The stromal microenvironment modifies MM.1S sensitivity to S63845 and venetoclax. MM.1S-luc cells were co-cultured with pMSCs for 48 hours with S63845 or venetoclax at the indicated doses. MM.1S-luc growth was assessed by luciferase bioluminescence signal, which was normalized relative to the growth of MM.1S-luc cells alone and in the absence of drug treatment. Graphs show the mean (n=3) ± SD.

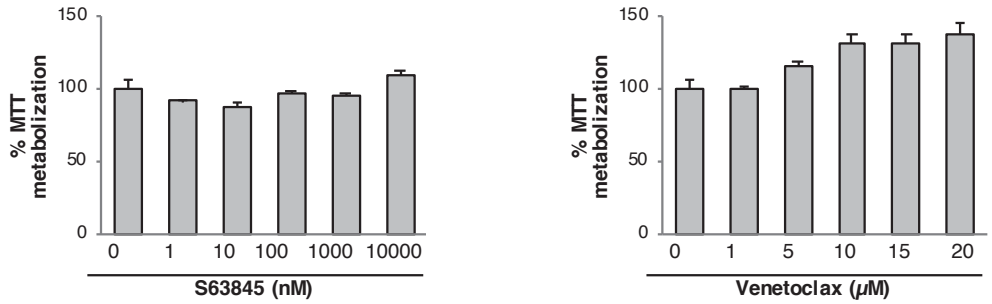

Figure 2.2. S63845 and venetoclax do not reduce pMSCs viability. pMSCs isolated from a MM patient were treated with increasing doses of S63845 or venetoclax for 48 hours, and cell viability was measured by the MTT assay. Average absorbances relative to the percentage of the control are shown. Data presented are means (n=3) ± SD.

pMSCs modify the expression of anti-apoptotic proteins MCL-1 and BCL-2 on MM cells

In an attempt to elucidate mechanisms triggered by the stromal BM microenvironment that could be modifying the activity of S63845 and venetoclax, we subsequently analyzed the expression of MCL-1 and BCL-2 anti-apoptotic proteins on MM.1S cells cultured for 48 hours in direct contact with pMSCs isolated from four MM patients. The co-culture with pMSCs induced an increase in the expression of MCL-1 and a decrease in BCL-2 levels on MM cells with respect to MM.1S cells in monoculture (Figure 2.3).

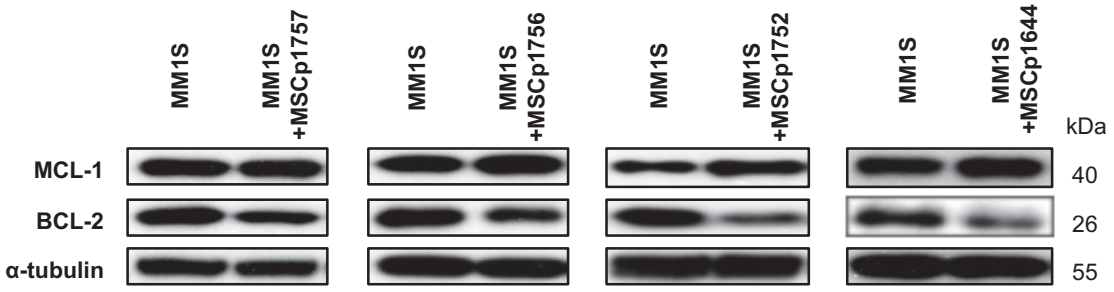

Figure 2.3. pMSCs modify MCL-1 and BCL-2 expression on MM.1S cells. Immunoblot analysis of MCL-1 and BCL-2 in MM.1S cells in monoculture and in co-culture with pMSCs for 48 hours. α-tubulin was used as a loading control.

We also evaluated the expression of these proteins in a series of five MM cell lines co-cultured with pMSCs under the same conditions (Figure 2.4). Similarly to MM.1S cells,

RPMI-8226 and NCI-H929 cell lines showed augmented MCL-1 protein levels when co-cultured with pMSCs. However, no noticeable changes in MCL-1 expression were observed in JJN3 and KMS12-BM cells. BCL-2 protein levels, contrary to MCL-1, were reduced in MM.1S, JJN3, RPMI-8226 and NCI-H929 cell lines in co-culture with pMSCs as compared to cells in monoculture. In KMS12-BM cells, BCL-2 expression remained unchanged.

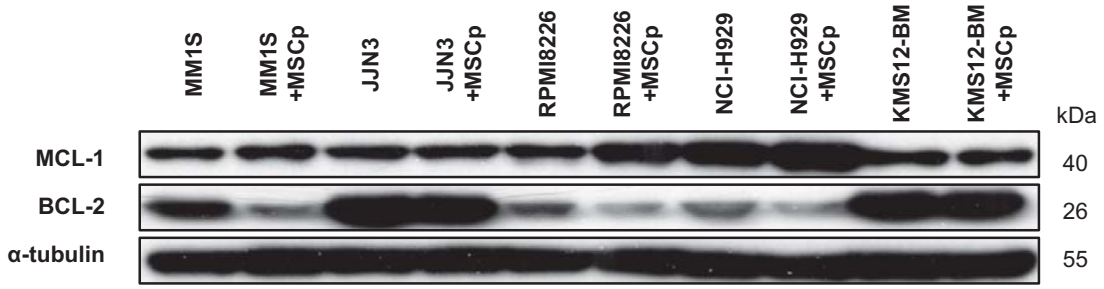

Figure 2.4. Co-culture with pMSCs modifies MCL-1 and BCL-2 expression in different MM cell lines. Western blot evaluation of MCL-1 and BCL-2 in MM.1S, JJN3, RPMI-8226, NCI-H929 and KMS12-BM cells cultured in absence or presence of pMSCs (from the same patient). α-tubulin was used as a loading control.

Regulation of MCL-1 and BCL-2 protein expression induced by pMSCs on MM cells is, at least partially, mediated by miRNAs

To gain insight into possible mechanisms by which pMSCs could be modifying the expression of MCL-1 and BCL-2 proteins on MM cells and eventually affecting the efficacy of S63845 and venetoclax, we focused on post-transcriptional regulation of anti-apoptotic proteins by miRNAs. First, we studied changes produced on the miRNA expression profile of MM.1S when this cell line was co-cultured with pMSCs for 48 hours (Affymetrix GeneChip miRNA 4.0 Array; previous data from our group). We then resorted to the Target Scan algorithm with the aim of identifying potential miRNAs targeting *MCL1* and *BCL2* mRNAs. The bioinformatic analysis predicted a total of 53 miRNAs with an evolutionary conserved binding site in the 3´UTR of *MCL1* mRNA (Table 2.1) and 58 in that of *BCL2* (Table 2.2).

Table 2.1: miRNAs with evolutionary conserved binding sites in the 3´ UTR of *MCL1* mRNA among mammals.

hsa-miR-125a-5p
hsa-miR-4319
hsa-miR-125b-5p
hsa-miR-29a-3p
hsa-miR-29b-3p
hsa-miR-29c-3p
hsa-miR-526b-3p
hsa-miR-106a-5p
hsa-miR-20b-5p
hsa-miR-93-5p
hsa-miR-519d-3p
hsa-miR-17-5p
hsa-miR-20a-5p
hsa-miR-106b-5p
hsa-miR-520f-3p
hsa-miR-302c-3p.2
hsa-miR-133a-3p.1
hsa-miR-133b
hsa-miR-133a-3p.2
hsa-miR-373-3p
hsa-miR-372-3p
hsa-miR-520a-3p
hsa-miR-520d-3p
hsa-miR-520e
hsa-miR-302d-3p
hsa-miR-302b-3p
hsa-miR-302c-3p.1
hsa-miR-520c-3p
hsa-miR-302a-3p
hsa-miR-520b
hsa-miR-302e
hsa-miR-135a-5p
hsa-miR-135b-5p
hsa-miR-153-3p
hsa-miR-4262
hsa-miR-181b-5p
hsa-miR-181a-5p
hsa-miR-181d-5p
hsa-miR-181c-5p
hsa-miR-5590-3p
hsa-miR-142-5p
hsa-miR-193a-3p
hsa-miR-193b-3p
hsa-miR-4465
hsa-miR-26b-5p
hsa-miR-26a-5p
hsa-miR-1297
hsa-miR-101-3p.1
hsa-miR-101-3p.2
hsa-miR-325-3p
hsa-miR-873-5p.1
hsa-miR-381-3p
hsa-miR-300

Table 2.2: miRNAs with evolutionary conserved binding sites in the 3´ UTR of *BCL2* mRNA among mammals.

hsa-miR-16-5p
hsa-miR-6838-5p
hsa-miR-195-5p
hsa-miR-424-5p
hsa-miR-15a-5p
hsa-miR-15b-5p
hsa-miR-497-5p
hsa-miR-4262
hsa-miR-181d-5p
hsa-miR-181b-5p
hsa-miR-181a-5p
hsa-miR-181c-5p
hsa-miR-125a-5p
hsa-miR-125b-5p
hsa-miR-4319
hsa-miR-153-3p
hsa-miR-182-5p
hsa-miR-30d-5p
hsa-miR-30e-5p
hsa-miR-30a-5p
hsa-miR-30b-5p
hsa-miR-30c-5p
hsa-miR-449a
hsa-miR-449b-5p
hsa-miR-34a-5p
hsa-miR-34c-5p
hsa-miR-96-5p
hsa-miR-1271-5p
hsa-miR-200b-3p
hsa-miR-429
hsa-miR-200c-3p
hsa-miR-365b-3p
hsa-miR-365a-3p
hsa-miR-204-5p
hsa-miR-211-5p
hsa-miR-140-3p.2
hsa-miR-21-5p
hsa-miR-590-5p
hsa-miR-6088
hsa-miR-143-3p
hsa-miR-4770
hsa-miR-383-5p.2
hsa-miR-383-5p.1
hsa-miR-23b-3p
hsa-miR-130a-5p
hsa-miR-23c
hsa-miR-23a-3p
hsa-miR-202-5p
hsa-miR-448
hsa-miR-342-3p
hsa-miR-503-5p
hsa-miR-382-3p
hsa-miR-219a-2-3p
hsa-miR-374c-5p
hsa-miR-655-3p
hsa-miR-323a-3p
hsa-miR-6835-3p
hsa-miR-224-5p

From the predicted miRNAs targeting *MCL1* mRNA, we identified four (miR-193b-3p, miR-17-5p, miR-93-5p and miR-106a-5p) with a significant reduced expression in MM.1S cells after 48 hours of co-culture with pMSCs in the miRNA microarray data set, being miR-193b the most significantly deregulated (Figure 2.5). On the other hand, miR-21-5p was the only miRNA that by bioinformatic prediction targeted *BCL2* mRNA and was found to be significantly upregulated in MM cells after their interaction with pMSCs (Figure 2.5).

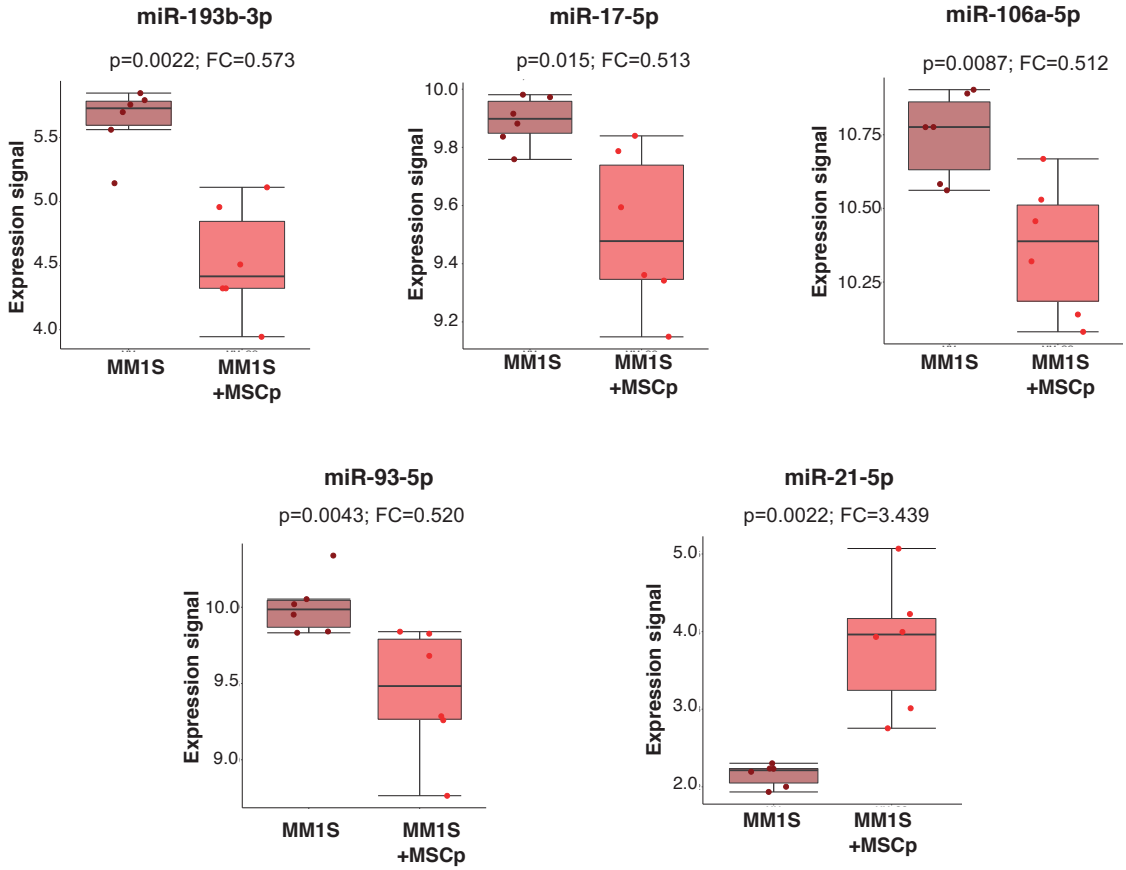

Figure 2.5. Normalized expression signal of miRNAs targeting MCL-1 and BCL-2 which are significatively deregulated in MM1S cells in monoculture *versus* MM1S cells after co-culture with pMSCs. The expression of miRNAs was taken from Affymetrix GeneChip miRNA 4.0 Array, and boxplots of the miRNAs which were predicted to target *MCL1* (miR-193b-3p, miR-17-5p, miR106b-5p and miR-93-5p) and *BCL2* (miR-21-5p) are shown. The Wilcoxon rank-sum test was used to determine the significance between the monoculture and co-culture conditions, and the fold-change (FC) was calculated as the ratio of the mean expression of each miRNA in each of the two groups compared, transformed to lineal escale using the antilog of the ratio.

Subsequently, the significantly lower miR-193b-3p and higher miR-21-5p expression detected in MM.1S cells in co-culture with pMSCs as compared to MM.1S cells in monoculture by microarrays was confirmed by qRT-PCR analysis (Figure 2.6).

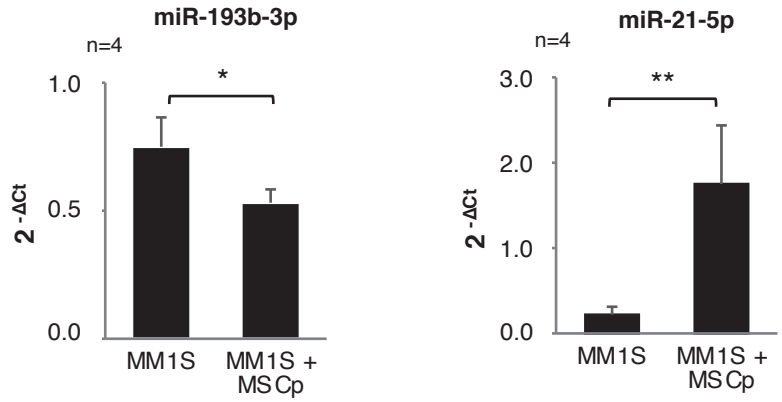

Figure 2.6. mir-193b-3p and miR-21-5p are deregulated on MM.1S cells in co-culture with pMSCs. Normalized expression of miR-193b-3p and miR-21-5p in MM.1S cells alone or co-cultured with pMSCs for 48 hours as assessed by qRT-PCR. Results are expressed as the mean ± SEM. Student t test (*, $p < 0.05$; **, $p < 0.01$).

To study the putative role of miR-193b-3p and miR-21-5p as regulators of MCL-1 and BCL-2 expression, the MM.1S cell line was transiently transfected with correspondent miRNA mimics or inhibitors, and the expression of anti-apoptotic proteins was determined 48 hours post-transfection (Figure 2.7). Importantly, MM.1S cells transfected with miR-193b-3p or miR-21-5p mimics clearly decreased MCL-1 and BCL-2 levels, as compared with negative control (NC) transfected cells. By contrast, MCL-1 and BCL-2 expression were respectively increased upon transfection with miR-193b-3p and miR-21-5p inhibitors. Taken together, these results seem to be indicative of 193b-3p and miR-21-5p negatively modulating the expression of MCL-1 and BCL-2.

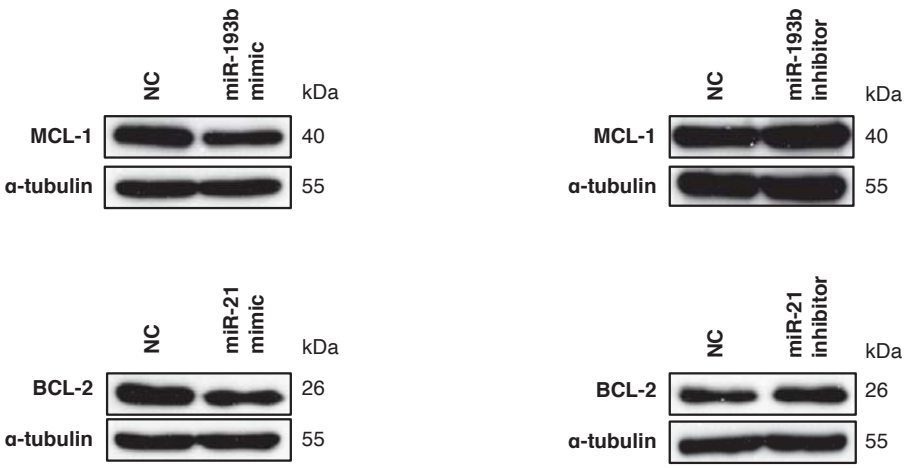

Figure 2.7. MCL-1 and BCL-2 expression are respectively modulated by miR-193b-3p and miR-21-5p in the MM.1S cell line. Western blot evaluation of MCL-1 expression after transfection with miR-193b-3p mimic (upper left) or inhibitor (upper right) or the correspondent Negative Controls (NC). Similarly, MM.1S cells were transfected with miR-21-5p mimics (lower left) or inhibitors (lower right) and their respective NCs, and BCL-2 levels were subsequently analyzed by immunoblotting.

To establish a functional link between the diminished expression of miR-193b-3p or the augmented expression of miR-21-5p in MM cells in co-culture with pMSCs and the altered S63845 and venetoclax cytotoxic effect observed in these conditions, MM.1S-luc cells were transiently transfected with miR-193b-3p inhibitors or miR-21-5p mimics and their respective NCs. Subsequently, cells were treated with S63845 50 nM or venetoclax 2.5 μM and bioluminescence was measured 48 hours post-transfection (Figure 2.8). In concordance with results obtained in the presence on the stroma, mir-193b-3p inhibitor significantly increased S63845 efficacy as compared to NC, whereas no significant changes on venetoclax activity were observed. In the same line, after the overexpression of miR-21-5p, a general decrease in both venetoclax and S63845 efficacies was observed with respect to NCs.

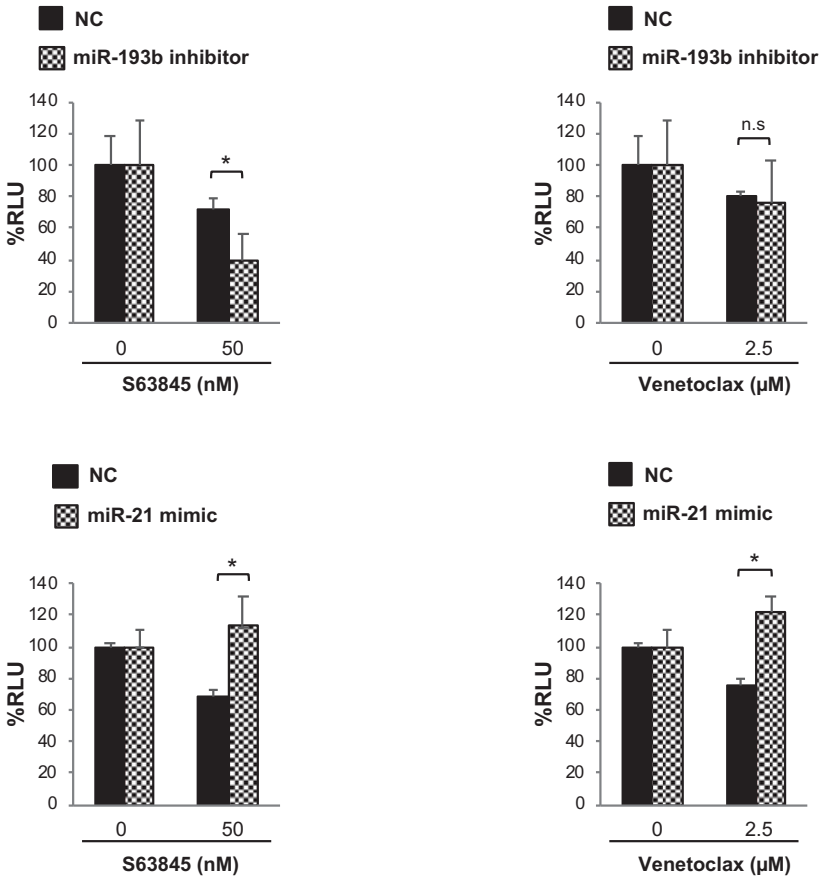

Figure 2.8. miR-193b inhibition and miR-21 overexpression modifies MM.1S sensitivity to S63845 and venetoclax. MM.1S-luc cells were transiently transfected with miR-193b-3p inhibitor or miR-21-5p mimic and NCs and treated with 50 nM S63845 and 2.5 μM venetoclax for 48 hours. MM cell viability was assessed by bioluminescence, which was normalized relative to the growth of NC transfected untreated cells. Results are expressed as the mean (n=3) ± SD. Student t test (*, $p < 0.05$).

MCL-1 is directly regulated by miR-193b-3p, whereas miR-21-5p does not have BCL-2 as a direct target

In order to validate *MCL1* as a target of miR-193b-3p and *BCL2* as a target of miR-21-5p, luciferase reporter assays were performed using miRNA binding sites in their 3′UTR mRNAs. *MCL1 and BCL2* wild-type (WT) 3′UTR sequences, respectively containing miR-193b-3p and miR-21-5p binding sites, were cloned into a dual luciferase-reporter plasmid. In parallel, 3′UTR sequences harboring mutant (MUT) binding sites were cloned into the same reporter plasmid and used as negative controls. HEK293 cells were co-transfected with WT or MUT constructs and the corresponding miRNA or negative control (NC) mimics. The expression of luciferase activity was measured 24 hours post-transfection (Figure 2.9). Luciferase activity of cells co-transfected with *MCL1* WT 3′UTR and miR-

193b-3p mimics was significantly lower ($p<0.05$) than that exhibited by MM.1S cells transfected with the NC miRNAs. By contrast, luciferase activity of transfected MUT constructs was not significantly affected by the presence of miR-193b-3p. On the other hand, no reduction in luciferase activity was observed in cells co-transfected with either *BCL2* WT and MUT 3′UTR constructs and miR-21-5p mimics. Taken together, these data indicate that miR-193b-3p binds to the 3´UTR of *MCL1* precluding its translation into protein, thus being *MCL1* transcript a direct target of miR-193b-3p. However, miR-21-5p does not bind to the 3´UTR of *BCL2*, indicating that it is not directly modulating BCL-2 protein expression.

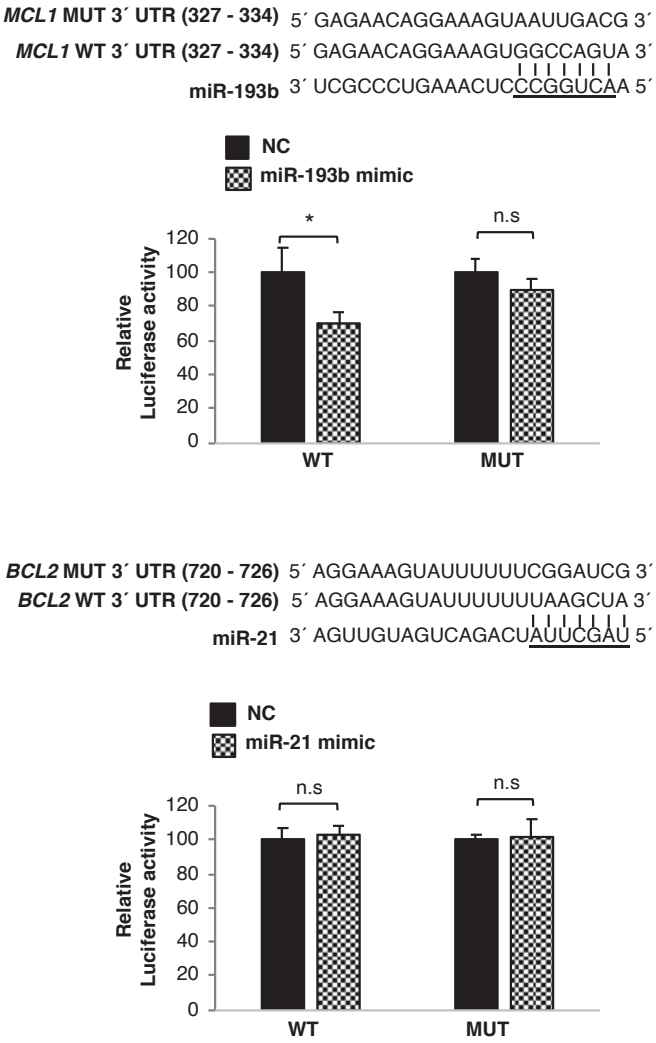

Figure 2.9. miR-193b-3p targets *MCL1* 3´UTR mRNA whereas miR-21-5p does not directly bind to *BCL2* 3´UTR transcript. Luciferase activity was measured in HEK293 cells co-transfected with miR-193b-3p / miR-21-5p and NC mimics and pmiR-Glo plasmids containing the wild-type (WT) or the mutated (MUT) miRNAs binding site of the 3´UTR *MCL1* / *BCL2* genes cloned downstream of the luciferase reporter gene. Firefly luciferase activity was normalized using to that of *Renilla*. All results are presented as the mean (n=3) ± SD. Significant differences with respect to cells transfected with NC mimics were assessed with the Student t test (*, $p < 0.05$).

Interactions of anti-apoptotic proteins with BIM in untreated and S63845 or venetoclax treated MM.1S cells are modified by the presence of stromal cells

Considering changes induced by pMSCs on the expression of MCL-1 and BCL-2 proteins and their influence on S63845 and venetoclax efficacy, we next investigated whether pMSCs were also affecting interactions of these anti-apoptotic proteins with the pro-apoptotic protein BIM. For that purpose, MM.1S cells were cultured alone or in presence of pMSCs and exposed or not to S63845 and venetoclax. After 48 hours, immunoprecipitation assays were performed (Figure 2.10).

In untreated cells, despite the increased MCL-1 expression previously observed in total lysates, MCL-1/BIM complexes were slightly diminished or remained unaffected by the presence of pMSCs. On the other hand, the decreased BCL-2 total protein levels observed on MM.1S cells when co-cultured with pMSCs were accompanied by a drop in the levels of BCL-2 bound to BIM. Given the fact that decreased interactions of BCL-2 with BIM were not resulting in the formation of extra MCL-1/BIM complexes, we sought to investigate the anti-apoptotic protein BCL-X_L, non-targeted by any of the BH3-mimetics assessed in this study. Interestingly, the reduced amount of BCL-2/BIM complexes detected in presence of pMSCs seemed to be balanced by the formation of additional BCL-X_L/BIM complexes.

Under treatment with S63845, interactions of MCL-1 with BIM were impaired in MM.1S cells both in monoculture and in co-culture with pMSCs. However, no increase of BCL-2/BIM complexes and higher BCLX_L/BIM levels were detected on MM cells cultured in the presence of the stroma and exposed to S63845 as compared with non-treated cells. On the other hand, with venetoclax treatment, the interaction between BCL-2 and BIM was completely impaired leading to a noticeable increase in MCL-1/BIM complexes either in MM cells in monoculture and in co-culture with pMSCs as compared with untreated cells. However, BCL-X_L/BIM levels augmented in cells in monoculture whereas decreased in co-culture conditions.

Finally, our group, as shown in chapter one, has demonstrated that the simultaneous treatment of MM cells with S63845 and venetoclax is a promising strategy for improved efficacy and for overcoming resistance to each of these agents in monotherapy. Consequently, we also wanted to investigate the effect of the stromal BM microenvironment on S63845 in combination with venetoclax. The S63845 + venetoclax

combination completely blocked interactions of BCL-2 with BIM and precluded the formation of additional compensatory MCL-1/BIM complexes, which were induced by venetoclax in monotherapy. Interestingly, interactions of BCL-X_L with BIM did not increase with respect to treatments in monotherapy, either in monoculture or co-culture conditions.

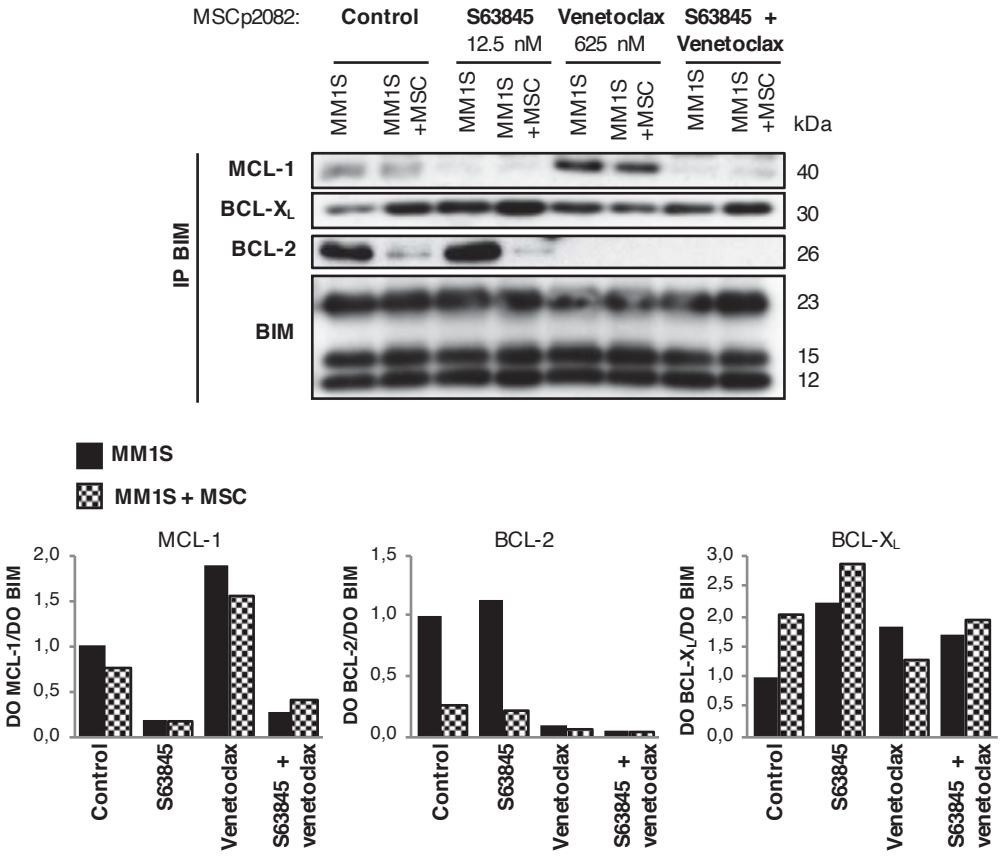

Figure 2.10. pMSCs modify the interactions between anti-apoptotic proteins and BIM in MM.1S cells. MM.1S cells were treated with S63845 12.5 nM and venetoclax 625 nM alone or in combination and cultured in the absence or presence of pMSCs for 48 hours. Protein lysates were subjected to immunoprecipitation with an anti-BIM antibody. MCL-1, BCL-X_L and BCL-2 bound to BIM were then analyzed by immunoblotting.

S63845 potently synergizes with venetoclax in presence of pMSCs

In view of our results, we subsequently analyzed whether the S63845 + venetoclax combination was synergistic in MM.1S cells in co-culture with pMSCs. Therefore, MM.1S-luc cells co-cultured with pMSCs were treated with increasing concentrations of S63845 and venetoclax alone and in combination for 48 hours and tumor cell viability was measured by bioluminescence. The double combination had a strong anti-myeloma effect

even in the presence of the tumor-associated stromal microenvironment (Figure 2.11), demonstrating its superiority over S63845 and venetoclax in monotherapy in co-culture with pMSCs. As was observed with the drugs in monotherapy, the double combination did not affect pMSCs viability (Figure 2.12).

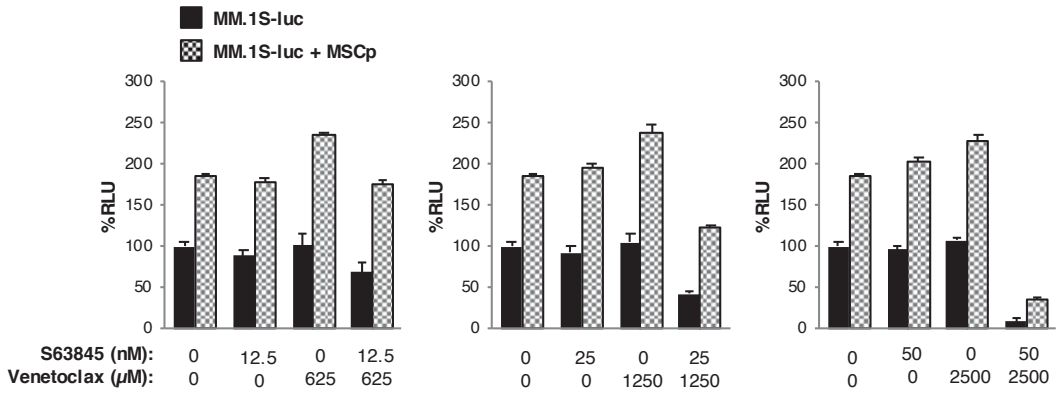

Figure 2.11. The S63845 + venetoclax combination remains efficient in the presence of the BM stromal microenvironment. MM.1S-luc cells were co-cultured with pMSCs for 48 hours with S63845 + venetoclax combination at the indicated doses. MM.1S-luc growth was assessed by the luciferase bioluminescence signal, which was normalized relative to the growth of MM.1S-luc cells alone and in the absence of drug treatment. Graphs show the mean (n=3) ± SD.

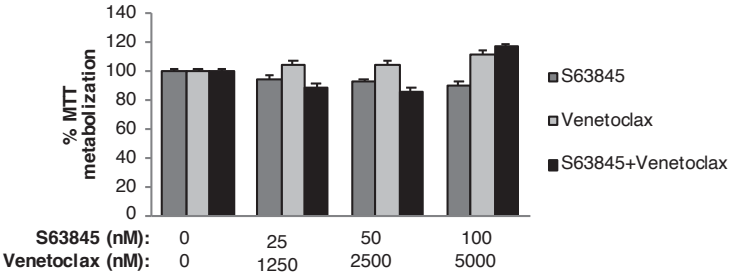

Figure 2.12. The S63845 + venetoclax combination does not reduce pMSCs viability. pMSCs isolated from a MM patient were treated with increasing doses of S63845 + venetoclax for 48 hours, and cell viability was measured by the MTT assay. Average absorbances relative to the percentage of the control are shown. Data presented are means (n=3) ± SD.

5. DISCUSSION

Multiple myeloma is a disease in which therapeutic approaches have drastically advanced in past two decades. Consequently, MM patients' survival has significantly improved in the last years. However, MM remains incurable mainly due to continuous relapses that are progressively more resistant to subsequent treatments. Therefore, the development of new drugs with novel mechanisms of action being effective even in the presence of the BM microenvironment either in monotherapy or in combination is still fundamental. Moreover, moving nowadays towards a precision medicine with the development of more specific and selective targeted therapies, it is becoming of upmost importance to better identify the therapy most suitable for each subgroup of patients. Therefore, it is crucial to deeply investigate the molecular mechanisms behind the response to a drug in order to anticipate the development of potential mechanisms of resistance either by the tumor cell itself or prompted by the BM microenvironment.

Apoptosis evasion is a hallmark of malignancy[136] and the addiction of cancer cells to one or more anti-apoptotic proteins makes them particularly vulnerable to agents targeting these proteins. Therefore, in recent years, substantial progress has been made in the development of small molecules capable of selectively inhibiting anti-apoptotic proteins. This PhD work shows a detailed and extensive preclinical study of two novel agents, the BH3-mimetic targeting MCL-1 S63845 and the BH3-mimetic targeting BCL-2 venetoclax, currently under evaluation for the treatment of MM.

We confirmed in a large panel of MM cell lines the recently reported strong anti-myeloma activity of S63845 *in vitro*[103]. No significant correlation was found between the sensitivity to these drugs *in vitro* with the cytogenetic alterations or the basal protein expression of different members of the BCL-2 family. Considering the levels of BCL-2 family proteins, there tended to be higher levels of BCL-X_L or BCL-2 in cell lines that were less sensitive to S63845. By contrast, we observed higher expression of BCL-X_L or MCL-1 in cell lines that were less sensitive to venetoclax, implying that these cells might be more dependent on the proteins that are not targeted by the given agent. From these results we should also point out that, while BCL-2 and BCL-X_L were only expressed by some cell lines (at least at levels detectable with Western blot analyses), all the cell lines tested showed notable MCL-1 levels, which may reflect the importance of MCL-1 for MM cell survival with respect to the other anti-apoptotic proteins.

Regarding the *ex vivo* data for venetoclax, within the eight evaluated patients, only one, bearing the t(11;14) translocation, responded to venetoclax, while the others, even

one of them that also harbored this translocation, did not respond. This situation is consistent with clinical data in which less than half of the t(11;14) patients respond to venetoclax[88]. Most interestingly, all the patients showed some response to S63845, independently of the presence of the translocation. Notably, patients who responded best to S63845 featured a 1q amplification, where the locus of the *MCL1* gene is located. This result has been later confirmed by Slomp *et al.* in a higher number of patient samples[137]. This finding may be of particular interest since 1q amplification is a cytogenetic feature demonstrated to have an adverse prognosis in this disease. However, whether 1q amplification is a bona-fide marker of response to MCL-1 inhibitors remains to be tested in other ongoing preclinical and clinical studies.

As far as the mechanism of action is concerned, in accordance with the findings of previous studies[75,87,103], we have demonstrated that S63845 and venetoclax do not significantly reduce the expression of their respective targets in MM cells. This result is particularly important for the MCL-1 inhibitor since this protein, apart from preventing apoptosis, has other essential functions in non-malignant cells[138] and a substantial reduction of its levels could lead to serious toxicity. Our results show that the mechanism of action of S63845 and venetoclax is mainly based on the impairment of the interactions between MCL-1 or BCL-2 with the pro-apoptotic protein BIM, which is in line with what has been previously described for venetoclax[75,91]. Interestingly, the shift in the binding to BIM from MCL-1 to BCL-2 and BCL-X_L with S63845, and from BCL-2 to MCL-1 and BCL-X_L with venetoclax, suggests a mechanism of resistance to these drugs. This hypothesis is reinforced by the fact that these changes are particularly evident in the less sensitive cell lines. In fact, this mechanism raises the possibility of using the combination of an MCL-1 inhibitor with venetoclax as a treatment strategy for MM. In this regard, we demonstrate the strong *in vitro* synergism of the combination of S63845 + venetoclax through the simultaneous inhibition of the binding of MCL-1 and BCL-2 to BIM. This combination was also effective *ex vivo* in all evaluated patients, irrespective of the cytogenetic pattern. Interestingly, patients who were refractory to venetoclax in monotherapy showed a higher relative increase in the apoptosis induced by the combination, which is a marker of a potential reversion of the resistance to this agent probably mediated, at least in part, by the upregulation of MCL-1/BIM complexes. More importantly, one patient, neither harboring t(11;14) or 1q amplification and unresponsive to S63845 and venetoclax in monotherapy, was highly sensitive to the double combination, suggesting an expansion of the group of patients who could benefit from the S63845 + venetoclax regimen.

Our in vivo data in an aggressive model of disseminated MM, corroborated the efficacy observed *in vitro* and *ex vivo*, with a clear potentiation of the S63845 + venetoclax combination. Toxicity might be a concern when simultaneously targeting MCL-1 and BCL-2, although our *ex vivo* and *in vivo* data showed good tolerability. In the *ex vivo* experiments, a clear therapeutic window was observed when comparing the citotoxicity on plasma cells with that on normal lymphocytes. No significant reduction in mouse body weight or other evident signs of toxicity were observed *in vivo*, although S63845 has a considerable weaker affinity for murine MCL-1[103], and therefore rat studies or novel models will be required to better evaluate the safety margins of this combination.

Subsequently, the influence of the stromal-associated BM microenvironment on MM cell sensitivity to S63845 and venetoclax was analyzed. Although both agents remained active, the co-culture with pMSCs revealed that S63845, in contrast to venetoclax, was more effective within the BM tumor microenvironment, with a lower IC_{50} in cells co-cultured with pMSCs.

IL6-mediated signals have been shown to promote MCL-1 overexpression and dependence in MM[139,140], with phosphorylation of BIM shifting its binding from BCL-2 and BCL-X_L to MCL-1[100]. In our hands, the direct co-culture with primary pMSCs augmented MCL-1 total protein levels in MM.1S cells. By contrast, the presence of stromal cells induced a decrease in BCL-2 expression in this cell line. Interestingly, the increased expression of MCL-1 was found to be associated with concomitant reduced levels of miR-193b-3p. We demonstrate that the inhibition of miR-193b-3p in MM.1S cells in monoculture, conveying the co-culture condition, induced the overexpression of MCL-1. Consistently, *MCL1* transcript was later corroborated as a direct target of miR-193b-3p. In concordance with these results, miR-193a belonging to the same miRNA family as miR-193b, has also been shown to directly target *MCL1* mRNA in the context of dexamethasone resistant MM cell lines[141] and in colorectal cancer[142]. In relation with BCL-2 expression, we found that its reduced levels in MM.1S cells after their interaction with pMSCs was associated with increased miR-21-5p expression. However, miR-21-5p was not found to directly bind to the *BCL2* 3´UTR mRNA in luciferase reporter assays. Contradictory findings about whether mir-21 positively or negatively regulates BCL-2 expression have been published in other tumors[143–147]. In MM, our results only suggest an indirect negative regulation of BCL-2 upon miR-21-5p overexpression.

Besides the expression of anti-apoptotic proteins, the co-culture with pMSCs also modified their interactions with the pro-apoptotic protein BIM in untreated MM cells. Despite the augmented MCL-1 total protein levels observed in MM.1S cells in direct co-culture with primary pMSCs, a significant increase in MCL-1/BIM complexes was not detected. These results may be explained by previously reported data indicating that the overexpression of MCL-1 in some MM cell lines, including MM.1S, does not result in augmented MCL-1/BIM complexes[148]. On the contrary, the reduced BCL-2 expression observed in MM.1S cells after direct co-culture with primary pMSCs, led to a decrease in the interactions of BCL-2 with BIM. Reduced BCL-2/BIM complexes seem to be balanced by an increase of BCL-X_L/BIM complexes. Overall, these results suggest that in MM.1S cells, the direct contact with pMSCs preserves MCL-1 cell dependence unchanged while inducing a shift from BCL-2 to BCL-X_L dependence.

Given the later data, we hypothesized that the presence of the BM stroma would alter anti-apoptotic and BIM interactions in MM cells treated with S63845 and venetoclax. Importantly, S63845 and venetoclax remained active in presence of pMSCs, being able to impair the interactions of their targets with the pro-apoptotic protein BIM. Besides, in concordance with the shift from BCL-2 to BCL-X_L dependence observed in untreated MM.1S cells when co-cultured in presence of pMSCs, the mechanism of resistance to S63845 treatment in presence of the BM microenvironment seemed to be mediated by the formation of additional BCL-X_L/BIM instead of BCL-2/BIM complexes. However, resistance to venetoclax was mainly mediated by increased MCL-1/BIM levels in co-culture conditions. Finally, the S63845 + venetoclax combination was also assessed and, besides diminishing MCL-1/BIM and BCL-2/BIM complexes, it also impeded the increased formation of BCL-X_L/BIM complexes.

Moreover, we showed that the simultaneous inhibition of MCL-1 and BCL-2 by S63845 + venetoclax combination was highly effective regardless of MM.1S cells being in mono-culture or co-culture with pMSCs. This is in line with previous observations reported by our group and others, showing high synergism for the mentioned combination *in vitro, ex vivo* and *in vivo*[131,137]. Whether the use of combinations of BH3-mimetics targeting MCL-1 and BCL-2 may be suitable for MM patients, may probably rely on the feasible management of hematologic and cardiac toxicities[82].

Considering the different patterns of responses exhibited by MM cells based on the heterogeneity showed with respect to MCL-1, BCL-2 and/or BCL-X_L dependencies and co-dependencies, the identification of biomarkers that could reveal subgroups of MM patients that may benefit more from each of these therapies is now an imperative issue. In addition, it becomes of upmost importance to better understand potential mechanisms of resistance acquired by MM cells exposed to these agents, and to identify synergistic combinations in order to prevent or overcome their appearance by the administration of more effective treatment combinations.

To identify genes modulating the response to venetoclax and S63845 in MM, in this PhD work a genome-wide CRISPRa screen was performed with both BH3-mimetics in monotherapy. The use of this novel technology has allowed the interrogation the complete human genome reveling known and novel genes whose overexpression confer sensitivity or resistance to MCL-1 or BCL-2 inhibition.

MRD1 is a protein known to pump many drugs out of the cell (such as PIs, alkylating agents and IMiDs) thereby decreasing their intracellular accumulation and limiting their efficacy[149]. Since we demonstrated that S63845 was a MDR1 substrate, and a high enrichment of this protein could impede the identification of other hits, this agent was combined with an MDR1i. Despite the fact that the combination of S63845 with an MDR1i did not precluded the enrichment of *ABCB1* overexpressing MM cells, this enrichment was not predominant so it did not hinder the appearance of other genes potentially involved in more S63845-specific mechanisms of resistance. By contrast, in the screen implemented with venetoclax in monotherapy, *ABCB1* was two-fold more enriched than the second positively selected hit, probably constituting a potential obstacle for the enrichment of other candidates.

In concordance with our previous findings reporting the ability of MM cells to shift their dependence to the non-targeted anti-apoptotic proteins with BH3-mimetics targeting MCL-1 and BCL-2[131,150,151], *BCL2L1* (BCL-X_L) overexpressing MM cells became highly enriched in both screens. In this same line, *BCL2* was also positively selected in the S63845 screen even to a greater extent than *BCL2L1*, perhaps suggesting a more important role of BCL-2 in the acquisition of resistance to the MCL-1 inhibitor. These results also validate previous studies reporting that high BCL-2 or BCL-X_L expression confers resistance against MCL-1 inhibition in MM cell lines[137]. Surprisingly, *MCL1* was not among the positively selected genes in the venetoclax screen. However, no increase in

MCL-1 protein levels was observed when MM cells were individually transduced with three of out of the six sgRNAs targeting *MCL1* that are contained in the Calabrese library (data not shown). Moreover, despite not being remarkably enriched, the overexpression of *BCL2A1*, a gene encoding for the less known anti-apoptotic protein BCL-2A1, was also found to be involved in the acquisition of resistance to S63845. Interestingly, previous reports had associated the overexpression of BCL-2A1 with the resistance to ABT-737 in CLL[152]; nevertheless, *BCL2A1* was not found significantly enriched in the CRISPRa screen performed with venetoclax in MM cells.

With respect to negatively selected genes from the BCL-2 family, according to the fact that BH3-mimetics induce tumor cell death *via* the intrinsic apoptotic pathway and given the indispensable role of the effector pro-apoptotic proteins BAX and BAK in that process, *BAX* overexpressing MM cells were significantly depleted in the final population from both screens. However, *BAK1* was only among the negatively selected genes in the S63845, but not in the venetoclax screen. This may be explained by the ability of BAX to interact with all anti-apoptotic proteins, whereas BAK has been reported to establish significant interactions with MCL-1, but not with BCL-2[153]. In addition, *PMAIP1* (NOXA), in accordance with its role inducing MCL-1 degradation[154] and given the involvement of MCL-1 in venetoclax resistance[75,92], was among the most negatively selected genes in the venetoclax screen. Moreover, the induction of NOXA expression has been reported to be the mechanism by which bortezomib sensitizes MM cells to venetoclax[91]. Interestingly, the MM subgroup harboring the translocation t(11;14), particularly sensitive to venetoclax treatment, has been associated with high *PMAIP1* expression[101]. Lastly, despite that elevated *BCL2/BCL2L1* (BCL-X_L) *and BCL2/MCL1* ratios have been correlated with higher sensitivity to venetoclax[57,69,72,150,151], *BCL2* overexpressing cells were not significantly depleted in the population treated during 28 days with venetoclax, suggesting low *MCL1* and/or *BCL2L1* (BCL-X_L) expression to be more determinant biomarkers of sensitivity for this agent.

In addition to members belonging to the BCL-2 family, other positively or negatively selected genes have also been identified in both screens. This may be of particular interest for the group of patients revealed to be resistant to all three classes of BH3-mimetics targeting MCL-1, BCL-2 and BCL-X_L in monotherapy[150], in order to uncover other targets that may sensitize MM cells to these agents. In this regard, we have identified *IRF1* as a gene sensitizing MM cells to venetoclax. Precisely, IFNα, which was a cytokine broadly used for the treatment of MM before the development of PIs and IMiDs[155], is known to

induce *IRF1* upregulation in MM cells[156]. Therefore, our data point out the potential of combining venetoclax with IFNα for the treatment of MM. Additionally, IMiDs increase the production of IFNγ by immune effector cells from the BM microenvironment[157,158], another cytokine more strongly stimulating the expression of *IRF1* than IFNα. Thus, IMiDs, inducing the secretion of IFNγ by effector immune cells, may induce *IRF1* overexpression on MM cells sensitizing them to venetoclax. Additionally, the role of *IRF4*, *IKZF1* and *IKZF3* as sensitizers for S63845 is also particularly important. It is well-known that the mechanism of action of IMiDs is, in part, based on the degradation of the proteins encoded by these genes, Ikaros and Aiolos, also resulting in a reduced *IRF4* expression[134]. Therefore, attending to our CRISPRa results, the combination of S63845 with IMiDs may not be highly synergistic.

Finally, *CCND1*, being significantly depleted in the CRISPRa screen performed with venetoclax, was not validated. This fact reveals the existance of false positive candidate genes in these screens. Possibly this could be attributed to the intermediate doses administrated, as indicated by absence of numerous strong negative and positive drivers (avrgFCs in control treatment *vs* pDNA). However, the intermediate doses allowed us to analyze both enriched and depleted genes within the same experiment. On the other hand, dose-response analyses performed after only 48 hours of treatment may not be enough to show significant differences, since in the CRISPRa screens MM cells were treated for 28 days. Thus, longer exposure times could be needed for detecting significant differences for some genes.

Altogether, genome-wide CRISPRa screens successfully revealed known and novel genes potentially conferring resistance or constituting synergistic/antagonistic partners to S63845 and venetoclax treatments in MM.1S cells. However, variances among different MM cell lines may be expected given the heterogeneity in S63845 and venetoclax responses shown on MM cell lines in several studies. Probably, more accurate candidates will be identified by future studies evaluating a focus library containing a selection of the sgRNAs targeting the top-100 enriched and depleted genes found in our whole-genome CRISPRa screens on different MM cell lines.

Overall, the data collected in this doctoral dissertation confirm the efficacy and mechanism of action of S63845 and venetoclax in monotherapy and have revealed the efficacy of the S63845 and venetoclax combination. Additionally, intrinsic (mechanisms potentially developed by the tumor cells themselves) and extrinsic (such as the BM

microenvironment) factors modulating MM cell response to these agents have been identified, allowing to predict synergistic or non-synergistic combinations with other standard treatments. Therefore, this PhD work may help to determine those patients who will most likely benefit from these treatments and also to anticipate how these MM patients, attending to their particular alterations, will respond to them.

6. CONCLUDING REMARKS

CHAPTER 1: PRECLINICAL EVALUATION OF SINGLE AND DUAL INHIBITION OF MCL-1 AND BCL-2 WITH S63845 AND VENETOCLAX IN MULTIPLE MYELOMA

- MM cell lines with different cytogenetic alterations exhibit different sensitivity profiles to the MCL-1 and BCL-2 inhibitors in monotherapy *in vitro*, with the most resistant cell lines generally expressing high basal levels of the non-targeted anti-apoptotic proteins.
- Tumor cells derived from MM patients with 1q amplifications are significantly more sensitive to S63845.
- S63845 and venetoclax induce apoptosis without decreasing the expression of MCL-1 and BCL-2, respectively, but impairing their interaction with the pro-apoptotic protein BIM.
- Treatment with S63845 and venetoclax in monotherapy induces a shift in the interaction of the non-targeted anti-apoptotic proteins with the pro-apoptotic protein BIM, revealing a potential mechanism of resistance.
- The S63845 + venetoclax combination is highly effective *in vitro*, *ex vivo* and *in vivo*, and abrogates the respective increased binding of BCL-2 and MCL-1 to BIM induced by each of the drugs in monotherapy.

CHAPTER 2: EVALUATION OF THE STROMA-INDUCED DRUG RESISTANCE TO S63845 AND VENETOCLAX MEDIATED BY THE DEREGULATION OF miRNAs TARGETING MCL-1 and BCL-2 IN MULTIPLE MYELOMA

- S63845 and venetoclax remain active in presence of the stromal BM microenvironment, being MCL-1 inhibition, contrary to BCL-2 inhibition, more effective in the context of the BM tumor microenvironment.
- The stroma-associated BM microenvironment increases the expression of MCL-1 and decreases that of BCL-2 in MM.1S cells.
- The increased MCL-1 levels in MM.1S cells in co-culture with pMSCs is, in part, mediated by the reduction of miR-193b expression observed in this condition, and augments S63845 efficacy.
- The augmented miR-21 expression observed in MM.1S cells co-cultured with pMSCs is not directly responsible for the decreased BCL-2 expression in MM cells observed in this setting, and may participate in a more general stroma-mediated mechanism of resistance to both drugs.

- Changes on MCL-1 and BCL-2 expression in MM.1S cells co-cultured with pMSCs results into modified interactions with BIM, which may affect developed mechanisms of resistance.
- The combination of S63845 with venetoclax is highly effective even in the presence of the stromal BM microenvironment.

CHAPTER 3: IDENTIFICATION OF GENES MODULATING THE RESPONSE TO S63845 AND VENETOCLAX IN MULTIPLE MYELOMA BY CRISPR ACTIVATION SCREENS

- Whole-genome CRISPR activation screens have demonstrated to be a useful strategy for confirming already decribed apoptosis-related genes and reveling others involved in other signaling pathways as regulators of S63845 and venetoclax activity.
- The individual overexpression of BCL-X_L conferred resistance to S63845 and venetoclax in MM.1S cells.
- BCL-2 and, for first time described, BCL2A1, overexpression were also confirmed to decrease S63845 activity. Interestingly, high BCL-2 levels did not influence the efficacy of venetoclax.
- The overexpression of NOXA, pro-apoptotic protein involved in MCL-1 degradation, sensitized MM.1S cells to venetoclax.
- Independent from the BCL-2 family, *IRF1* overexpression confers sensitivity to venetoclax, supporting the combination of this agent with IFNα or IMiDs.
- IRF4, Ikaros and Aiolos overexpression sensitize MM.1S cells to S63845, which may suggest that the combination with IMiDs may not be highly synergistic.

7. REFERENCES

1. Siegel RL, Miller KD, Jemal A. Cancer statistics, 2016: Cancer Statistics, 2016. *CA: A Cancer Journal for Clinicians*. 2016;66(1):7–30.

2. Cowan A, Libby EN, Fitzmaurice C, Global Burden of Disease Cancer Collaboration. Global burden of multiple myeloma: A systematic analysis for the Global Burden of Disease study 2016. *JCO*. 2018;36(15_suppl):e20023–e20023.

3. Surveillance, Epidemiology, and End Results (SEER) Program. SEER cacner statistic factsheets: Myeloma. https:// seer.cancer.gov/statfacts/html/mulmy.html. Accessed October 1, 2019.

4. Rajkumar SV, Dimopoulos MA, Palumbo A, et al. International Myeloma Working Group updated criteria for the diagnosis of multiple myeloma. *The Lancet Oncology*. 2014;15(12):e538–e548.

5. Kyle RA, Therneau TM, Rajkumar SV, et al. A Long-Term Study of Prognosis in Monoclonal Gammopathy of Undetermined Significance. *N Engl J Med*. 2002;346(8):564–569.

6. Kyle RA, Remstein ED, Therneau TM, et al. Clinical Course and Prognosis of Smoldering (Asymptomatic) Multiple Myeloma. *N Engl J Med*. 2007;356(25):2582–2590.

7. Mateos M-V, Hernández M-T, Giraldo P, et al. Lenalidomide plus Dexamethasone for High-Risk Smoldering Multiple Myeloma. *N Engl J Med*. 2013;369(5):438–447.

8. Mateos M-V, Hernández M-T, Giraldo P, et al. Lenalidomide plus dexamethasone versus observation in patients with high-risk smouldering multiple myeloma (QuiRedex): long-term follow-up of a randomised, controlled, phase 3 trial. *The Lancet Oncology*. 2016;17(8):1127–1136.

9. González D, van der Burg M, García-Sanz R, et al. Immunoglobulin gene rearrangements and the pathogenesis of multiple myeloma. *Blood*. 2007;110(9):3112–3121.

10. Barwick BG, Gupta VA, Vertino PM, Boise LH. Cell of Origin and Genetic Alterations in the Pathogenesis of Multiple Myeloma. *Front. Immunol.* 2019;10:1121.

11. Kumar SK, Rajkumar SV. The multiple myelomas — current concepts in cytogenetic classification and therapy. *Nat Rev Clin Oncol*. 2018;15(7):409–421.

12. on behalf of the International Myeloma Working Group, Chng WJ, Dispenzieri A, et al. IMWG consensus on risk stratification in multiple myeloma. *Leukemia*. 2014;28(2):269–277.

13. Palumbo A, Avet-Loiseau H, Oliva S, et al. Revised International Staging System for Multiple Myeloma: A Report From International Myeloma Working Group. *JCO*. 2015;33(26):2863–2869.

14. Lakshman A, Alhaj Moustafa M, Rajkumar SV, et al. Natural history of t(11;14) multiple myeloma. *Leukemia*. 2018;32(1):131–138.

15. Fonseca R, Bailey RJ, Ahmann GJ, et al. Genomic abnormalities in monoclonal gammopathy of undetermined significance. *Blood*. 2002;100(4):1417–1424.

16. Avet-Loiseau H, Daviet A, Saunier S. Chromosome 13 abnormalities in multiple myeloma are mostly monosomy 13. 2.

17. Binder M, Rajkumar SV, Ketterling RP, et al. Prognostic implications of abnormalities of chromosome 13 and the presence of multiple cytogenetic high-risk abnormalities in newly diagnosed multiple myeloma. *Blood Cancer J.* 2017;7(9):e600–e600.

18. Li F, Hu L, Xu Y, et al. Identification of characteristic and prognostic values of chromosome 1p abnormality by multi-gene fluorescence in situ hybridization in multiple myeloma. *Leukemia*. 2016;30(5):1197–1201.

19. Shah GL, Landau H, Londono D, et al. Gain of chromosome 1q portends worse prognosis in multiple myeloma despite novel agent-based induction regimens and autologous transplantation. *Leukemia & Lymphoma*. 2017;58(8):1823–1831.

20. Avet-Loiseau H, Attal M, Moreau P, et al. Genetic abnormalities and survival in multiple myeloma: the experience of the Intergroupe Francophone du Myélome. *Blood*. 2007;109(8):3489–3495.

21. Avet-Loiseau H, Gerson F, Magrangeas F, et al. Rearrangements of the c-myc oncogene are present in 15% of primary human multiple myeloma tumors. *Blood*. 2001;98(10):3082–3086.

22. Affer M, Chesi M, Chen WD, et al. Promiscuous MYC locus rearrangements hijack enhancers but mostly super-enhancers to dysregulate MYC expression in multiple myeloma. *Leukemia*. 2014;28(8):1725–1735.

23. Chapman MA, Lawrence MS, Keats JJ, et al. Initial genome sequencing and analysis of multiple myeloma. *Nature*. 2011;471(7339):467–472.

24. Walker BA, Boyle EM, Wardell CP, et al. Mutational Spectrum, Copy Number Changes, and Outcome: Results of a Sequencing Study of Patients With Newly Diagnosed Myeloma. *JCO*. 2015;33(33):3911–3920.

25. Alzrigat M, Párraga AA, Jernberg-Wiklund H. Epigenetics in multiple myeloma: From mechanisms to therapy. *Seminars in Cancer Biology*. 2018;51:101–115.

26. Amodio N, D'Aquila P, Passarino G, Tassone P, Bellizzi D. Epigenetic modifications in multiple myeloma: recent advances on the role of DNA and histone methylation. *Expert Opinion on Therapeutic Targets*. 2017;21(1):91–101.

27. Glavey SV, Manier S, Sacco A, et al. Epigenetics in Multiple Myeloma. *Plasma Cell Dyscrasias*. 2016;169:35–49.

28. Esquela-Kerscher A, Slack FJ. Oncomirs — microRNAs with a role in cancer. *Nat Rev Cancer*. 2006;6(4):259–269.

29. Pichiorri F, Suh S-S, Ladetto M, et al. MicroRNAs regulate critical genes associated with multiple myeloma pathogenesis. *Proceedings of the National Academy of Sciences*. 2008;105(35):12885–12890.

30. Martino MTD, Gullà A, Cantafio MEG, et al. In Vitro and in Vivo Anti-tumor Activity of miR-221/222 Inhibitors in Multiple Myeloma. *Oncotarget*. 2013;4(2):242–255.

31. Roccaro AM, Sacco A, Thompson B, et al. MicroRNAs 15a and 16 regulate tumor proliferation in multiple myeloma. *Blood*. 2009;113(26):6669–6680.

32. Gutiérrez NC, Sarasquete ME, Misiewicz-Krzeminska I, et al. Deregulation of microRNA expression in the different genetic subtypes of multiple myeloma and correlation with gene expression profiling. *Leukemia*. 2010;24(3):629–637.

33. Misiewicz-Krzeminska I, Krzeminski P, Corchete L, et al. Factors Regulating microRNA Expression and Function in Multiple Myeloma. *ncRNA*. 2019;5(1):9.

34. Shay G, Hazlehurst L, Lynch CC. Dissecting the multiple myeloma-bone microenvironment reveals new therapeutic opportunities. *J Mol Med*. 2016;94(1):21–35.

35. Garcia-Gomez A. Multiple myeloma mesenchymal stromal cells: Contribution to myeloma bone disease and therapeutics. *WJSC*. 2014;6(3):322.

36. Mitsiades CS, Mitsiades NS, Munshi NC, Richardson PG, Anderson KC. The role of the bone microenvironment in the pathophysiology and therapeutic management of multiple myeloma: Interplay of growth factors, their receptors and stromal interactions. *European Journal of Cancer*. 2006;42(11):1564–1573.

37. McMillin DW, Negri JM, Mitsiades CS. The role of tumour-stromal interactions in modifying drug response: challenges and opportunities. *Nat Rev Drug Discov*. 2013;12(3):217–228.

38. Raimondi L, De Luca A, Morelli E, et al. MicroRNAs: Novel Crossroads between Myeloma Cells and the Bone Marrow Microenvironment. *Biomed Res Int*. 2016;2016:6504593–6504593.

39. Amodio N, Bellizzi D, Leotta M, et al. miR-29b induces SOCS-1 expression by promoter demethylation and negatively regulates migration of multiple myeloma and endothelial cells. *Cell Cycle*. 2013;12(23):3650–3662.

40. Raimondi L, Amodio N, Di Martino T, et al. Targeting of multiple myeloma-related angiogenesis by miR-199a-5p mimics: in vitro and in vivo anti-tumor activity. *Oncotarget;*

Vol 5, No 10. 2014;

41. Di Martino MT, Leone E, Amodio N, et al. Synthetic miR-34a Mimics as a Novel Therapeutic Agent for Multiple Myeloma: In Vitro and In Vivo Evidence. *Clin Cancer Res*. 2012;18(22):6260.

42. Zhao J-J, Lin J, Zhu D, et al. miR-30-5p Functions as a Tumor Suppressor and Novel Therapeutic Tool by Targeting the Oncogenic Wnt/β-Catenin/BCL9 Pathway. *Cancer Res*. 2014;74(6):1801.

43. Leotta M, Biamonte L, Raimondi L, et al. A p53-Dependent Tumor Suppressor Network Is Induced by Selective miR-125a-5p Inhibition in Multiple Myeloma Cells. *Journal of Cellular Physiology*. 2014;229(12):2106–2116.

44. Hao M, Zhang L, An G, et al. Bone marrow stromal cells protect myeloma cells from bortezomib induced apoptosis by suppressing microRNA-15a expression. *Leukemia & Lymphoma*. 2011;52(9):1787–1794.

45. Wang X, Li C, Ju S, et al. Myeloma cell adhesion to bone marrow stromal cells confers drug resistance by microRNA-21 up-regulation. *Leukemia & Lymphoma*. 2011;52(10):1991–1998.

46. Morelli E, Leone E, Cantafio MEG, et al. Selective targeting of IRF4 by synthetic microRNA-125b-5p mimics induces anti-multiple myeloma activity in vitro and in vivo. *Leukemia*. 2015;29(11):2173–2183.

47. Gulla A, Di Martino MT, Gallo Cantafio ME, et al. A 13 mer LNA-i-miR-221 Inhibitor Restores Drug Sensitivity in Melphalan-Refractory Multiple Myeloma Cells. *Clinical Cancer Research*. 2016;22(5):1222–1233.

48. Wang J, Faict S, Maes K, et al. Extracellular vesicle cross-talk in the bone marrow microenvironment: implications in multiple myeloma. *Oncotarget*. 2016;7(25):38927–38945.

49. Kumar SK, Rajkumar SV, Dispenzieri A, et al. Improved survival in multiple myeloma and the impact of novel therapies. *Blood*. 2008;111(5):2516–2520.

50. Kumar SK, Dispenzieri A, Lacy MQ, et al. Continued improvement in survival in multiple myeloma: changes in early mortality and outcomes in older patients. *Leukemia*. 2014;28(5):1122–1128.

51. Burwick N, Sharma S. Glucocorticoids in multiple myeloma: past, present, and future. *Ann Hematol*. 2019;98(1):19–28.

52. Pönisch W, Mitrou PS, Merkle K, et al. Treatment of Bendamustine and Prednisone in patients with newly diagnosed multiple myeloma results in superior complete response rate, prolonged time to treatment failure and improved quality of life compared to treatment

with Melphalan and Prednisone—a randomized phase III study of the East German Study Group of Hematology and Oncology (OSHO). *Journal of Cancer Research and Clinical Oncology*. 2006;132(4):205–212.

53. Dimopoulos MA, Moreau P, Palumbo A, et al. Carfilzomib and dexamethasone versus bortezomib and dexamethasone for patients with relapsed or refractory multiple myeloma (ENDEAVOR): a randomised, phase 3, open-label, multicentre study. *The Lancet Oncology*. 2016;17(1):27–38.

54. Stewart AK, Rajkumar SV, Dimopoulos MA, et al. Carfilzomib, Lenalidomide, and Dexamethasone for Relapsed Multiple Myeloma. *N Engl J Med*. 2014;372(2):142–152.

55. Vij R, Siegel DS, Jagannath S, et al. An open-label, single-arm, phase 2 study of single-agent carfilzomib in patients with relapsed and/or refractory multiple myeloma who have been previously treated with bortezomib. *British Journal of Haematology*. 2012;158(6):739–748.

56. Moreau P, Masszi T, Grzasko N, et al. Oral Ixazomib, Lenalidomide, and Dexamethasone for Multiple Myeloma. *N Engl J Med*. 2016;374(17):1621–1634.

57. Thibaudeau TA, Smith DM. A Practical Review of Proteasome Pharmacology. *Pharmacol Rev*. 2019;71(2):170–197.

58. Dou QP, Zonder JA. Overview of proteasome inhibitor-based anti-cancer therapies: perspective on bortezomib and second generation proteasome inhibitors versus future generation inhibitors of ubiquitin-proteasome system. *Curr Cancer Drug Targets*. 2014;14(6):517–536.

59. Hideshima T, Anderson KC. Preclinical Studies of Novel Targeted Therapies. *Hematology/Oncology Clinics of North America*. 2007;21(6):1071–1091.

60. Mogollón P, Díaz-Tejedor A, Algarín EM, et al. Biological Background of Resistance to Current Standards of Care in Multiple Myeloma. *Cells*. 2019;8(11):1432.

61. Glasmacher A, Hahn C, Hoffmann F, et al. A systematic review of phase-II trials of thalidomide monotherapy in patients with relapsed or refractory multiple myeloma. *British Journal of Haematology*. 2006;132(5):584–593.

62. Miguel JS, Weisel K, Moreau P, et al. Pomalidomide plus low-dose dexamethasone versus high-dose dexamethasone alone for patients with relapsed and refractory multiple myeloma (MM-003): a randomised, open-label, phase 3 trial. *The Lancet Oncology*. 2013;14(11):1055–1066.

63. Richardson PG, Oriol A, Beksac M, et al. Pomalidomide, bortezomib, and dexamethasone for patients with relapsed or refractory multiple myeloma previously treated with lenalidomide (OPTIMISMM): a randomised, open-label, phase 3 trial. *The*

Lancet Oncology. 2019;20(6):781–794.

64. Attal M, Richardson PG, Rajkumar SV, et al. Isatuximab plus pomalidomide and low-dose dexamethasone versus pomalidomide and low-dose dexamethasone in patients with relapsed and refractory multiple myeloma (ICARIA-MM): a randomised, multicentre, open-label, phase 3 study. *The Lancet*. 2019;394(10214):2096–2107.

65. Holstein SA, McCarthy PL. Immunomodulatory Drugs in Multiple Myeloma: Mechanisms of Action and Clinical Experience. *Drugs*. 2017;77(5):505–520.

66. Swan D, Lynch K, Gurney M, O'Dwyer M. Current and emerging immunotherapeutic approaches to the treatment of multiple myeloma. *Therapeutic Advances in Hematology*. 21.

67. San-Miguel JF, Hungria VTM, Yoon S-S, et al. Panobinostat plus bortezomib and dexamethasone versus placebo plus bortezomib and dexamethasone in patients with relapsed or relapsed and refractory multiple myeloma: a multicentre, randomised, double-blind phase 3 trial. *The Lancet Oncology*. 2014;15(11):1195–1206.

68. Ocio EM, San Miguel JF. The DAC system and associations with multiple myeloma. *Investigational New Drugs*. 2010;28(1):28–35.

69. Laubach JP, Richardson PG. CD38-Targeted Immunochemotherapy in Refractory Multiple Myeloma: A New Horizon. *Clinical Cancer Research*. 2015;21(12):2660–2662.

70. van de Donk NWCJ. Reprint of "Immunomodulatory effects of CD38-targeting antibodies." *Immunology Letters*. 2019;205:71–77.

71. Campbell KS, Cohen AD, Pazina T. Mechanisms of NK Cell Activation and Clinical Activity of the Therapeutic SLAMF7 Antibody, Elotuzumab in Multiple Myeloma. *Front. Immunol.* 2018;9:2551.

72. Lonial S, Weiss BM, Usmani SZ, et al. Daratumumab monotherapy in patients with treatment-refractory multiple myeloma (SIRIUS): an open-label, randomised, phase 2 trial. *The Lancet*. 2016;387(10027):1551–1560.

73. Lokhorst HM, Plesner T, Laubach JP, et al. Targeting CD38 with Daratumumab Monotherapy in Multiple Myeloma. *N Engl J Med*. 2015;373(13):1207–1219.

74. Syed YY. Selinexor: First Global Approval. *Drugs*. 2019;79(13):1485–1494.

75. Touzeau C, Dousset C, Le Gouill S, et al. The Bcl-2 specific BH3 mimetic ABT-199: a promising targeted therapy for t(11;14) multiple myeloma. *Leukemia*. 2014;28(1):210–212.

76. Youle RJ, Strasser A. The BCL-2 protein family: opposing activities that mediate cell death. *Nature Reviews Molecular Cell Biology*. 2008;9(1):47–59.

77. Ichim G, Tait SWG. A fate worse than death: apoptosis as an oncogenic process.

Nature Reviews Cancer. 2016;16(8):539–548.

78. Lessene G, Czabotar PE, Colman PM. BCL-2 family antagonists for cancer therapy. *Nat Rev Drug Discov*. 2008;7(12):989–1000.

79. Shamas-Din A, Brahmbhatt H, Leber B, Andrews DW. BH3-only proteins: Orchestrators of apoptosis. *Biochimica et Biophysica Acta (BBA) - Molecular Cell Research*. 2011;1813(4):508–520.

80. Birkinshaw RW, Czabotar PE. The BCL-2 family of proteins and mitochondrial outer membrane permeabilisation. *Seminars in Cell & Developmental Biology*. 2017;72:152–162.

81. Fernald K, Kurokawa M. Evading apoptosis in cancer. *Trends in Cell Biology*. 2013;23(12):620–633.

82. Vogler M, Walter HS, Dyer MJS. Targeting anti-apoptotic BCL2 family proteins in haematological malignancies - from pathogenesis to treatment. *British Journal of Haematology*. 2017;178(3):364–379.

83. Nifoussi SK, Vrana JA, Domina AM, et al. Thr 163 Phosphorylation Causes Mcl-1 Stabilization when Degradation Is Independent of the Adjacent GSK3-Targeted Phosphodegron, Promoting Drug Resistance in Cancer. *PLOS ONE*. 2012;7(10):e47060.

84. Peso L del, González-Garćia M, Page C, Herrera R, Nuñez G. Interleukin-3-Induced Phosphorylation of BAD Through the Protein Kinase Akt. *Science*. 1997;278(5338):687.

85. Tse C, Shoemaker AR, Adickes J, et al. ABT-263: A Potent and Orally Bioavailable Bcl-2 Family Inhibitor. *Cancer Research*. 2008;68(9):3421–3428.

86. Deeks ED. Venetoclax: First Global Approval. *Drugs*. 2016;76(9):979–987.

87. Souers AJ, Leverson JD, Boghaert ER, et al. ABT-199, a potent and selective BCL-2 inhibitor, achieves antitumor activity while sparing platelets. *Nature Medicine*. 2013;19(2):202–208.

88. Kumar S, Kaufman JL, Gasparetto C, et al. Efficacy of venetoclax as targeted therapy for relapsed/refractory t(11;14) multiple myeloma. *Blood*. 2017;130(22):2401–2409.

89. Matulis SM, Gupta VA, Nooka AK, et al. Dexamethasone treatment promotes Bcl-2 dependence in multiple myeloma resulting in sensitivity to venetoclax. *Leukemia*. 2016;30(5):1086–1093.

90. Kaufman JL, Gasparetto C, Schjesvold FH, et al. Phase I/II Study Evaluating the Safety and Efficacy of Venetoclax in Combination with Dexamethasone As Targeted Therapy for Patients with t(11;14) Relapsed/Refractory Multiple Myeloma. *Blood*.

2019;134(Supplement_1):926–926.

91. Punnoose EA, Leverson JD, Peale F, et al. Expression Profile of BCL-2, BCL-XL, and MCL-1 Predicts Pharmacological Response to the BCL-2 Selective Antagonist Venetoclax in Multiple Myeloma Models. *Molecular Cancer Therapeutics*. 2016;15(5):1132–1144.

92. Dousset C, Maïga S, Gomez-Bougie P, et al. BH3 profiling as a tool to identify acquired resistance to venetoclax in multiple myeloma. *British Journal of Haematology*. 2017;179(4):684–688.

93. Gomez-Bougie P, Wuilleme-Toumi S, Menoret E, et al. Noxa Up-regulation and Mcl-1 Cleavage Are Associated to Apoptosis Induction by Bortezomib in Multiple Myeloma. *Cancer Research*. 2007;67(11):5418–5424.

94. Moreau P, Chanan-Khan A, Roberts AW, et al. Promising efficacy and acceptable safety of venetoclax plus bortezomib and dexamethasone in relapsed/refractory MM. *Blood*. 2017;130(22):2392–2400.

95. Kumar S, Harrison SJ, Cavo M, et al. A Phase 3 Study of Venetoclax or Placebo in Combination with Bortezomib and Dexamethasone in Patients with Relapsed/Refractory Multiple Myeloma. *Clinical Lymphoma, Myeloma and Leukemia*. 2019;19(10):e31.

96. Moreau P, Harrison S, Cavo M, et al. Updated Analysis of Bellini, a Phase 3 Study of Venetoclax or Placebo in Combination with Bortezomib and Dexamethasone in Patients with Relapsed/Refractory Multiple Myeloma. *Blood*. 2019;134(Supplement_1):1888–1888.

97. Derenne S. Antisense strategy shows that Mcl-1 rather than Bcl-2 or Bcl-xL is an essential survival protein of human myeloma cells. *Blood*. 2002;100(1):194–199.

98. Zhang B. Myeloid cell factor-1 is a critical survival factor for multiple myeloma. *Blood*. 2002;99(6):1885–1893.

99. Gong J-N, Khong T, Segal D, et al. Hierarchy for targeting prosurvival BCL2 family proteins in multiple myeloma: pivotal role of MCL1. *Blood*. 2016;128(14):1834–1844.

100. Gupta VA, Matulis SM, Conage-Pough JE, et al. Bone marrow microenvironment–derived signals induce Mcl-1 dependence in multiple myeloma. *Blood*. 2017;129(14):1969–1979.

101. Gomez-Bougie P, Amiot M. Apoptotic Machinery Diversity in Multiple Myeloma Molecular Subtypes. *Frontiers in Immunology*. 2013;4:.

102. Wuillème-Toumi S, Robillard N, Gomez P, et al. Mcl-1 is overexpressed in multiple myeloma and associated with relapse and shorter survival. *Leukemia*. 2005;19(7):1248–1252.

103. Kotschy A, Szlavik Z, Murray J, et al. The MCL1 inhibitor S63845 is tolerable and effective in diverse cancer models. *Nature*. 2016;538(7626):477–482.

104. Tron AE, Belmonte MA, Adam A, et al. Discovery of Mcl-1-specific inhibitor AZD5991 and preclinical activity in multiple myeloma and acute myeloid leukemia. *Nat Commun*. 2018;9(1):5341.

105. Caenepeel S, Brown SP, Belmontes B, et al. AMG 176, a Selective MCL1 Inhibitor, is Effective in Hematological Cancer Models Alone and in Combination with Established Therapies. *Cancer Discov*. 2018;CD-18-0387.

106. Mojica FJM, Diez-Villaseñor C, Garcia-Martinez J, Soria E. Intervening Sequences of Regularly Spaced Prokaryotic Repeats Derive from Foreign Genetic Elements. *J Mol Evol*. 2005;60(2):174–182.

107. Brouns SJJ, Jore MM, Lundgren M, et al. Small CRISPR RNAs Guide Antiviral Defense in Prokaryotes. *Science*. 2008;321(5891):960.

108. Jinek M, Chylinski K, Fonfara I, et al. A Programmable Dual-RNA–Guided DNA Endonuclease in Adaptive Bacterial Immunity. *Science*. 2012;337(6096):816.

109. Mojica FJM, Díez-Villaseñor C, García-Martínez J, Almendros C. Short motif sequences determine the targets of the prokaryotic CRISPR defence system. *Microbiology*. 2009;155(3):733–740.

110. Mojica FJM, Montoliu L. On the Origin of CRISPR-Cas Technology: From Prokaryotes to Mammals. *Trends in Microbiology*. 2016;24(10):811–820.

111. Hartenian E, Doench JG. Genetic screens and functional genomics using CRISPR/Cas9 technology. *FEBS J*. 2015;282(8):1383–1393.

112. Pickar-Oliver A, Gersbach CA. The next generation of CRISPR–Cas technologies and applications. *Nat Rev Mol Cell Biol*. 2019;20(8):490–507.

113. Gilbert LA, Larson MH, Morsut L, et al. CRISPR-Mediated Modular RNA-Guided Regulation of Transcription in Eukaryotes. *Cell*. 2013;154(2):442–451.

114. Peters JM, Silvis MR, Zhao D, et al. Bacterial CRISPR: accomplishments and prospects. *Current Opinion in Microbiology*. 2015;27:121–126.

115. Shalem O, Sanjana NE, Zhang F. High-throughput functional genomics using CRISPR–Cas9. *Nat Rev Genet*. 2015;16(5):299–311.

116. Shi C-X, Kortüm KM, Zhu YX, et al. CRISPR Genome-Wide Screening Identifies Dependence on the Proteasome Subunit PSMC6 for Bortezomib Sensitivity in Multiple Myeloma. *Mol Cancer Ther*. 2017;16(12):2862–2870.

117. Sievers QL, Gasser JA, Cowley GS, Fischer ES, Ebert BL. Genome-wide screen identifies cullin-RING ligase machinery required for lenalidomide-dependent CRL4CRBN

activity. *Blood*. 2018;132(12):1293–1303.

118. Liu J, Song T, Zhou W, et al. A genome-scale CRISPR-Cas9 screening in myeloma cells identifies regulators of immunomodulatory drug sensitivity. *Leukemia*. 2019;33(1):171–180.

119. Ramkumar P, Abarientos AB, Tian R, et al. CRISPR-based screens uncover determinants of immunotherapy response in Multiple Myeloma. Cancer Biology; 2019.

120. Nechiporuk T, Kurtz SE, Nikolova O, et al. The TP53 Apoptotic Network Is a Primary Mediator of Resistance to BCL2 Inhibition in AML Cells. *Cancer Discov*. 2019;9(7):910–925.

121. Chen X, Glytsou C, Zhou H, et al. Targeting Mitochondrial Structure Sensitizes Acute Myeloid Leukemia to Venetoclax Treatment. *Cancer Discov*. 2019;9(7):890–909.

122. DeWeirdt PC, Sanson KR, Hanna RE, et al. Genetic screens in isogenic mammalian cell lines without single cell cloning. Genetics; 2019.

123. Kabir S, Cidado J, Andersen C, et al. The CUL5 ubiquitin ligase complex mediates resistance to CDK9 and MCL1 inhibitors in lung cancer cells. *eLife*. 2019;8:e44288.

124. Garcia-Gomez A, Quwaider D, Canavese M, et al. Preclinical Activity of the Oral Proteasome Inhibitor MLN9708 in Myeloma Bone Disease. *Clinical Cancer Research*. 2014;20(6):1542–1554.

125. McMillin DW, Delmore J, Weisberg E, et al. Tumor cell-specific bioluminescence platform to identify stroma-induced changes to anticancer drug activity. *Nat Med*. 2010;16(4):483–489.

126. Paíno T, Sarasquete ME, Paiva B, et al. Phenotypic, Genomic and Functional Characterization Reveals No Differences between CD138++ and CD138low Subpopulations in Multiple Myeloma Cell Lines. *PLoS ONE*. 2014;9(3):e92378.

127. Ocio EM, Maiso P, Chen X, et al. Zalypsis: a novel marine-derived compound with potent antimyeloma activity that reveals high sensitivity of malignant plasma cells to DNA double-strand breaks. *Blood*. 2009;113(16):3781–3791.

128. Maiso P, Carvajal-Vergara X, Ocio EM, et al. The Histone Deacetylase Inhibitor LBH589 Is a Potent Antimyeloma Agent that Overcomes Drug Resistance. *Cancer Research*. 2006;66(11):5781–5789.

129. Chou T-C. Drug Combination Studies and Their Synergy Quantification Using the Chou-Talalay Method. *Cancer Research*. 2010;70(2):440–446.

130. Li W, Xu H, Xiao T, et al. MAGeCK enables robust identification of essential genes from genome-scale CRISPR/Cas9 knockout screens. 2014;12.

131. Algarín EM, Díaz-Tejedor A, Mogollón P, et al. Preclinical evaluation of the

simultaneous inhibition of MCL-1 and BCL-2 with the combination of S63845 and venetoclax in multiple myeloma. *Haematologica*. 2019;haematol.2018.212308.

132. Lin EY, Orlofsky A, Berger MS, Prystowsky MB. Characterization of A1, a novel hemopoietic-specific early-response gene with sequence similarity to bcl-2. *J. Immunol.* 1993;151(4):1979.

133. Alsamman K, El-Masry OS. Interferon regulatory factor 1 inactivation in human cancer. *Bioscience Reports*. 2018;38(3):BSR20171672.

134. Agnarelli A, Chevassut T, Mancini EJ. IRF4 in multiple myeloma—Biology, disease and therapeutic target. *Leukemia Research*. 2018;72:52–58.

135. Kronke J, Udeshi ND, Narla A, et al. Lenalidomide Causes Selective Degradation of IKZF1 and IKZF3 in Multiple Myeloma Cells. *Science*. 2014;343(6168):301–305.

136. Hanahan D, Weinberg RA. Hallmarks of Cancer: The Next Generation. *Cell*. 2011;144(5):646–674.

137. Slomp A, Moesbergen LM, Gong J, et al. Multiple myeloma with 1q21 amplification is highly sensitive to MCL-1 targeting. *Blood Advances*. 2019;3(24):4202–4214.

138. Perciavalle RM, Opferman JT. Delving deeper: MCL-1's contributions to normal and cancer biology. *Trends in Cell Biology*. 2013;23(1):22–29.

139. Jourdan M, Veyrune J-L, Vos JD, et al. A major role for Mcl-1 antiapoptotic protein in the IL-6-induced survival of human myeloma cells. *Oncogene*. 2003;22(19):2950–2959.

140. Jourdan M, De Vos J, Mechti N, Klein B. Regulation of Bcl-2-family proteins in myeloma cells by three myeloma survival factors: interleukin-6, interferon-alpha and insulin-like growth factor 1. *Cell Death Differ*. 2000;7(12):1244–1252.

141. Wu Y, Wang H. LncRNA NEAT1 promotes dexamethasone resistance in multiple myeloma by targeting miR-193a/MCL1 pathway. *Journal of Biochemical and Molecular Toxicology*. 2018;32(1):e22008.

142. Lam LT, Lu X, Zhang H, et al. A MicroRNA Screen to Identify Modulators of Sensitivity to BCL2 Inhibitor ABT-263 (Navitoclax). *Mol Cancer Ther*. 2010;9(11):2943–2950.

143. Sims EK, Lakhter A, Anderson-Baucum E, et al. MicroRNA 21 targets BCL2 mRNA to increase cell apoptosis in rat and human beta cells. *Diabetologia*. 2017;60(6):1057–1065.

144. Wickramasinghe NS, Manavalan TT, Dougherty SM, et al. Estradiol downregulates miR-21 expression and increases miR-21 target gene expression in MCF-7 breast cancer cells. *Nucleic Acids Research*. 2009;37(8):2584–2595.

145. Liu K, Du J, Ruan L. MicroRNA-21 regulates the viability and apoptosis of diffuse

large B-cell lymphoma cells by upregulating B cell lymphoma-2. *Exp Ther Med*. 2017;

146. Dong J, Zhao Y-P, Zhou L, Zhang T-P, Chen G. Bcl-2 Upregulation Induced by miR-21 Via a Direct Interaction Is Associated with Apoptosis and Chemoresistance in MIA PaCa-2 Pancreatic Cancer Cells. *Archives of Medical Research*. 2011;42(1):8–14.

147. Li Y, Yan L, Zhang W, et al. miR-21 inhibitor suppresses proliferation and migration of nasopharyngeal carcinoma cells through down-regulation of BCL2 expression. 10.

148. Morales AA, Kurtoglu M, Matulis SM, et al. Distribution of Bim determines Mcl-1 dependence or codependence with Bcl-xL/Bcl-2 in Mcl-1-expressing myeloma cells. *Blood*. 2011;118(5):1329–1339.

149. Nass J, Efferth T. Drug targets and resistance mechanisms in multiple myeloma. *CDR*. 2018;

150. Gomez-Bougie P, Maiga S, Tessoulin B, et al. BH3-mimetic toolkit guides the respective use of BCL2 and MCL1 BH3-mimetics in myeloma treatment. *Blood*. 2018;132(25):2656–2669.

151. Siu KT, Huang C, Panaroni C, et al. BCL2 blockade overcomes MCL1 resistance in multiple myeloma. *Leukemia*. 2019;33(8):2098–2102.

152. Vogler M, Butterworth M, Majid A, et al. Concurrent up-regulation of BCL-XL and BCL2A1 induces approximately 1000-fold resistance to ABT-737 in chronic lymphocytic leukemia. *Blood*. 2009;113(18):4403–4413.

153. Willis SN. Proapoptotic Bak is sequestered by Mcl-1 and Bcl-xL, but not Bcl-2, until displaced by BH3-only proteins. *Genes & Development*. 2005;19(11):1294–1305.

154. Czabotar PE, Lee EF, van Delft MF, et al. Structural insights into the degradation of Mcl-1 induced by BH3 domains. *Proceedings of the National Academy of Sciences*. 2007;104(15):6217–6222.

155. Khoo. Interferon-Alpha in the Treatment of Multiple Myeloma. *cdt*. 2011;12(3):.

156. Otsuki T, Yamada O, Sakaguchi H, et al. Human myeloma cell apoptosis induced by interferon-a. *British Journal of Haematology*. 1998;12.

157. Chang DH, Liu N, Klimek V, et al. Enhancement of ligand-dependent activation of human natural killer T cells by lenalidomide: therapeutic implications. *Blood*. 2006;108(2):618–621.

158. Henry JY, Labarthe M-C, Meyer B, et al. Enhanced cross-priming of naive CD8+ T cells by dendritic cells treated by the IMiDs® immunomodulatory compounds lenalidomide and pomalidomide. *Immunology*. 2013;139(3):377–385.

8. SUPPLEMENTARY APPENDIX

Preclinical evaluation of the simultaneous inhibition of MCL-1 and BCL-2 with the combination of S63845 and venetoclax in multiple myeloma

Apoptotic evasion has been postulated as one of the main mechanisms of multiple myeloma (MM) cell survival.[1,2] The intrinsic apoptotic pathway, tightly regulated by the BCL-2 protein family, is initiated by intracellularly sensed stress signals and ultimately leads to the permeabilization of the outer mitochondrial membrane. Tumor cells can keep this pathway inactivated, in part, through the overexpression of BCL-2, BCL-XL or MCL-1 anti-apoptotic proteins,[3] which bind to and sequester pro-apoptotic proteins (e.g. BIM, NOXA, PUMA), thereby eluding apoptosis. Venetoclax is a drug that selectively binds to BCL-2, impeding its activity as an inhibitor of pro-apoptotic proteins.[4] In MM, a phase I clinical trial of venetoclax in monotherapy (*clinicaltrials.gov identifier: 01794520*) has been effective, predominantly in the subgroup of patients harboring the t(11;14) translocation.[5] Although co-dependencies with BCL-2 and BCL-XL have

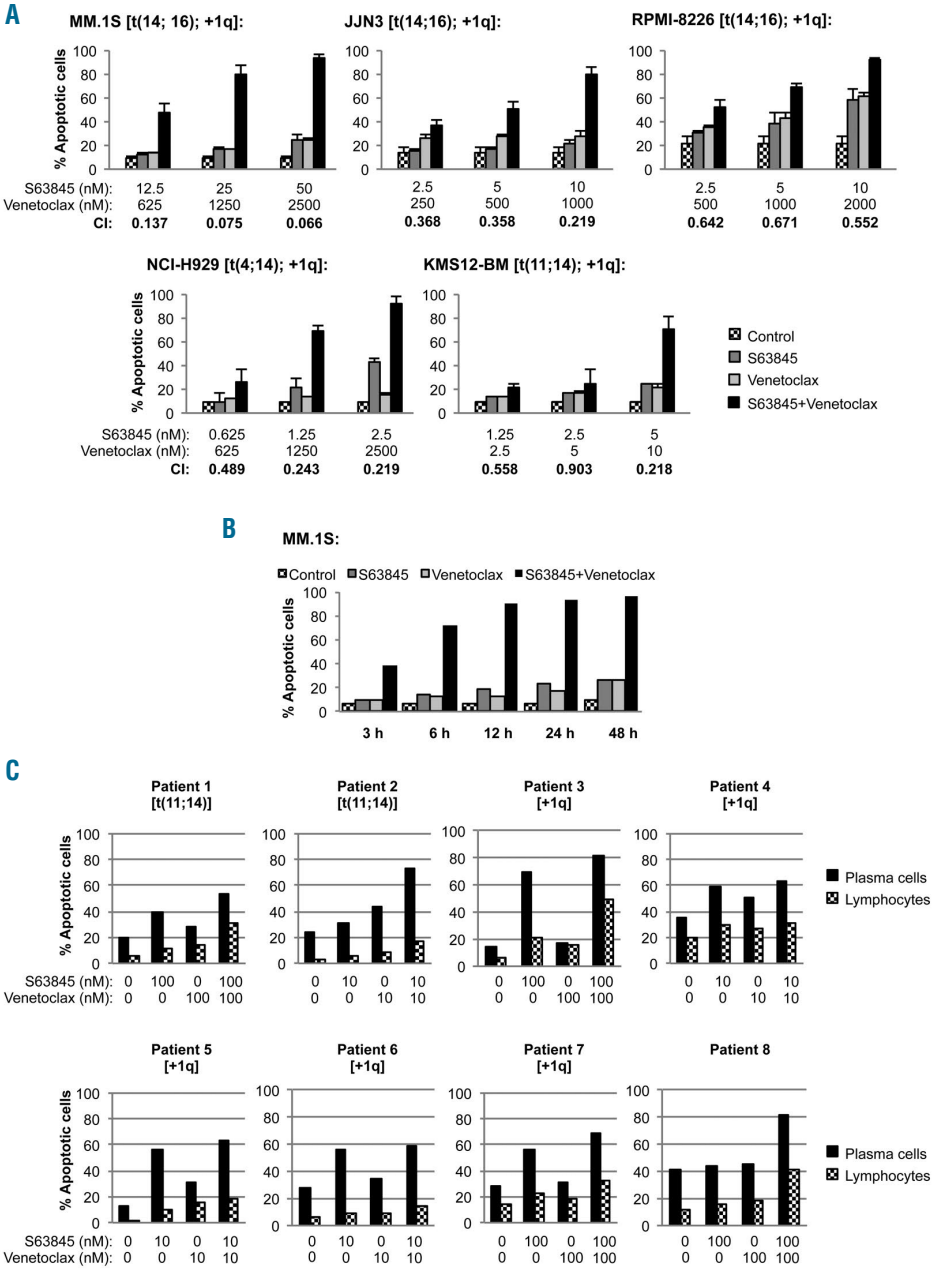

Figure 1. S63845 strongly synergizes with venetoclax *in vitro*. (A) Multiple myeloma (MM) cell lines were exposed to increasing doses of S63845+venetoclax for 48 hours (h), using a constant drug ratio combination design for each cell line. Apoptosis induction was analyzed by flow cytometry after Annexin-V binding and propidium iodide micromolar staining as represented in the graphs, and combination indices (CI) were calculated with the Calcusyn software (see also *Online Supplementary Figure S2*). A CI of 1 indicates an additive effect, CI <1 a synergistic effect and CI<1 antagonism. (B) MM.1S cells were treated with S63845 50 nM and venetoclax 2.5 nM for 3, 6, 12, 24 and 48 h, and the induction of apoptosis was assessed at indicated time points. (C) Bone marrow cells from eight MM patients were incubated with S63845 and venetoclax as single agents and in combination at indicated doses for 24 h. Apoptosis induction was analyzed by flow cytometry after Annexin-V binding in plasma cells ($CD38^{+bright}$, $CD45^{-/low}$, $SSC^{low/intermediate}$, CD56-/+) and lymphocytes ($CD45^{++}$, SSC^{low}).

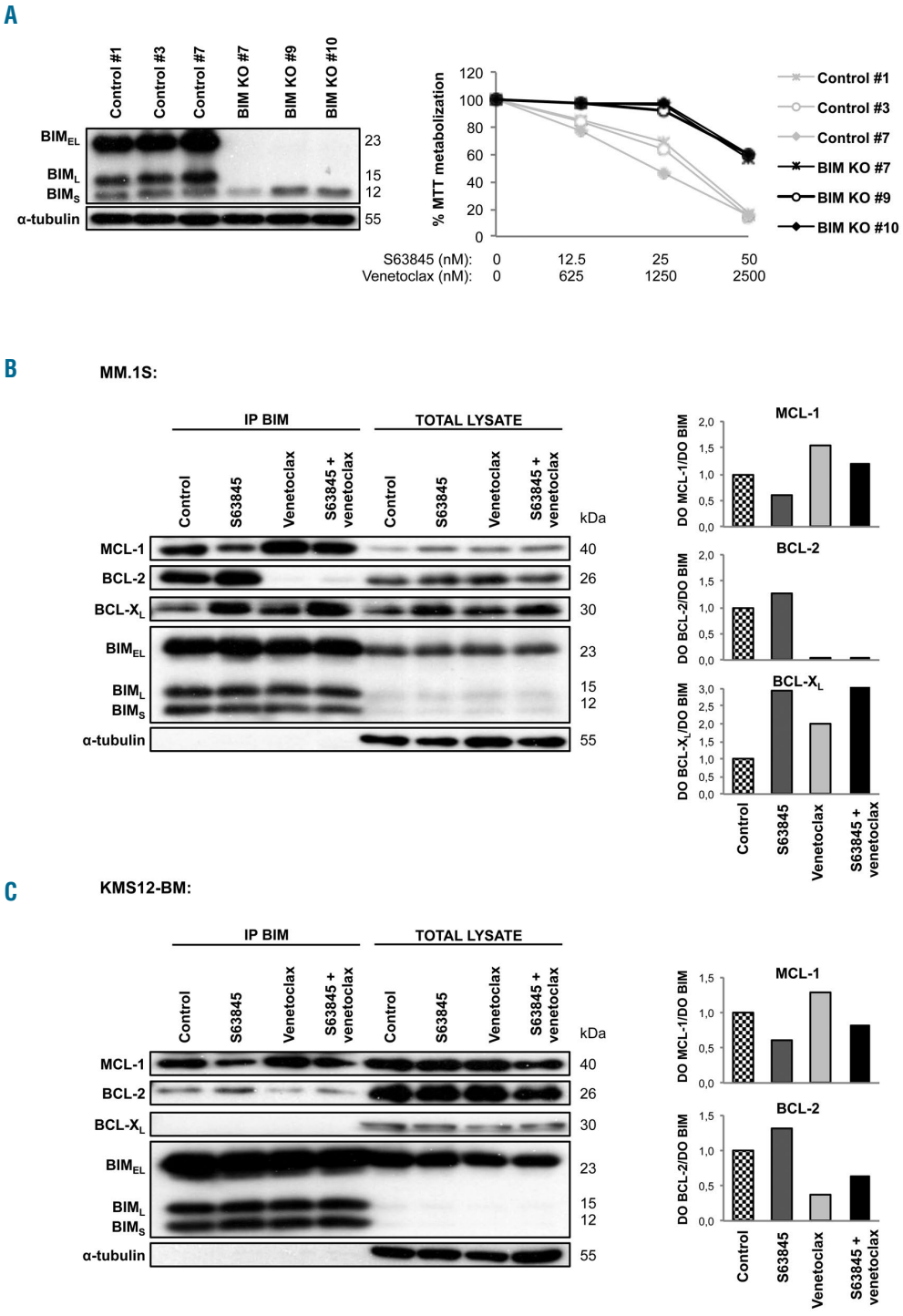

Figure 2. The S63845 + venetoclax combination impairs the interactions of MCL-1 and BCL-2 with the pro-apoptotic protein BIM. (A) BIM shows three major isoforms: BIM$_{EL}$, BIM$_L$ and BIM$_S$. MM.1S clones KO for BIM$_{EL}$ and BIM$_L$ isoforms were generated by electroporation of a Cas9 ribonucleoprotein complex [containing a guide RNA and a Cas9 enzyme (Integrated DNA Technologies)], using the Neon Transfection System (Thermo Fisher Scientific) and subsequent single cell sorting. Clones KO for BIM$_{EL}$ and BIM$_L$ isoforms and control clones (electroporated with the Cas9 enzyme only) were exposed to increasing doses of S63845+venetoclax for 24 hours, keeping a constant 1:50 S63845:venetoclax ratio. Cell viability was analyzed by MTT assay. (B and C) MM.1S and KMS12-BM cell lines (least sensitive and most sensitive to S63845 and venetoclax) were respectively treated with S63845 (12.5 and 2 nM) and venetoclax (625 and 4 nM), in monotherapy or in combination for 24 hours (S63845 and venetoclax doses were adjusted for each cell line so that the combination would induce 13-25% apoptosis as measured by Annexin-V and PI staining). Protein lysates were subjected to immunoprecipitation with an anti-BIM antibody, and MCL-1, BCL-2 and BCL-X$_L$ bound to BIM were then analyzed by immunoblotting. Their levels were quantified by densitometry analysis of bands using ImageJ software, normalized to those of BIM, and depicted as bar diagrams. Whole cell lysates of each cell line are also shown.

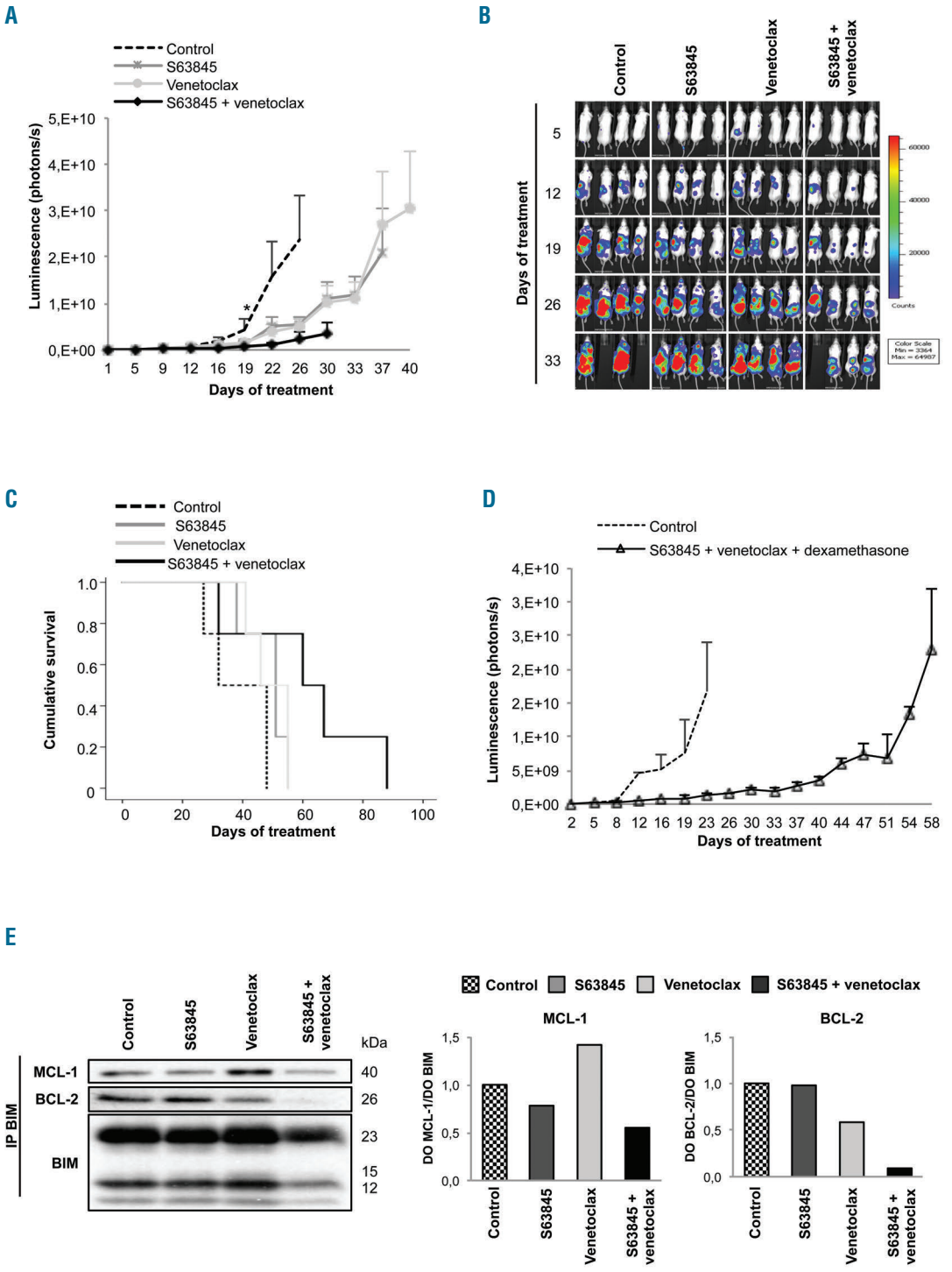

Figure 3. The S63845 + venetoclax combination has potent *in vivo* anti-myeloma activity. (A) *In vivo* efficacy of S63845+venetoclax in an RPMI-8226-luc xenograft model of disseminated multiple myeloma (MM) in BRG mice. Experimental groups included: control (vehicle), S63845 (12.5 mg/kg intravenous, weekly), venetoclax (100 mg/kg oral administration, 5 days per week), and the respective combination (n=4 per group). Mice were treated until death or sacrifice for humane reasons. Statistically significant differences (Kruskal-Wallis test followed by Dunn's post-hoc comparisons, **P*<0.05) were observed from day 19 onwards when comparing the combination with the control. Data are summarized as the mean±Standard Error of Mean (SEM). (B) Images representing the bioluminescence signal of each mouse by treatment group from day 5 to day 33 of treatment. (C) Kaplan-Meier curves representing the survival of each treatment group. (D) Efficacy of the triple combination S63845+venetoclax+dexamethasone using the doses and scheme as in (A) but with intraperitoneal dexamethasone administration (1 mg/kg, 2 days/week) (n=3 per group). Data are shown as mean±SEM. (E) RPMI-8226 cells were subcutaneously injected in CB17-SCID mice. When plasmacytomas reached 2 cm in one of their diameters, animals received one dose of vehicle, S63845 (12.5 mg/kg), venetoclax (100 mg/kg) or the respective combination (n=2 per group). Tumors were excised 24 hours after treatment and protein lysates from tumors were subjected to immunoprecipitation with an anti-BIM antibody. MCL-1, BCL-2 and BCL-Xʟ anti-apoptotic proteins bound to BIM were then analyzed by immunoblotting, quantified by densitometry analysis of bands normalized to those of BIM using ImageJ software, and represented in bar diagrams.

been described,[6,7] MM cells are heavily dependent on MCL-1[8,9] and high levels of MCL-1 have been associated with venetoclax resistance.[2,10] In this regard, a new selective MCL-1 inhibitor, S63845, has recently demonstrated single-agent anti-tumor effect in MM.[11] Within this scenario, we sought to test the potential synergistic apoptotic induction of S63845 and venetoclax in MM. Mechanistically, the shift in MM-cell dependence to different anti-apoptotic proteins observed with each agent in monotherapy was greatly overcome with the double combination, translating into important anti-myeloma efficacy *in vitro*, *ex vivo* and *in vivo*.

We selected five myeloma cell lines with different sensitivities to S63845 and venetoclax in monotherapy (MM.1S being the most resistant and KMS12-BM the most sensitive), and evaluated the cytotoxic effect of the combination of both agents by flow cytometry (Figure 1A) and MTT assay (*Online Supplementary Figure S1*). Overall, our *in vitro* findings show that the S63845+venetoclax combination clearly increased apoptotic cell death and reduced cell viability, with combination indexes (CI) reaching a strong synergism (0.1 <CI <0.3) in almost all cell lines (*Online Supplementary Figures S2 and S3)*. This effect was dose- and time-dependent, and short drug exposures of 3-6 hours already triggered the apoptotic effect (Figure 1A and B). Given the clinical interest of the addition of dexamethasone in the current backbone of MM treatment, the triple combination of S63845+venetoclax+dexamethasone was also evaluated. Dexamethasone clearly increased the efficacy of both S63845 and venetoclax, and the triple combination showed an even stronger synergism than the S63845+venetoclax doublet in MM.1S (best CI=0.054) and RPMI-8226 (best CI=0.099) cells (*Online Supplementary Figure S4A and B*).

The anti-tumoral effect of S63845 and venetoclax was further investigated *ex vivo* in cells isolated from eight MM patients. Patients 1 and 2 harbored the t(11;14) translocation, Patients 3 to 7 had 1q gain, and Patient 8 did not bear any of those cytogenetic alterations. S63845 in monotherapy was active in almost all patients (*Online Supplementary Figure S5A*), although those patients with 1q amplification (thus harboring the locus of the MCL1 gene) were significantly more sensitive to this agent (Student *t*-test, $P<0.05$) (*Online Supplementary Figure S5B*). Whether 1q amplification is a bona-fide marker of response to MCL-1 inhibitors is being tested in ongoing preclinical and clinical studies. On the other hand, only Patient 2 bearing the t(11;14) translocation was clearly sensitive to venetoclax as single agent (*Online Supplementary Figure S5C*). This situation is consistent with the clinical data in which less than half of the t(11;14) patients responded to venetoclax.[5] Finally, in 5 of the 8 evaluated patients (Patients 1, 2, 3, 7 and 8), the combination enhanced the apoptotic induction of both agents in monotherapy, but, interestingly, this was particularly evident in Patient 2 [venetoclax responder harboring the t(11;14) translocation] and Patient 8 [insensitive to both drugs in monotherapy without t(11;14) translocation or +1q gain alterations] (Figure 1C). The toxicity on normal lymphocytes was clearly lower than that on tumor cells, suggesting a therapeutic window for both drugs (Figure 1C and *Online Supplementary Figure S5A-C*).

Next, we explored the mechanism of action of the S63845+venetoclax combination. BIM is a pro-apoptotic protein which has already been shown to be involved in the mechanism of action of S63845 and venetoclax in monotherapy.[12-14] Accordingly, using CRISPR/Cas9 gene editing in MM.1S cells, we selected BIM knock-out clones for 2 of the 3 major BIM isoforms (BIM_{EL} and BIM_L), which showed notably decreased sensitivity to the S63845+venetoclax combination (Figure 2A). Since these data prove the involvement of BIM in the mechanism of action of the double combination, the binding of MCL-1, BCL-2 and BCL-X_L anti-apoptotic proteins to BIM was next explored in the MM.1S and KMS12-BM cell lines (Figure 2B and C). S63845 treatment clearly disrupted MCL-1/BIM complexes, but also induced a compensatory increase in BCL-2/BIM complexes over control levels in both cell lines. BCL-X_L/BIM complexes were also increased after S63845 treatment in the MM.1S cell line, but these complexes were absent in KMS12-BM cells. These results imply that S63845 treatment may change MM-cell dependence from MCL-1 to BCL-2, and also to BCL-X_L in cells particularly dependent on this protein, thus suggesting a potential mechanism of resistance. On the other hand, and consistent with previous reports,[2,13] venetoclax impaired the formation of BCL-2/BIM complexes and also increased the binding of MCL-1 to BIM over control levels in KMS12-BM cells and the binding of both MCL-1 and BCL-X_L to BIM in MM.1S cells, suggesting a parallel situation to that observed with S63845. Importantly, after treatment with the S63845+venetoclax combination, BCL-2/BIM complexes remained low in both cell lines tested. However, in MM.1S cells, MCL-1 was still able to interact with BIM, although to a lesser extent than with venetoclax in monotherapy, thereby diminishing the previously described venetoclax escape mechanism. Regarding BCL-X_L/BIM complexes, their increase with S63845 and venetoclax treatments in monotherapy was not further potentiated by the double combination. Whole cell lysates did not show major changes on MCL-1, BCL-2, BCL-X_L and BIM levels in MM.1S and KMS12-BM cells treated with S63845 and venetoclax alone and in combination (Figure 2B and C). Finally, we immunoprecipitated MCL-1 and BCL-2 anti-apoptotic proteins, and analyzed BIM binding by immunoblotting (*Online Supplementary Figure S6A and B*); the results obtained were in accordance with those from BIM immunoprecipitation. MCL-1/NOXA and BCL-2/PUMA complexes were also evaluated, but low expression of these pro-apoptotic proteins precluded evaluation of their role in response to the drugs (*data not shown*).

Furthermore, the efficacy of S63845+venetoclax was explored *in vivo* in an aggressive disseminated model of MM. The double treatment delayed tumor growth, and in contrast to the agents in monotherapy, produced a statistically significant benefit with respect to the control from day 19 onwards (Figure 3A). Of note, at day 32, a mouse treated with S63845+venetoclax, despite only having a relatively localized bioluminescence signal, developed hind-limb paralysis and was euthanized for humane reasons (Figure 3B). Nevertheless, the efficacy in controlling tumor growth translated into improved survival of mice treated with S63845+venetoclax, with a median survival of 60 days (range: 32-88 days) compared with 51 days for S63845 (range: 38-55 days) and 46 days for venetoclax (range: 41-55 days) (Figure 3C), although these differences were not statistically significant. Remarkably, none of the treatments caused a significant reduction in body weight (*Online Supplementary Figure S7A*) or other signs of toxicity. It should be noted that S63845 has weaker affinity for murine MCL-1,[11] and therefore other models[15] would be required to better evaluate the safety margins of this combination.

Similarly to *in vitro* studies, we also evaluated the activ-

ity and toxicity of the triple combination of S63845+venetoclax+dexamethasone in the previously mentioned *in vivo* disseminated model of MM. The triple combination induced approximately 30 days delay in tumor growth compared with the control group (Figure 3D). Most importantly, the tolerability of this triple combination was excellent, without significant body weight loss (*Online Supplementary Figure S7B*) or other signs of toxicity.

Finally, we performed mechanistic studies on tumor cells from large RPMI-8226 plasmacytomas excised 24 hours after one dose of treatment (Figure 3E). In accordance with *in vitro* data, treatment with S63845 and venetoclax in monotherapy, respectively, impaired the binding of MCL-1 and BCL-2 to the pro-apoptotic protein BIM. Moreover, there was a compensatory upregulation of MCL-1/BIM complexes in tumors from mice treated with venetoclax, but no increase in BCL-2/BIM complexes in tumors from mice treated with S63845. Remarkably, the S63845+venetoclax combination completely disrupted BCL-2/BIM complexes and was able to counteract the compensatory upregulation of MCL-1 bound to BIM in tumors treated with venetoclax in monotherapy. Thus, *in vivo*, benefit is observed with the double combination relative to the disruption of BIM complexes with MCL-1 and BCL-2.

In conclusion, we have shown the high preclinical efficacy and synergism of the S63845 and venetoclax combination on MM cells, mediated at least in part by the simultaneous inhibition of the binding of MCL-1 and BCL-2 to BIM. Our preclinical results provide a strong rationale for the clinical investigation of the combination of an MCL-1 inhibitor with venetoclax for the treatment of MM patients. In addition, based on the preliminary results obtained with the triple combination, the addition of dexamethasone may also be considered.

Esperanza M Algarín,[1] Andrea Díaz-Tejedor,[1] Pedro Mogollón,[1] Susana Hernández-García,[1] Luis A. Corchete,[1] Laura San-Segundo,[1] Montserrat Martín-Sánchez,[1] Lorena González-Méndez,[1] Marie Schoumacher,[2] Sébastien Banquet,[2] Laurence Kraus-Berthier,[2] Ioana Kloos,[2] Alix Derreal,[2] Ensar Halilovic,[3] Heiko Maacke,[4] Norma C. Gutiérrez,[1] María-Victoria Mateos,[1] Teresa Paíno,[1] Mercedes Garayoa[1] and Enrique M. Ocio[1,5*]*

**MG and EMO contributed equally to this work.*

[1]University Hospital of Salamanca (IBSAL)-Cancer Research Center (IBMCC-CSIC-USAL), Salamanca, Spain; [2]Institut de Recherches Servier, Suresnes, France; [3]Novartis Institutes for Biomedical Research, Cambridge, MA, USA; [4]Novartis Institutes for Biomedical Research, Basel, Switzerland and [5]University Hospital Marqués de Valdecilla (IDIVAL); University of Cantabria, Santander, Spain

Correspondence: ENRIQUE M. OCIO
ocioem@unican.es
doi:10.3324/haematol.2018.212308

Funding: this work was supported by the Spanish ISCIII-FIS and FEDER Funds (PI 15/00067 and PI 15/02156) and the Regional Health Council of Castilla y León (GRS 1604/A/17). EMA was supported by a grant from the Regional Education Council of Castilla y León co-financed by the European Social Fund.

Information on authorship, contributions, and financial & other disclosures was provided by the authors and is available with the online version of this article at www.haematologica.org.

References

1. Witzig T, Timm M, Larson D, Therneau T, Greipp P. Measurement of apoptosis and proliferation of bone marrow plasma cells in patients with plasma cell proliferative disorders. Br J Haematol. 1999;104(1):131–137.
2. Touzeau C, Dousset C, Le Gouill S, et al. The Bcl-2 specific BH3 mimetic ABT-199: a promising targeted therapy for t(11;14) multiple myeloma. Leukemia. 2014;28(1):210–212.
3. Vogler M, Walter HS, Dyer MJS. Targeting anti-apoptotic BCL2 family proteins in haematological malignancies - from pathogenesis to treatment. Br J Haematol. 2017;178(3):364–379.
4. Souers AJ, Leverson JD, Boghaert ER, et al. ABT-199, a potent and selective BCL-2 inhibitor, achieves antitumor activity while sparing platelets. Nat Med. 2013;19(2):202–208.
5. Kumar S, Kaufman JL, Gasparetto C, et al. Efficacy of venetoclax as targeted therapy for relapsed/refractory t(11;14) multiple myeloma. Blood. 2017;130(22):2401–2409.
6. Gomez-Bougie P, Maiga S, Tessoulin B, et al. BH3-mimetic toolkit guides the respective use of BCL2 and MCL1 BH3-mimetics in myeloma treatment. Blood. 2018;132(25):2656–2669.
7. Touzeau C, Ryan J, Guerriero J, et al. BH3 profiling identifies heterogeneous dependency on Bcl-2 family members in multiple myeloma and predicts sensitivity to BH3 mimetics. Leukemia. 2016;30(3):761–764.
8. Gong J-N, Khong T, Segal D, et al. Hierarchy for targeting prosurvival BCL2 family proteins in multiple myeloma: pivotal role of MCL1. Blood. 2016;128(14):1834–1844.
9. Derenne S. Antisense strategy shows that Mcl-1 rather than Bcl-2 or Bcl-xL is an essential survival protein of human myeloma cells. Blood. 2002;100(1):194–199.
10. Dousset C, Maïga S, Gomez-Bougie P, et al. BH3 profiling as a tool to identify acquired resistance to venetoclax in multiple myeloma. Br J Haematol. 2017;179(4):684–688.
11. Kotschy A, Szlavik Z, Murray J, et al. The MCL1 inhibitor S63845 is tolerable and effective in diverse cancer models. Nature. 2016;538(7626):477–482.
12. Morales AA, Kurtoglu M, Matulis SM, et al. Distribution of Bim determines Mcl-1 dependence or codependence with Bcl-xL/Bcl-2 in Mcl-1-expressing myeloma cells. Blood. 2011;118(5):1329–1339.
13. Punnoose EA, Leverson JD, Peale F, et al. Expression Profile of BCL-2, BCL-XL, and MCL-1 Predicts Pharmacological Response to the BCL-2 Selective Antagonist Venetoclax in Multiple Myeloma Models. Mol Cancer Ther. 2016;15(5):1132–1144.
14. Merino D, Whittle JR, Vaillant F, et al. Synergistic action of the MCL-1 inhibitor S63845 with current therapies in preclinical models of triple-negative and HER2-amplified breast cancer. Sci Transl Med. 2017;9(401):eaam7049.
15. Brennan MS, Chang C, Dewson G, et al. Humanized Mcl-1 mice enable accurate pre-clinical evaluation of MCL-1 inhibitors destined for clinical use. Blood. 2018;132(15):1573–1583.